LIFETIME ESTIMATION OF STEEL TUBING BY CORROSION ANALYSIS FOR PETROLEUM

Atiwat Ketsukmanote

A Thesis Submitted in Partial Fulfillment of the Requirements for the

Degree of Master of Engineering in Geotechnology

Suranaree University of Technology

Academic Year 2016

การประเมินอายุการใช้งานของท่อเหล็กโดยการวิเคราะห์การกัดกร่อน สำหรับอุตสาหกรรมปิโตรเลียม

นายอธิวัฒน์ เกษสุขมาโนช

วิทยานิพนธ์นี้เป็นส่วนหนึ่งของการศึกษาตามหลักสูตรปริญญาวิศวกรรมศาสตรมหาบัณฑิต
สาขาวิชาเทคโนโลยีธรณี
มหาวิทยาลัยเทคโนโลยีสุรนารี
ปีการศึกษา 2559

LIFETIME ESTIMATION OF STEEL TUBING BY CORROSION ANALYSIS FOR PETROLEUM

Suranaree University of Technology has approved this thesis submitted in partial fulfillment of the requirements for a Master's Degree.

Thesis Examining Committee

_____

(Prof. Dr. Kittitep Fuenkajorn)

Chairperson

_____

(Asst. Prof. Dr. Akkhapun Wannakomol)

Member (Thesis Advisor)

_____

(Assoc. Prof. Kriangkrai Trisarn)

Member

_____ _____

(Prof. Dr. Sukit Limpijumnong) (Assoc. Prof. Flt. Lt. Dr. Kontorn Chamniprasart)

Vice Rector for Academic Affairs and Innovation

Dean of Institute of Engineering

อธิวัฒน์ เกษสุขมาโนช : การประเมินอายุการใช้งานของท่อเหล็กโดยการวิเคราะห์การกัดกร่อนสำหรับอุตสาหกรรมปิโตรเลียม (LIFETIME ESTIMATION OF STEEL TUBING BY CORROSION ANALYSIS FOR PETROLEUM) อาจารย์ที่ปรึกษา : ผู้ช่วยศาสตราจารย์ ดร.อัฆพรรค์ วรรณโกมล, 115 หน้า.

การวิจัยนี้มีวัตถุประสงค์หลักเพื่อการศึกษาอัตราการกัดกร่อนและ คาดการณ์อายุการใช้งานของท่อผลิตน้ำมันเกรด L80-13Cr และ K55 ตามมาตรฐาน API 5CT ซึ่งถูกใช้อย่างแพร่หลายในอุตสาหกรรมการผลิตปิโตรเลียม การทดสอบได้ใช้หลักการทางไฟฟ้าเคมีต่อตัวอย่างที่มีลักษณะพื้นผิวหยาบแตกต่างกันโดยใช้น้ำจากแหล่งกักเก็บที่ได้จากแหล่งกักเก็บที่ได้จากแหล่งน้ำมันพิษณุโลกมาเป็นของเหลวที่ใช้ในการทดสอบที่ใช้ทดสอบการกัดกร่อน การศึกษาครั้งนี้ยังทำการทดสอบการสึกหรอจากทรายร่วมด้วย ผลที่ได้จากการทดลองพบว่าอัตราการกัดกร่อนของท่อผลิตเหล็กเกรด L80-13Cr ที่ได้ผ่านการเตรียมพื้นผิวด้วยกระดาษทรายเบอร์ 1200 และ 600 นั้นมีค่าเป็น 0.0138 และ 0.0169 มิลลิเมตรต่อปี ในขณะที่ของท่อเหล็กเกรด K55 นั้นมีค่าเป็น 0.0376 และ 0.0465 มิลลิเมตรต่อปี ตามลำดับ เมื่อได้พิจารณาถึงถึงอิทธิพลของความหยาบของผิวท่อผลิตต่อความต้านทานการกัดกร่อนพบว่าอัตราการกัดกร่อนที่เกิดขึ้นบนผิวที่ถูกเตรียมด้วยกระดาษทรายเบอร์ 1200 นั้นมีค่าน้อยกว่าที่เกิดขึ้นบนพื้นผิวที่ถูกเตรียมด้วยกระดาษทรายเบอร์ 600 ผลที่ได้จากการทดสอบการสึกหรอโดยทรายแสดงให้เห็นว่าการสูญเสียน้ำหนักของท่อผลิตเกรด K55 นั้นมีค่าเกือบเป็นสองเท่าของท่อเกรด L80-13Cr ด้วยเหตุนี้ค่าอัตราการกัดกร่อนที่คำนวณได้นี้สามารถนำมาใช้ในการคาดการณ์อายุการใช้งานของท่อผลิตตามเกณฑ์มาตรฐาน API 5CT ได้เป็น 58.70 และ 47.93 ปี สำหรับท่อเกรด L80-13Cr ที่ผ่านการเตรียมพื้นผิวด้วยกระดาษทรายเบอร์ 1200 และ 600 และเป็น 21.54 ปี และ 17.42 ปี สำหรับท่อเกรด K55 ที่ผ่านการเตรียมพื้นผิวด้วยกระดาษทรายเบอร์ 1200 และ 600 ตามลำดับ

สาขาวิชา <u>เทคโนโลยีธรณี</u> ลายมือชื่อนักศึกษา_____

ปีการศึกษา 2559 ลายมือชื่ออาจารย์ที่ปรึกษา_____

ATIWAT KETSUKMANOTE : LIFETIME ESTIMATION OF STEEL TUBING BY CORROSION ANALYSIS FOR PETROLEUM. THESIS ADVISOR : ASST. PROF. AKKHAPUN WANNAKOMOL, Ph.D., 115 PP.

EROSION-WARE/ CORROSION RATE/ ELECTROCHEMICAL/ ESTIMATE LIFETIME OF TUBE/ PETROLEUM PRODUCTION

The main objective of this research is to study the corrosion rate and to estimate lifetime of steel tubing grade L80-13Cr and K55 according to API 5CT standard which are widely used in petroleum production industry. The test had been conducted based on electrochemical method to the different surface roughness samples by using reservoir water of Phitsanulok Oil Field as corrosion solution. This study also conducted the wear tests by sand. Results from experiments showed that the corrosion rate of steel tubing grade L80-13Cr having surface prepared with sandpaper 1200 and 600 grit number were 0.0138 and 0.0169 mm/year, while those of steel tubing grade K55 were 0.0376 and 0.0465 mm/year, respectively. When considered the effect of tubing surface roughness to the corrosion resistant, it was found that the corrosion rate taken place on sandpaper 1200 grit number surface preparing was less than those of the sandpaper 600 grit number. Results from wear test by sand indicated that the weight-less of tubing grade K55 was almost two-times of tubing grade L80-13Cr. Consequently, the calculated corrosion rate could be used for the lifetime estimation of tubing according to the API 5CT standard as 58.70 and 47.93 year for the tubing grade L80-13Cr having surface preparing by sandpaper 1200

and 600 grit number, and 21.54 and 17.42 year for the tubing grade K55 having surface preparing by sandpaper 1200 and 600 grit number respectively.

School of Geotechnology

Academic Year 2016

Student's Signature_____

Advisor's Signature_____

ACKNOWLEDGEMENTS

First I would like to thank Assistant Professor Dr. Akkhapun Wannakomol and the Institute of Geotechnology and Metallurgical engineering for providing me the tools and advice to conduct my research and the opportunity to do so.

The special appreciation is also extending to Assoc. Prof. Dr. Pornwasa Wongpanya, Assoc.Prof. Kriangkrai Trisarn, Dr. Bantita Terakulsatit and Dr. Jongkol Srithorn for knowledge and helpful suggestion to steer my research to the right path. The authors wish to special thanks to Mr. Natthaphong Konkhunthot and Miss. Thipusa Wongpinij who teach me about potentiostat analysis. And I would like to thank Dr. Boonarong Arsairai, Mr. Sakchai Glumglomjit and Miss Pimabsorn Ruxnark for providing me with his specialized support. I thank all of the students for helping in laboratory.

I thank my mother and sister for having faith with me and listening to all of my wild ideas while continually to work harder. I thank Mr. Makara Laigranok and Mr Theeradech Thongsumrit for being there as great friends and helping me get over the research. There are truly too many people to list whom. I owe thanks; so, a thank you goes out to them as well.

Finally, I would like to thank all my friends and seniors who have patiently extended all sorts of help for accomplishing this undertaking during graduate studies at Suranaree University of Technology.

Atiwat Ketsukmanote

TABLE OF CONTENTS

Page

TABLE OF CONTENTS (Continued)

Page

TABLE OF CONTENTS (Continued)

Page

TABLE OF CONTENTS (Continued)

Page

LIST OF TABLES

Table **Page**

TABLE OF CONTENTS (Continued)

Page

LIST OF TABLES (Continued)

Table **Page**

LIST OF FIGURES

Figure **Page**

LIST OF FIGURES (Continued)

Figure **Page**

LIST OF FIGURES (Continued)

Figure **Page**

LIST OF FIGURES (Continued)

Figure **Page**

SYMBOLS AND ABBREVIATIONS

ROMAN ABBREVIATIONS:

A	=	Ampere
Ag	=	Silver
AgCl	=	Silver Chloride
AISI	=	American Iron and Steel Institute
API	=	American Petroleum Institute
ASME	=	American Society of Mechanical Engineers
ASTM	=	American Society of Testing and Materials
CE	=	Counter Electrode
cm^2	=	Square centimeter
cm^3	=	Cubic centimeter
CO_2	=	Carbon dioxide
Cr	=	Chromium
CR	=	Corrosion Rate
CRAs	=	Corrosion Resistant alloys
E.W	=	Equivalent weight
Ecorr	=	Potential of corrosion
EDS	=	Energy Dispersive X-ray Spectroscopy
F	=	Degree Fahrenheit
Fe_2O_3	=	Ferrous Oxide
FeS	=	Iron Sulphide

SYMBOLS AND ABBREVIATIONS (Continued)

ROMAN ABBREVIATIONS:

g	=	gram
H_2O	=	Water
H_2S	=	Hydrogen sulphide
Icorr	=	Current density of corrosion
KCl	=	Potassium Chloride
Mo	=	molybdenum
Ni	=	Nikel
OM	=	Optical Microscope
pH	=	A numeric scale used to specify the acidity or basicity
RE	=	Reference Electrode
SEM	=	Scanning Electron Microscopy
SiC	=	Silicon carbide
WE	=	Work Electrode

GREEK ABBREVIATIONS:

μ	=	Micrometer
ρ	=	Density

CHAPTER I

INTRODUCTION

1.1 Background and rationale

Pipeline and other oilfield equipment frequently operate at high fluid pressures, while proper equipment design, materials selection, and corrosion control can result in monetary savings, a perhaps more important reason for corrosion control is safety. A U.S. government report estimate the cost of corrosion in upstream operation and pipeline was $1372 billion per year with the largest expenses associated with pipelines followed by down hole tubing and increasing capital expenditures. The most important opportunity for savings is the prevention of failures that lead to lost production. Therefore, the emphasis on erosion corrosion rate analysis is needed for the pipeline lifetime estimating.

1.2 Research objectives

The specific objectives of this study can be defined as follows:

1) To study the corrosion rate (CR) of two grade tubing; L80-13Cr and K55, by electrochemical corrosion potentiostat method at different surface roughness.

2) To study the erosion-wear characteristics of tubing grade L80-13Cr and K55 by sand.

1.3 Scope and Limitations of the Study

1) The materials for corrosion testing is K55 and L80-13Cr (API 5CT).

2) Corrosion testing was conducted based on electrochemical (potentiostat) method to study the behavior of wet corrosion caused by reservoir water which was separated from crude oil of Phitsanulok oil field, PH 6-7, under room temperature and atmospheric pressure.

1.4 Research methodology

This study was conducted following the step as depicted in Figure 1.1, including 1) Literature reviewed, 2) Design and select materials and solution, 3) Sample preparation and analyze in physical and chemical composition, 4) Corrosion by electrochemical method in laboratory and wear testing, 5) Results analytical and comparisons, 6) Results of the experiment conclusions and discussion, and 7) Thesis and report writing, respectively.

1.5 Thesis contents

Chapter I introduces the thesis by briefly describing the background and rationale of the study, research objectives, scope and limitations of the study and methodology. Chapter II summarizes the results of the literature review. Chapter III describes the materials, equipment for samples preparation, chemical, corrosion testing and surface analysis. Chapter IV describes the results from the laboratory experiments, including corrosion testing, SEM & EDS analysis. Chapter V discusses

and concludes the research results and provides recommendations for future research studies, respectively

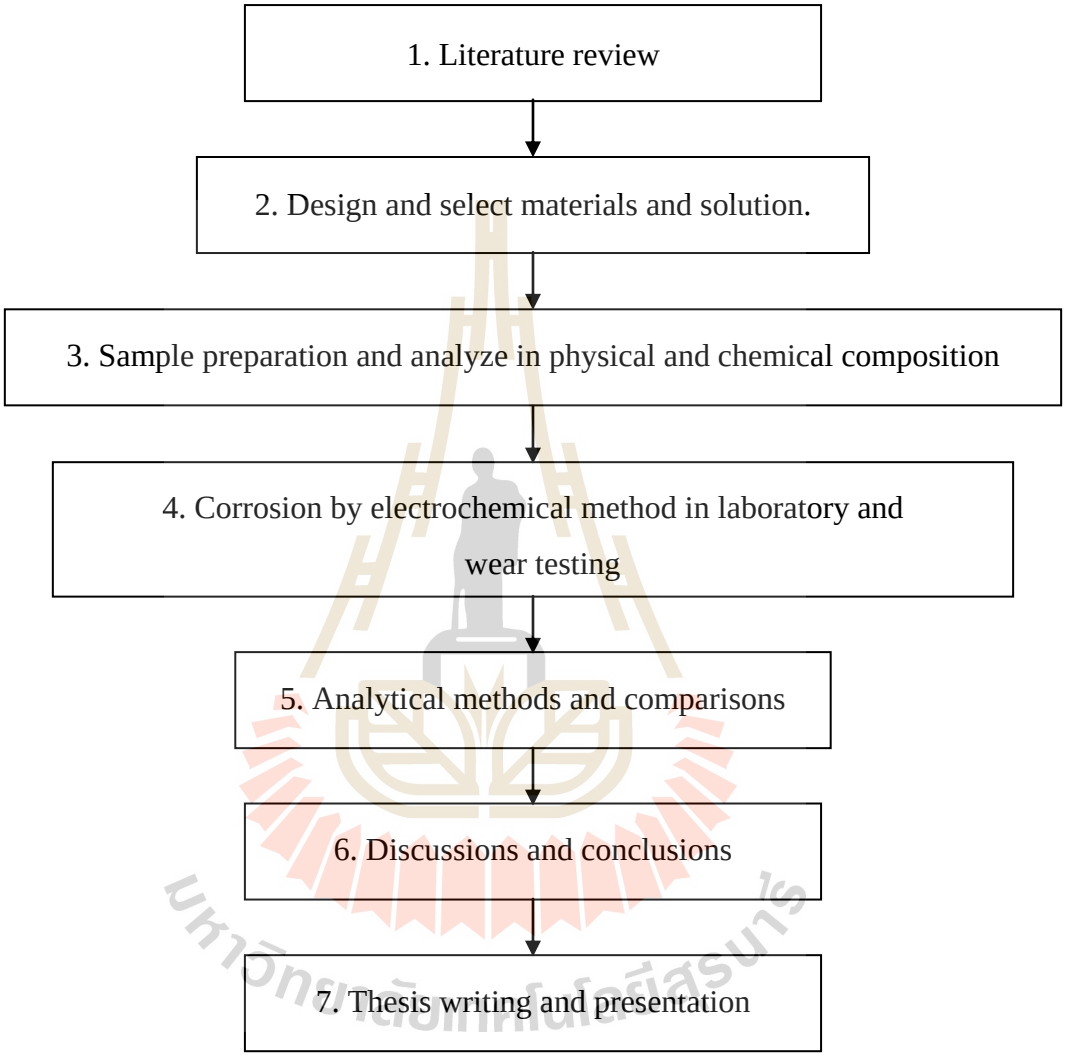

Figure 1.1 Research plan.

CHAPTER II

LITERATURE REVIEW

2.1 Introduction

The American Petroleum Institute (API) divides the petroleum industry into the following categories:

1) Upstream

2) Downstream

3) Pipelines

Kane (2006) suggests that other organizations use terms like production, pipelining, transportation, and refining. This book will discuss upstream operations, with an emphasis on production, and pipelines, which are closely tied to upstream operations. Many pipelines could also be termed gathering lines or flow lines, and the technologies involved in materials selection and corrosion control are similar for all three categories of equipment. Until the 1980s, metals used in upstream production operations were primarily carbon steels. Developments of deep, hot gas wells in the 1980s led to the use of corrosion-resistant alloys (CRAs), and this trend continues as the industry becomes involved in deeper and more aggressive environments. Nonetheless, the most used metal in oil and gas production is carbon steel or low alloy steel, and nonmetallic materials are used much less than metals. Increased emphasis on reliability also contributes to the use of newer or more corrosion-resistant materials. Many oil fields that were designed with anticipated operating lives

of 20-30 years are still economically viable after more than 50 years. This life extension of oil fields is the result of increases in the market value of petroleum products and the development of enhanced recovery techniques that make possible the recovery of larger fractions of the hydrocarbons in down hole formations. Unfortunately, this tendency to prolong the life of oil fields creates corrosion and reliability problems in older oil fields when reductions in production and return on investment cause management to become reluctant to spend additional resources on maintenance and inspection. These trends have all led to an industry that tends to design for much longer production lives and tries to use more reliable designs and materials. The previous tendency to rely on maintenance is being replaced by the trend to design more robust and reliable systems instead of relying on inspection and maintenance. The reduction in available trained labor for maintenance also drives this trend.

Heidersbach (2011) suggests that pipeline and other oilfield equipment frequently operate at high fluid pressures, while proper equipment design, materials selection, and corrosion control can result in monetary savings, a perhaps more important reason for corrosion control is safety. A U.S. government report estimate the cost of corrosion in upstream operation and pipeline was $1372 billion per year with the largest expenses associated with pipelines followed by down hole tubing and increasing capital expenditures. The most important opportunity for savings is the prevention of failures that lead to lost production. Therefore, the emphasis on corrosion rate analysis is needed for the pipeline lifetime estimating.

Papadakis (1999) also supports that oil and gas distribution via pipeline requires high level of safety and trust aiming at the reduction of approximately 40%

of the world wide pipeline network has reached its project life (estimated in 20 years) and efforts have been continually applied to further extend its residual life. The structural integrity evaluation of pipelines is an important tool to minimize the risks of leakage and its impact on the environment, enhancing the vital importance of the study of defect (crack and corrosion pits) on the material's integrity. According to the U.S. environmental Protection Agency, the number of oil spills has been reduced to less than 1% of the total volume handled each year (250 billion gallons of oil and petroleum products), meaning that over 2.5 billion gallons of oil and petroleum are still spilled every year only in the U.S. Accidents can happen during the oil production, distribution, storage and consumption process and it is very important to possess a detailed contingency plan (containment and recovery actions) to reduce the harmful effects of the oil spill.

Tawancy et al. (2013) point out up to now pipeline in perhaps the most economical and efficient means of large scale fluid transportation for crude oil and natural gas. Pipeline is commonly made of carbon steel due to some reason, i.e. carbon steel has good mechanical properties, low cost and wider availability despite their corrosion resistance is relatively low. Rodriguez et al. (2007) and Palmer and King (2004) conclude that normally, as oil and ages, the production of oil starts to decline whereas water and gas flow rate tend to increase. The presence of high corrosive agents such as CO_2, H_2S and chlorine compounds which are dissolved in the fluid can accelerate corrosion process inside the pipeline. Therefore, the impact of changes in fluid composition on a pipeline should be anticipated during maintenance program. Recently, oil leaks have been reported to occur at a horizontal crude oil subsea pipeline after 27 years in service. Ilman and Kusmono (2014) also support that

during operation, crude oil was pumped from subsea wells into the horizontal pipeline. The crude oil then flowed out the pipeline directly into a long radius elbow section which turned the crude oil flow vertically allowing the flow to pass through a riser for further processing in platform.

Shreir (1979) points out that although carbon steels can develop a passive layer of iron oxide, ingress of aggressive environment such as chlorides can lead to breakdown of the passive layer accelerating the corrosion of unprotected surface ultimately leading to the formation of hydrated iron oxide (rust): Fe_2O_3 H_2O. This is because complete removal of water from oil is rather difficult and therefore, it can act as an electrolyte as well as a hydrolyzing agent for chloride phases leading to formation of acidic environment, which accelerate the corrosion rate. Tawancy et al. (2013) support that water can mix with dirt falling out of the oil to form sludge at the inner surface of the pipe, which breads bacteria acting as source of sulfur enhancing corrosion attack. Such problems can be encountered in sections of pipeline where the flow of oil is not fast enough to maintain water in suspended state. Therefore, oil and gas pipeline made of carbon steels can be susceptible to internal localized corrosion.

Bellarby (2009) suggests that the main forms of corrosion found with completions and the associated metallurgies designed to prevent corrosion and limit erosion. The section also covers some of the elastomers and plastics that form seals with in completion components. Finally, various coatings and linings are covered, these coatings being designed to prevent corrosion whilst still allowing the use of less expensive metals.

In common with the analysis of many aspects of production chemistry, material selection is a highly specialized area. Most major oil and gas companies and

the service companies employ specialists to advice on appropriate materials for down hole use. Independent consultants are also available in some areas. This section is designed to give an overview of the issues rather than a definitive guide to material selection. It is therefore recommended that materials and corrosion experts be consulted when available.

Before starting to analyze corrosion and material selection, it is worthwhile considering the service conditions for the completion. Some of the different environments (Figure 2.1).

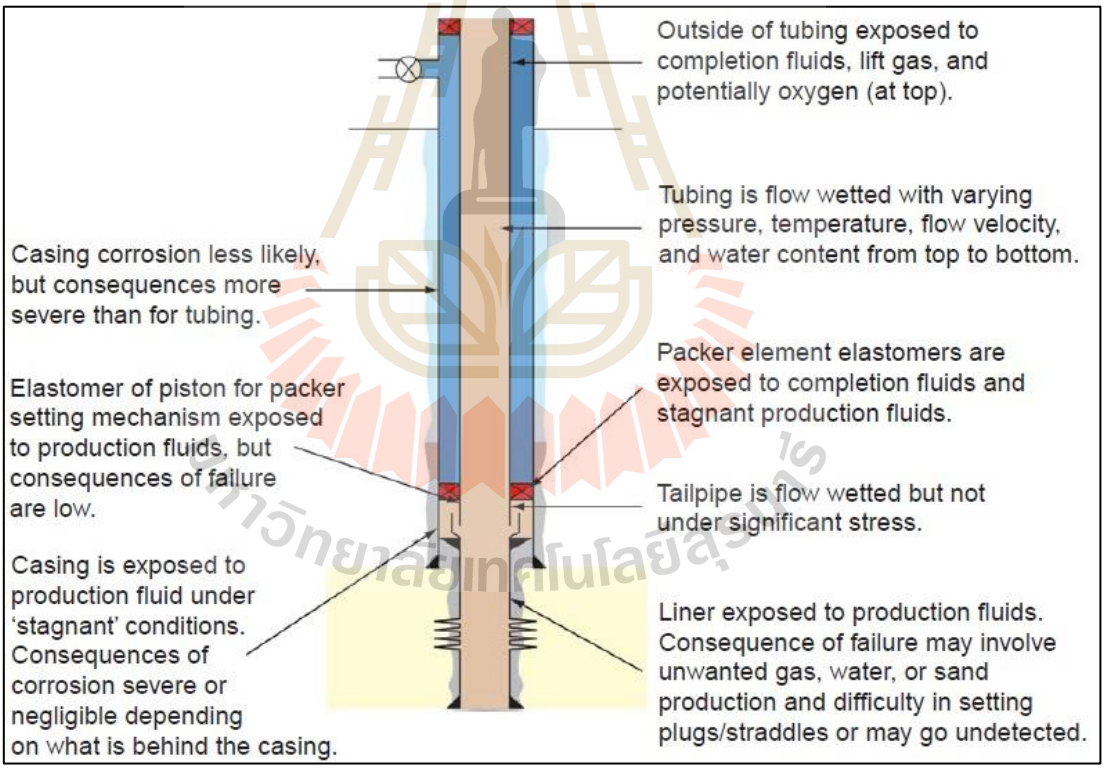

Figure 2.1 Materials selection environments (after Bellarby, 2009)

All forms of corrosion create corrosion products that have their own consequences such as iron scales. The consequences of corrosion also depend on the

life of the completion, the cost of deferred production caused by a well being shut in and the predictability of the failure.

2.2 Materials

Bellarby (2009) suggests that all completion components (wellhead, tree, packer, etc.) are metallic alloys, and the vast majority of tubing is metal with plastic pipe available for low-pressure applications. Almost all the metal used is some form of steel, with a niche application of titanium. Some completion equipment will incorporate components made from titanium, brass, copper, zinc, nickel, etc. and even gold; however, the structural components will again normally be steel.

2.2.1 Low-alloy steel

Bellarby (2009) suggests that steel is an alloy of iron and carbon. The amount of carbon in steel is less than 2.5 wt%, typically around 0.3 wt%. Other elements can be added to improve corrosion or strength properties or to aid in manufacturing. These alloying elements can be present up to 5% by weight in a low-alloy steel (above 5%, they are called alloy steels).

Clark and Varney (1952) indicate that iron is significantly cheaper than other metals, so the starting point for material selection is a low-alloy steel. The mixture of iron and carbon can form different phases (different crystalline structures) depending on the relative concentration of iron and carbon and the temperature (Figure 2.2).

Bhavsar and Montani (1998) point out that different designations are used for completion components compared with the API standards for low-alloy and L80-13Cr tubing (API 5CT, 2005). This problem is evident when specifying the

metallurgy for completion accessories to match a tubing selection. The low-alloy tubing can be specified by API 5CT, for example L80 pipe, but not the completion component unless it is manufactured from tubing. Most completion components are manufactured from bar stock. That is a solid bar of metal manufactured under standards from the AISI (American Iron and Steel Institute), the ASTM (American Society of Testing and Materials), or the ASME (American Society of Mechanical Engineers).

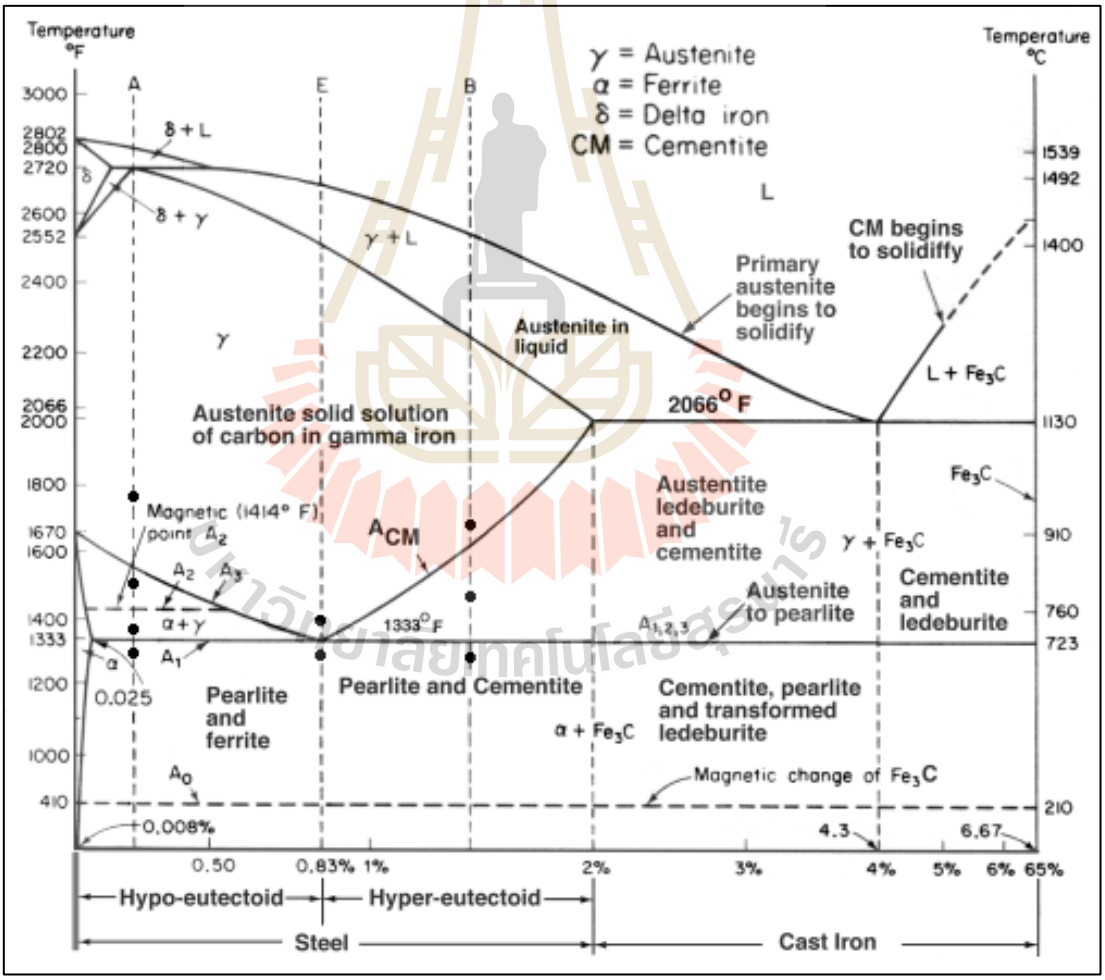

Figure 2.2 Fe-Fe3C Phase Diagram (after Pollack, 1988).

The previous discussion of the phases above 1333F might seem irrelevant to oilfield metallurgy as temperatures are not this high under down hole conditions. However, the structure of pearlite and ferrite is a direct result of cooling from above these high temperatures. The microscopic structure can be directly related to physical properties and corrosion resistance. The rate of cooling also has a marked effect on crystallization structure, and if cooling is quick enough, it can freeze in phases that would otherwise transform at the lower temperatures.

2.2.2 Heat treatment

Bellarby (2009) suggests that by varying the cooling rate of steel the structure of the metal is changed. By increasing the cooling rate, the grain sizes will reduce. This effect is common to all crystalline solidification processes from the formation of snow to the cooling of magma. Metals with smaller grain sizes are not only generally stronger (higher grade) but also more brittle (less ductile). If the cooling rate for low-alloy steels is increased further, instead of the laminar pearlite, a non-laminar form of cementite and ferrite is formed.

2.2.3 Alloy steels

Bellarby (2009) suggests that metals and other elements other than iron in concentrations above 5% define alloy steels. These are sometimes called corrosion-resistant alloys (CRAs). The additional elements and their purposes are:

1) Chromium improves corrosion resistance, particularly in the presence of carbon dioxide. Chromium also improves strength under high temperatures.

2) Nickel improves the toughness and provides corrosion resistance in conjunction with chromium, especially in the presence of hydrogen sulphide. Nickel is an austenite stabilizer.

3) Molybdenum and tungsten increase high temperature strength and make it easier to harden the metal and maintain hardness during heat treatments (good hardenability). They also improve an alloy's resistance to forms of localized corrosion (pitting).

4) Manganese ties up and prevents free sulphur and also increases hardenability.

5) Titanium strengthens the steel.

6) Silicon and aluminium tie up oxygen. Silicon can also be used to increase strength in certain heat-treated steels.

7) Niobium (also called columbium) and vanadium are added to improve hardening and increase strength.

8) Nitrogen is used as a strengthener in very low concentrations.

The API recognize the alloy L80-13Cr, that is similar to L80 carbon steel but with 13% chromium (and effectively no nickel or molybdenum). The additional chromium produces a martensitic structure. L80-13Cr tubing is common with the majority of offshore wells containing L80-13Cr or better tubing. The approximate AISI equivalent of L80-13Cr is 420 mod, although ASTM F6NM may be superior (and more expensive). The designations for some common stainless steel alloys are shown in Table 2.1 (Bellarby, 2009)

Table 2.1 Stainless steel alloys commonly used down hole (after Bellarby, 2009)

Designation	Structure	Carbon(%)	Chromium(%)	Nikel(%)	Molybdenum(%)
AISI 304	Austenitic	0.08	18-20	8-10	-
AISI 316	Austenitic	0.08	10-14	10-14	2-3
AISI 316L	Austenitic	0.08	10-14	10-14	2-3
AISI 410	Martensitic	0.15	-	-	-
AISI 420	Martensitic	0.15 min	-	-	-
AISI 420 mod	Martensitic	0.15-0.22	-	-	0.5
ASTM F6NM	Martensitic	0.05	3.5-4.5	3.5-4.5	0-5

2.3 Corrosion in oilfield

2.3.1 Down hole corrosion

Corrosion requires three conditions:

1) Metal

2) Water or electrolyte (saline solution)

3) A corrode (something to create the corrosion such as oxygen, acid or H_2S)

Gair and Moulds (1988) suggest that corrosion also comprises two reactions (Figure 2.3). Note that there are variations for both the anodic and the cathodic reactions, but the requirement for two reactions remains. If either reaction is stopped then corrosion ceases. The anode and cathode in Figure 2.3 are both on the surface of the metal. The anode emits electrons, and the cathode receives them. It is possible to create an electro potential (voltage difference) on the surface of the metal

by differences in the grains (crystals) caused by variations in composition, roughness or surface film within the metal structure.

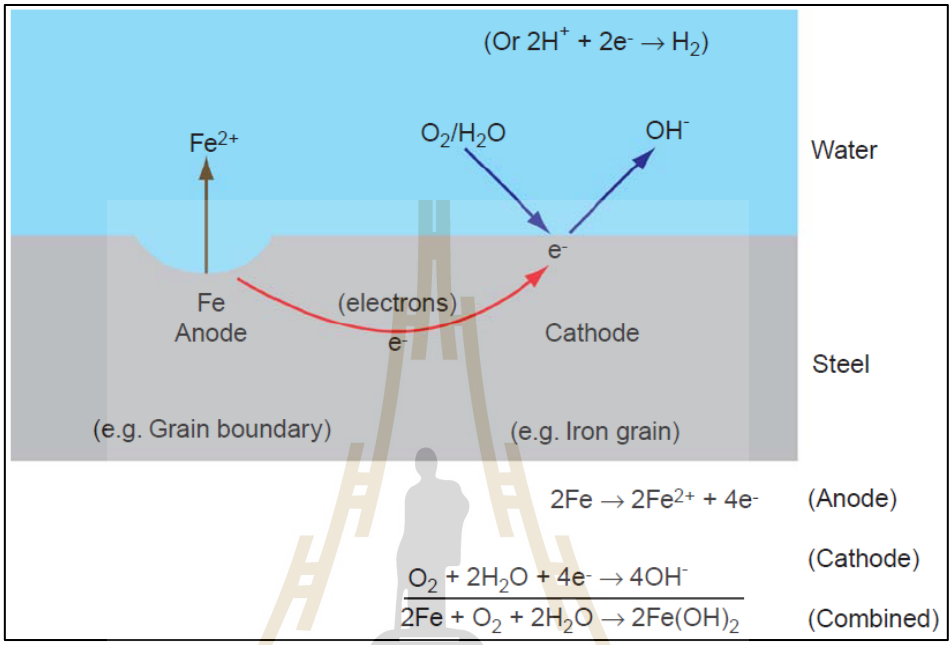

Figure 2.3 Corrosion reactions (after Bellarby, 2009)

2.3.2 Carbon dioxide corrosion

Waard et al. (1991) suggests that carbon dioxide or sweet corrosion attacks metals due to the acidic nature of dissolved carbon dioxide (carbonic acid). The acidity (pH) of the solution will depend on the partial pressure of the carbon dioxide. This is discussed further can be used to predict the down hole pH as a function of partial pressure, temperature, salinity and the bicarbonate ion concentration. Salinity, especially bicarbonate, acts to buffer the pH demonstrates the huge variations in bicarbonate concentrations and salinity in formation waters. Fresh water, for example water of condensation in a gas well, will generally have a lower pH than water from a saline aquifer. For the same pH, the weak carbonic acid is more

corrosive than strong acids (e.g. hydrochloric acid), as carbonic acid can rapidly dissociate at the metal surface to provide a steady supply of the hydrogen ions needed at the cathode (Figure 2.3). One of the earliest attempts to quantify the effect of pH caused by carbonic acid on corrosion rates was by Waard et al. (1991). The equation they developed almost always predicts excessive corrosion rates for carbon steel under down hole conditions. For example at a down hole temperature of 2401F, a pressure of 1000 psia and 1% mol of CO_2, the corrosion rate predicted is around 20 mm/year (3/4 in./year). These corrosion rates are unrealistically high except in a fresh water environment at very high flow rates. In addition to the buffering effect of dissolved solids, semi-protective scales or films have a significant role in reducing corrosion rates. The formation and removal of these scales is temperature dependent. The highest corrosion rate for carbon steel is at around 2001F. The role of temperature on carbonic acid corrosion (Figure 2.4).

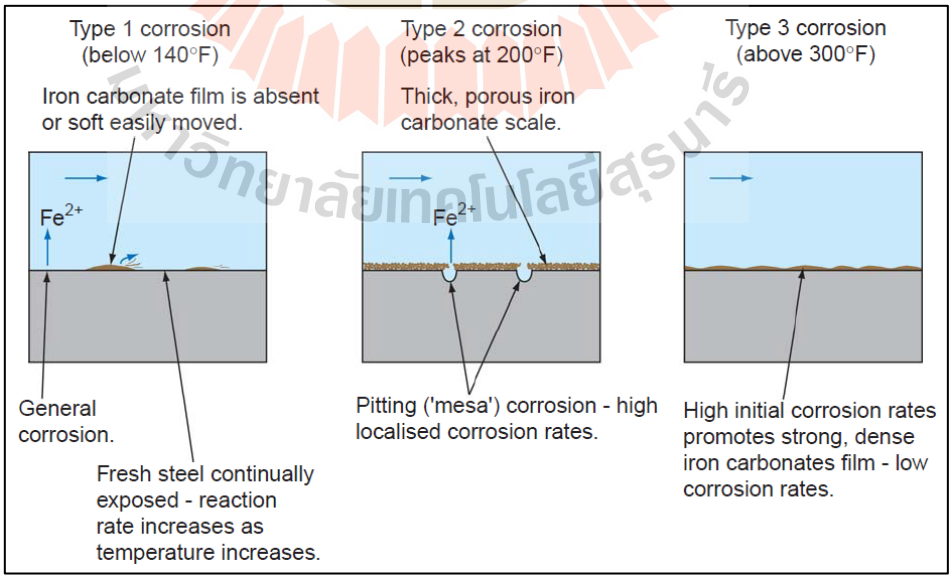

Figure 2.4 Corrosion of carbon steel by carbon dioxide (after Bellarby, 2009)

Chen et al. (2005) indicate that the continuous higher temperatures across a reservoir section combined with the reduced consequences can sometimes be used to justify a carbon steel liner in a well with L80-13Cr tubing. Adding chromium to the steel promotes the strength and adherence of the corrosion product to the steel surface through the presence of chromium oxides and reduces the film conductivity. Even a small amount of chromium can have a significant improvement at low temperatures. At higher temperatures, the effect is reduced and chromium steels may even corrode at higher rates than carbon steel. During the 1980s and 1990s, 9Cr material was used extensively. However, in recent years, the availability of 13Cr and the small cost increment over 9Cr have reduced the use of 9Cr tubing. For low to moderate temperature environments (less than 3001F) containing carbon dioxide, little or no H_2S and low chlorides, 13Cr has become the standard tubing metallurgy and L80-13Cr is included as an API specification. The semi-protective film that protects 13Cr steels from continuous corrosion can be removed by high velocities or erosive solids. Figure 2.5 shows 13Cr steel tubing with localized corrosion. Here, corrosion has been exacerbated on the low side of the tubing by small amounts of sand production at high rates. The semi-protective film is evident as orange deposits. The pits have a diameter of around 1/4 in. A generalized corrosion rate for carbon steel and various chromium content steels (Figure 2.6). The conditions are 435 psia partial pressure of CO_2 and 5 wt% sodium chloride.

Figure 2.5 Corrodes 13Cr tubing

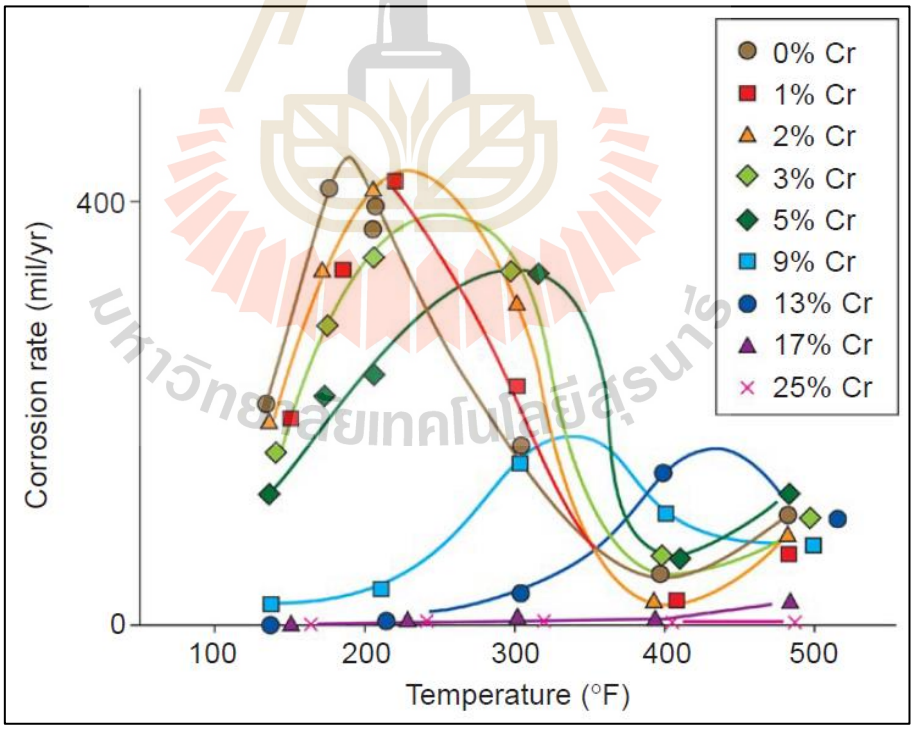

Figure 2.6 Corrosion rate as a function of chromium content (after Chen et al., 2005)

Note that at high temperatures, the carbon steel corrosion rate is reducing whilst the 13Cr corrosion rate is increasing and may exceed that of carbon steel. At high temperatures (above 3001F), the use of 13Cr tubing becomes borderline. Blackburn (1994) reports that dynamic autoclave testing for a 2000 psia bubble point, 3001F reservoir with 2.7% CO_2, 40 ppm H_2S and 12,000 ppm chlorides. The pitting test results showed high initial corrosion rates for carbon steel (80 mil/year), quickly reducing to 4.3 mil/year. 13Cr, by comparison, had low initial corrosion rates, but these increased to around 60 mil/year after 30 days. Failures of carbon steel tubing under these conditions were still observed, but primarily with high-rate wells. The modern solution of using modified 13Cr (2Mo–5Ni) was not available at that time.

Kimura et al. (2007) report that modified (2Mo–5Ni) 13Cr alloys and duplex steels provide higher-temperature carbon dioxide corrosion resistance as well as increasing resistance to hydrogen sulphide. Modified (2Mo–5Ni) 13Cr being effective in an environment containing a carbon dioxide partial pressure of 1500 psia at 3201F, 20 wt% sodium chloride, but without flow. 15Cr was acceptable to 3901F under similar conditions. In some circumstances, for example in the presence of strong acids, martensitic steels can provide corrosion resistance superior to that of duplex steels; in the duplex steels, the ferrite phase is selectively dissolved.

2.3.3 Hydrogen sulphide corrosion

Whereas carbon dioxide is considered sweet, hydrogen sulphide is regarded as a sour gas.

Bellarby (2009) indicates that hydrogen sulphide (H_2S) in produced fluids reacts with steel to form a semi-protective film of iron sulphide (FeS) in a

fashion similar to the formation of iron carbonate discussed in Section 2.3.2. Unfortunately, iron sulphide is rarely uniform and can be removed by flow, exposing fresh metal to hydrogen sulphide. The exposed site is anodic and small in area compared to the surrounding iron sulphide film. Thus, the exposed metal rapidly and preferentially corrodes, causing pitting (Figure 2.7). Fortunately, hydrogen sulphide levels in most produced fluids are low, typically tens of parts per million compared to low percentages for carbon dioxide. Sulphide-induced pitting is therefore relatively rare.

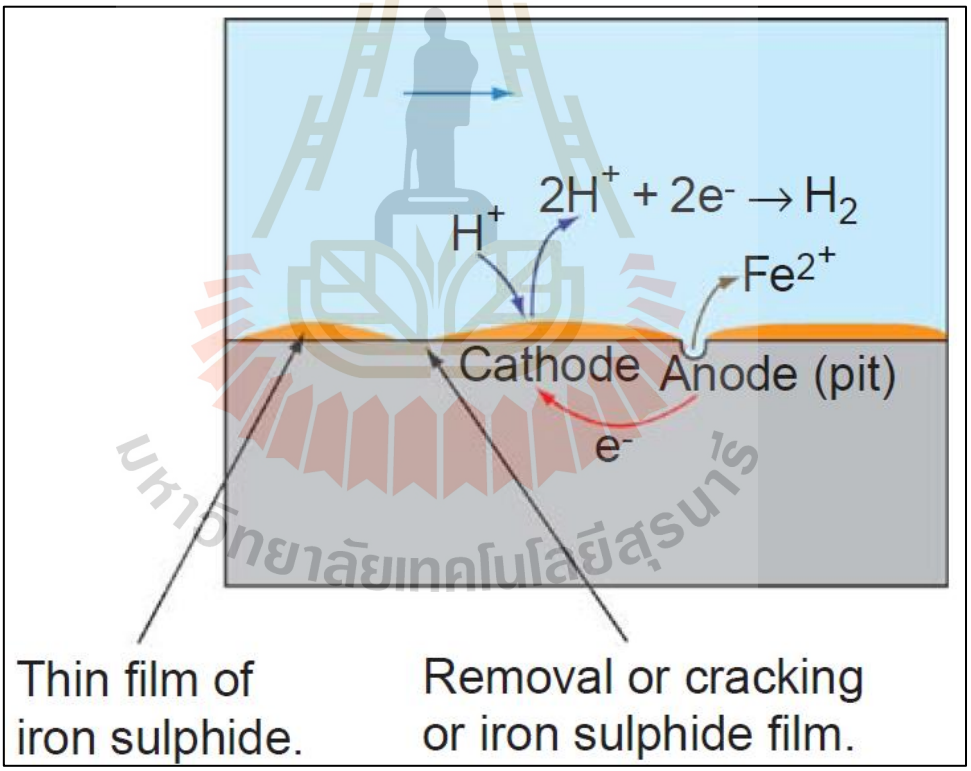

Figure 2.7 Hydrogen sulphide pitting (after Bellarby, 2009)

2.4 Erosion-wear corrosion

Heidersbach (2011) suggests that erosion corrosion is the result of a combination of an aggressive chemical environment and high fluid-surface velocities. It can be the result of fast fluid flow past a stationary object or it can result from the quick motion of an objective in a stationary fluid. Other terms include flow-enhance or flow-accelerated corrosion, which also include mechanisms not relate to erosion corrosion. These other flow-enhance corrosion subjects are discussed elsewhere in this proposal, for example, in the section on pipelines. In erosion corrosion mechanical effects predominate. Surfaces which have undergone erosion corrosion are generally fairly clean, unlike the surfaces from many other forms of corrosion. Some of Heriderbach's works and others an erosion-corrosion can be summarized as follows.

2.4.1 Mechanism

Erosion corrosion is often the result of the wearing a way of a protective scale or coating on the metal surface. Erosion corrosion is normally associated with turbulent flow because all practical piping systems require turbulent flow. Most erosion corrosion is caused by multiphase fluid flow. The flow regime map shown below in Figure 2.8 indicates the distribution of liquid (dark areas) and vapor (light areas) in vertical and horizontal flow. Slug flow has serious velocity-related problems, but none of these patterns produce erosion corrosion in straight piping in the absence of entrained solids. Where a flow pattern change, for example, at a rough pipe connection, or a wellhead, liquid droplets or gas bubbles, which can collapse and produce shock waves that spall the protective surface film, or solid particles can cause accelerated attack by removing the protective film, either a passive

film, mineral scale, or corrosion inhibitor film. These flow regime maps do not sand, corrosion products, or scale, all of which are known to accelerate erosion corrosion.

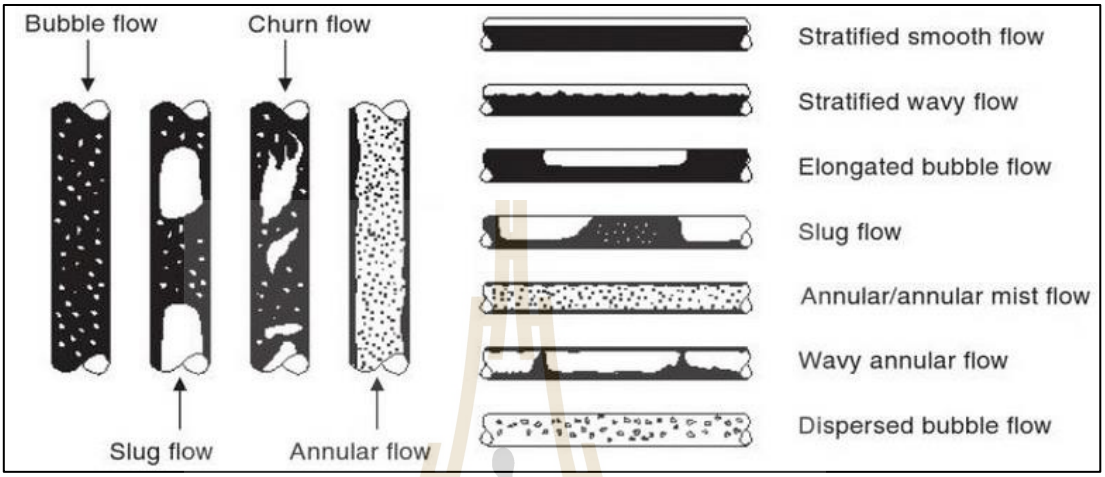

Figure 2.8 Multi fluid flow regimes in straight runs of vertical or horizontal pipeline (after Heidersbach, 2011)

2.4.2 Velocity effect

Heidersbach (2011) suggests that most metals have a critical velocity, which is the highest fluid velocity that can be tolerated before erosion corrosion will occur. For topside equipment piping, this is defined by formula in American National Standard Institute (ANSI)/American Petroleum Institute (API) Recommend Practice14E.

Solid-containing lines should have significantly reduced maximum allowable velocities, although no specific guidelines are offered.

The same recommended practice suggests a minimum velocity in two phase flow of approximately 10 ft/s (3 m/s) to minimize slugging in separation equipment. This is more important if elevation changes are involved.

The practice does not consider fluid properties such as velocity, effects of solid particles, substrate materials properties such as hardness, and geometric properties such as elbows and flow constrictions. All of these properties are known to affect erosion corrosion resistance.

2.4.3 Down hole applications

Heidersbach (2011) suggests that while the ANSI/API recommended practice is written for topside service piping systems, it has also been used for down hole production tubing and for injection wells. If the recommended maximum velocities are too conservative and operate with C-factors of 400 or greater and injection water (not multiphase fluid) velocity of up to 50 ft/s (15 m/s) for corrosion resistant alloys (CRAs).

2.4.4 Effect of different environments on maximum velocity

Heidersbach (2011) suggests that some companies have developed proprietary in-house guidelines on how to calculate maximum allowable velocities. Variable included in some of these guidelines are shown in Table 2.2.

The question of appropriate maximum velocities for down hole applications is a subject of continuing controversy and ongoing research. The subject is complicated; no consensus on this subject is likely.

Table 2.2 Erosion-corrosion variables for choosing C-factor in ANSI/API RP14E (Heidersbach, 2011)

Systems	Material Choice
Seawater	Carbon steel without inhibition
Single phase production (all liquid)	Carbon steel with inhibition
Multiphase production (oil wells or gas wells)	15Cr and modified 13Cr
Dry gas injection (no corrosion, no liquids)	Duplex Stainless steel
Methanol (no corrosion)	Super Duplex Stainless Steel
	Ni-Based CRAs

2.4.5 Cavitation

Kane (2006) suggests that the erosion corrosion that has been discussed so far has been due to moving fluid or solids impacting against a stationary metal surface. Cavitation is somewhat different, because it usually causes damage due to rapid movement of a metal surface in such a manner that a liquid, for example, in a pump, undergoes a rapid loss of pressure which causes the liquid to form vapor bubbles. This release of vapor bubbles is not harmful but if the same bubbles collapse against a metal surface, as shown in Figure 2.9, damage of the surface film(s) results in fresh metal exposures which then corrode. Cavitation pump impellers and housing can undergo rapid attack. Designing pumping system to avoid the occurrence of cavitation, normally by maintaining a positive head on the liquid, is one means avoiding this problem. Another is to hard-facing alloys on pump component.

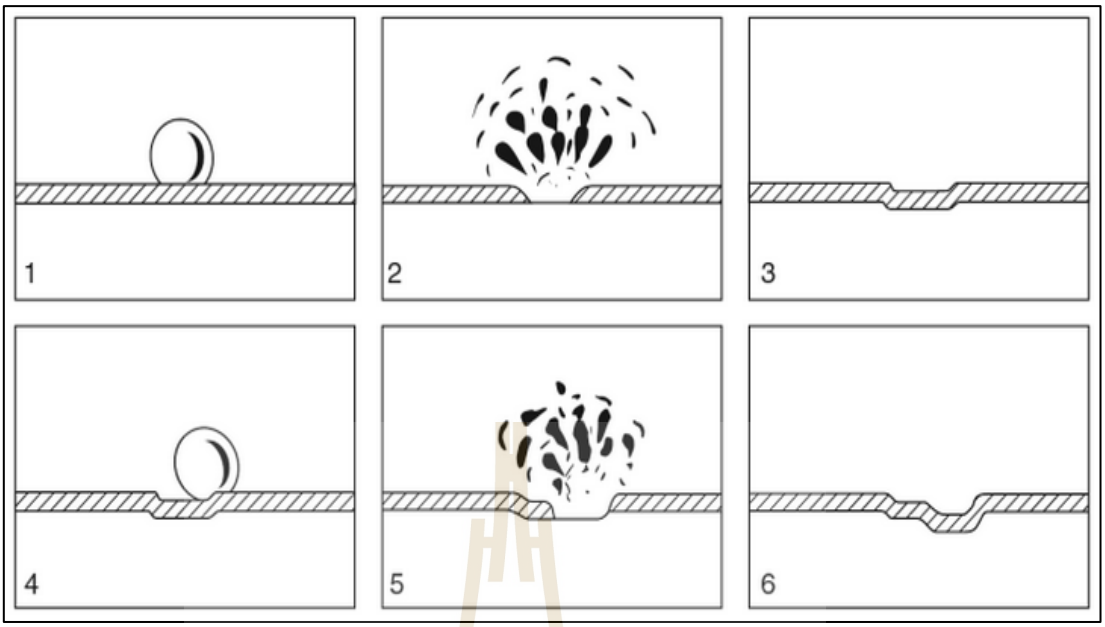

Figure 2.9 Cavitation bubble collapse and subsequence corrosion (after Kane, 2006)

2.4.6 Area of concern

Erosion corrosion is possibility whenever changes in fluid flow patterns occur, especially when they are accompanied by concurrent changes in pressure or temperature. This can be downstream of flow restrictions, where additional turbulence and phase changes have introduced, as well as at locations of local flow disruption.

2.4.7 Down hole tubing

Down hole tubing can have erosion-corrosion problems caused by localized turbulence near joints. This platform received major attention when down hole erosion was reported shortly after production started. Down hole multiphase fluid flow regimes are seldom as simple as shown in Figure 2.8. Deviations from vertical flow can often exceed 45 degrees and can sometimes approach horizontal flow. This

means that inspection tools must check in the most likely locations for damage, and asymmetrical damage of down hole tubing has been reported.

This is due to a combination of protective iron carbonate scales from the production fluid and the action of corrosion inhibitors where the scales have been breached. The corrosion inhibitor dosages may be inadequate to cover the exposed metal surface sand thee fluid velocities may be too fast and erode the inhibitor films from the exposed metal.

2.4.8 Erosion in elbows and bends in piping

The addition turbulence at sharp bends in piping causes accelerated erosion, especially when solids are entrained in the system. Liquid droplets can also impinge at piping bends and produce similar erosion patterns. Notice the localized erosion damage. It is very important to inspect in the proper locations to monitor if erosion is occurring. Placing an ultrasonic probe only a few centimeters away from the damage would miss it entirely. This problem has caused many utility systems to develop erosion modeling software to allow plant inspectors to determine where their periodic inspections should occur. The miles of piping in a typical power plant are too expensive to allow 100% inspection.

Steam injection systems in oilfield operations are even more complicated than power plant piping, and software for predicting where inspections should occur is not available. Any potential inspections are complicated, because most erosion-subject steam injection piping is covered with insulation, and the quality of steam (presence or absence of water droplets) is likely to be lower in injection systems.

One potential remedy to minimized erosion corrosion in steam piping is to increase the radius of any bends in the piping. This, of course, means increased installation costs, and space limitation, especially offshore, will often prevent this approach.

2.4.9 Control

Erosion corrosion can be controlled by the use of harder alloys (including flame-sprayed or welded hard facings) or by using a more corrosion-resistant alloy. Alterations in fluid velocity and charges in flow patterns can also reduce the effects of erosion corrosion. Chemical treatment with corrosion inhibitors many requires in the absence of erosion corrosions. This is because erosion removal of protective films may expose much higher bare metal surface areas. If solid particle erosion is involved, most corrosion inhibitors will adhere (chemisorb) to the particles as well as to bare metal.

Prediction of erosion corrosion locations and severity is limited, and there is no clear consensus on how to determine erosion thresholds. For this reason, monitoring in likely erosion locations once production has started is primary means of controlling the effects of erosion corrosion.

2.5 Tolerances on dimensions and masses of pipe

2.5.1 Wall thickness

Each length of pipe shall be measured to verify conformance with wall thickness requirements. Wall thickness measurements shall be made with a mechanical caliper, a go/no-go gauge or with a properly calibrated of appropriate accuracy.

For pipe, the wall thickness at any place shall not be less than the tabulated thickness the permissible under-tolerance specified is show in Table 2.3. (API Specification 5CT, 2005)

Table 2.3 Tolerances apply to the outside diameter and thickness of pipe (after API Specification 5CT, 2005)

Outside diameter (d_{OD})		**Thickness (t)**
Pipe diameter (mm)	**Tolerance (mm)**	**Tolerance (mm)**
< 114.3 (4 1/2 inch.)	± 0.79%	-12.5%
≥ 114.3 (4 1/2 inch.)	-0.5%, +1%	

2.5.2 Mass (weight)

The pipe manufacturer applying the markings to the pipe body shall be responsible for weighing the pipe to determine conformance with mass tolerance is shown in Table 2.4. (after API Specification 5CT, 2005)

Table 2.4 Tolerances apply to the mass (weight) of pipe (after API Specification 5CT, 2005)

Amount	**Tolerance**
Single lengths	+6.5%, -3.5%

2.6 Classification of corrosion

Corrosion has been classified in many different ways. One method divides corrosion into low-temperature and high-temperature corrosion. Another separates

corrosion into direst combination (or oxidation) and electrochemical corrosion. The preferred classification here is 1) wet corrosion and 2) dry corrosion (Figure 2.10). Corrosion of this study was set to be Fontana (1986) describes that wet corrosion. Wet corrosion occurs when a liquid is present. This usually involves aqueous solution or electrolytes and accounts for the greatest amount of corrosion by far. (Fontana, 1986)

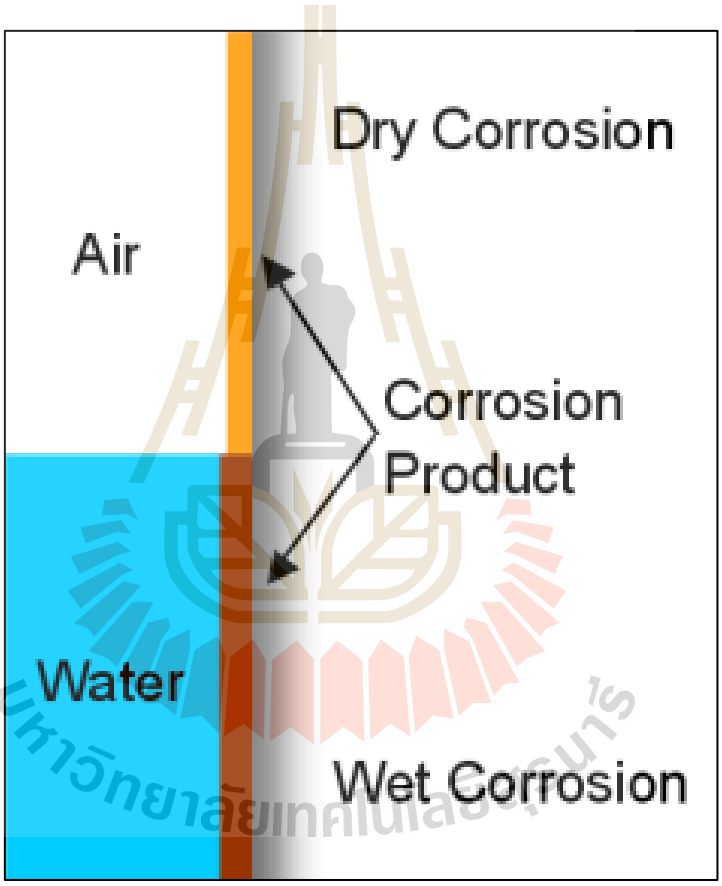

Figure 2.10 Environmental of wet and dry corrosion (after Fontana, 1986)

Fontana (1986) suggests that wet corrosion is the most common form of corrosion. It will occur if an “electrochemical cell” is produced. An electrochemical cell consists of an Anode, a Cathode, a Connection, and an Electrolyte. The anode is the metal that corrodes. It undergoes oxidation and therefore loses electrons. The

cathode can be a metal or any other conducting material. It undergoes reduction and therefore gains electrons. The reaction that occurs at the cathode is not necessarily related to the material that it is made from. The connection is necessary for the electrons to travel between the anode and cathode and can be either physical direct contact or some form of wire. An electrolyte must also be present to allow for migration of ions between the cathode and anode and participate in the formation of corrosion products (Figure 2.11).

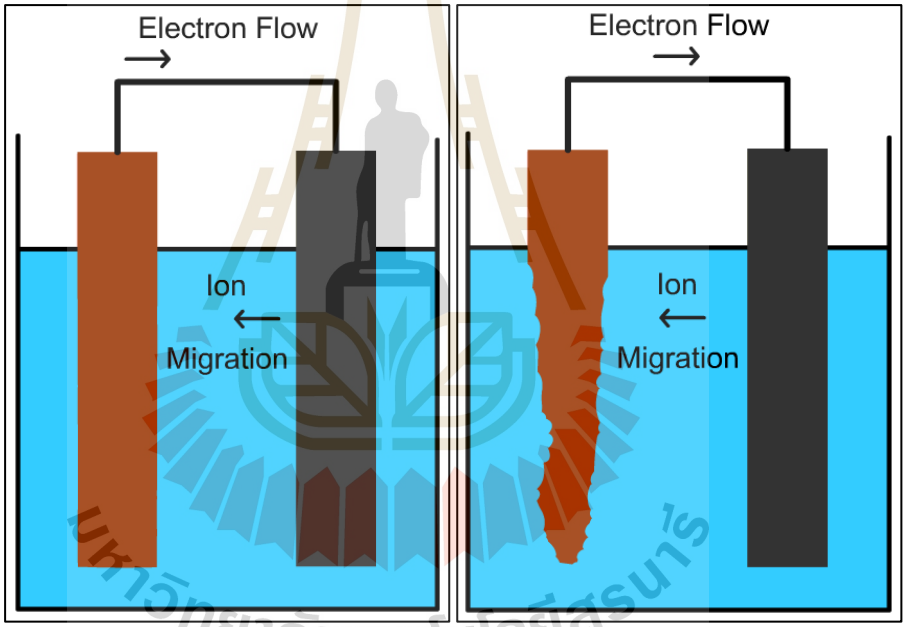

Figure 2.11 Electrochemical cell (after Fontana, 1986)

2.7 Chemistry of corrosion

Heidersbach (2011) Suggests that corrosion, the degradation of a material due to reaction with the environment, is usually, but not always, electrochemical in nature. For this reason, an understanding of basic electrochemistry is necessary to the

understanding of corrosion. More detailed descriptions of all phenomena discussed in this chapter are available in many general corrosion textbooks.

2.7.1 Electrochemical of corrosion

Most corrosion involves the oxidation of a metal which is accompanied by equivalent reduction reactions which consume the electrons associated with the corrosion reaction. The overall corrosion reactions are often referred to separately as "half-cell" reactions, but both oxidation and reduction are interrelated, and the electrical current of both anodes, where oxidation is prevalent, and cathodes, where reduction predominates, must be equal in order to conserve electrical charges in the overall system.

2.7.2 Electrochemical Reactions

A typical oxidation reaction for carbon steel would be:

$$Fe \rightarrow Fe^{+2} + 2e^{-} \quad (2.1)$$

Common reduction reactions associated with corrosion include:

Hydrogen evolution $2H^{+} + 2e \rightarrow H_2$ (2.2)

Oxygen reduction

In acid solutions $O_2 + 4H^{+} + 4e^{-} \rightarrow 2H_2O$ (2.3)

In neutral or $O_2 + 2H_2O + 4e^{-} \rightarrow 4OH^{-}$ (2.4)

Basic solutions

Metal ion reduction or deposition is also possible:

$$Fe^{+3} + e^{-} \rightarrow Fe^{+2} \quad (2.5)$$

$$Fe^{+2} + 2e^{-} \rightarrow Fe \quad (2.6)$$

The reduction reaction is usually corrosion - rate controlling because of the low concentrations of the reducible species in most environments compared with

the high concentration (essentially 100%) of the metal. As one example, the dissolved oxygen concentration in most air exposed surface waters is slightly lower than 10 ppm (parts per million). This relatively low dissolved oxygen concentration is usually much higher than the concentration of any other reducible species, and the control of air leakage into surface facilities is a primary means of controlling internal corrosion in topside equipment and piping.

More than one oxidation or reduction reaction may be occurring on a metal surface, for example, if an alloy is corroding or if an aerated acid has high levels of dissolved oxygen in addition to the hydrogen ions of the acid.

Electrochemical reactions occur at anodes, locations of net oxidation reactions, and at cathodes, locations of net reduction reactions. These anodes and cathodes can be very close, for example different metallurgical phases on a metal surface, or they can have wide separations, for example, in electrochemical cells caused by differences in environment or galvanic cells between anodes and cathodes made of different materials.

The heart of an electrochemical corrosion measurement system is the potentiostat. A potentiostat can be viewed as a box (Figure 2.12) which performs two main functions:

1) It controls the potential difference between the reference electrode (RE) and the working electrode (WE).

2) It measures the current flow between the working electrode (WE) and the counter electrode (CE). This is the i_{total} measurement referred to in the previous section.

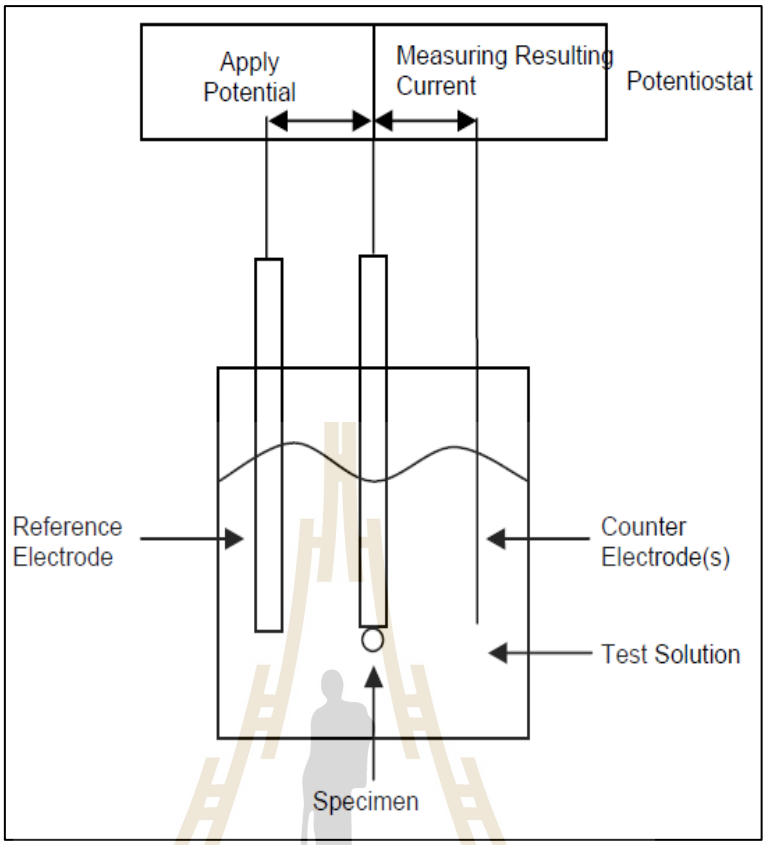

Figure 2.12 Potentiostat operation

2.8 Corrosion rate

2.8.1 Polarization curve

As stated earlier, most oilfield corrosion rates are determined by the concentration of the reducible chemicals in the environment. Figure 2.13(a) shows how the reduction of hydrogen ions determines the corrosion rate, Icorr, and the corrosion potential, Ecorr for a generic metal. For surface equipment, most corrosion rates are determined by the concentration of dissolved oxygen in whatever water is available (Figure 2.13(b)). The oxidation line showing Tafel behavior intersects the vertical (concentration limited) portion of the reduction reaction (Heidersbach, 2011).

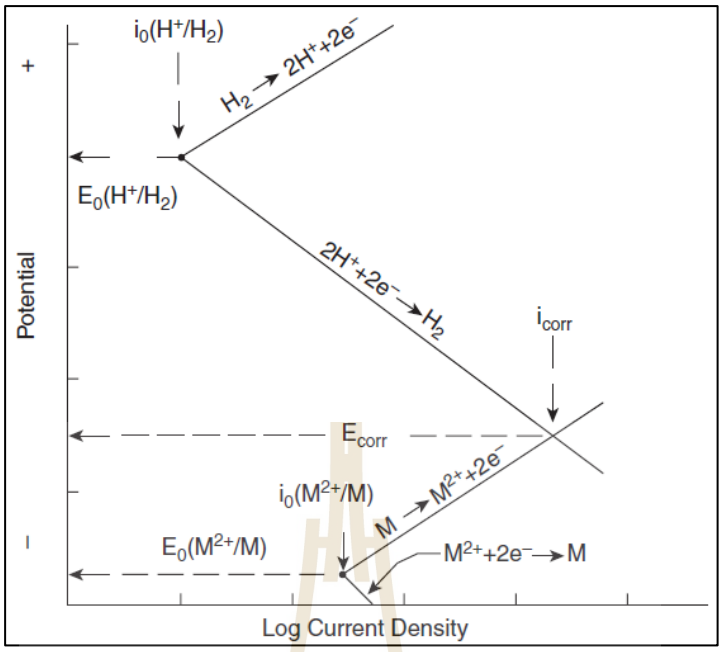

(a)

Figure 2.13 (a) Corrosion current and potential determined by the polarization of iron and the hydrogen reduction reaction (after Heidersbach, 2011)

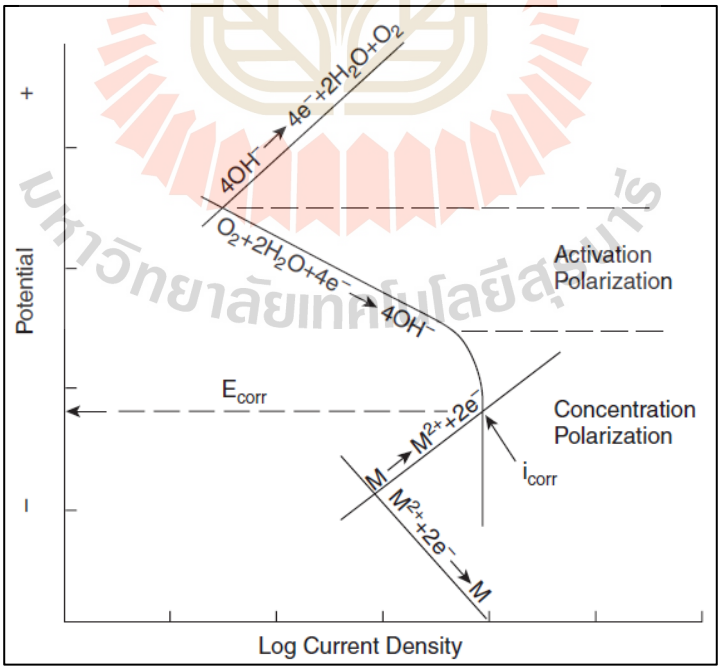

(b)

Figure 2.13 (b) Corrosion current and potential determined by the polarization of iron and the oxygen (after Heidersbach, 2011)

2.8.2 Corrosion rate expression

The simplest of these concepts to understand is depth of penetration. It can be expressed in mm/year (millimeters per year) or mpy (mils or thousandths of an inch per year). The loss of wall thickness is often used to determine remaining equipment life or safe operating pressures for piping systems, storage tanks, and so on. Table 2.5 shows a commonly used classification of relative corrosion rates. The U.S. Standard units, mpy, produce small numbers that are easy to understand, and corrosion rates in mpy are commonly used worldwide, although other expressions are also common.

Table 2.5 Relative corrosion resistance versus annual penetration rates (after Heidersbach, 2011)

Relative Corrosion Resistance	**Corrosion rate**	
	mpy	**mm/year**
Outstanding	< 1	< 0.02
Excellent	1-5	0.02-0.1
Good	5-20	0.1-0.5
Fair	20-50	0.5-1
Poor	50-200	1-5
Unacceptable	200+	5+

To calculate the corrosion rate, the corrosion current (Icorr) must be first determined. To determine the corrosion current from the Polarization Resistance plot, the Tafel constants are needed (the slopes of the anodic and cathodic linear

regions of the curve). Once Icorr is determined, the corrosion rate (in millimeter per year) can be calculated from the following equation.

$$\text{Corrosion Rate (CR)} = 0.00327 \times Icorr \times EW / \rho \quad (2.7)$$

where

E.W = equivalent weight

Icorr = area ($\mu A/cm^2$)

ρ = density (g/cm^3)

Therefore,

$$EW = 1 / N_{EQ} \quad (2.8)$$

and,

$$N_{EQ} = \Sigma[fi \times ni / Wi] \quad (2.9)$$

where

ni = The number of electrons that the loss of the elements.

fi = The proportion by mass of the elements i in the metal.

Wi = The atomic weight of the element i in the metal.

2.9 Previous works

2.9.1 Study of corrosion rate

Tawancy et al. (2013) points out that the carbon steels are commonly used as structural materials of piping systems used in these vessels because of their lower cost and wider availability despite their relatively lower corrosion resistance. Example of corrosive species in crude oil includes hydrogen sulfide, elemental sulfur,

carbon dioxide, inorganic salts including various metal chlorides such as calcium chloride, magnesium chloride, and sodium chloride.

A problem was encountered in the piping system of an oilfield separator vessel. According to design specifications, the piping system was made of SA-106 Grade C carbon steel. After an unspecified operating time, an elbow section developed a pinhole. The failed section was removed for metallurgical evaluation to determine the most probable cause of failure.

Pinhole is formed as a result of localized corrosion involving a sequential chlorination and sulfidation reactions. This is correlated with the formation of hydrochloric acid by hydrolysis of inorganic salts in the crude oil particularly calcium chloride and reactions involving hydrogen sulfide.

Ilman and Kusmono (2014) indicate that the pipeline is commonly made of carbon steels due to some reasons, i.e. Carbon steels have good mechanical properties, low cost and wider availability despite their corrosion resistance is relative low. The presence of high corrosive agents such as CO_2, H_2S and chlorine compounds which dissolved in the fluids can accelerate the corrosion process in the pipeline.

Failure of a subsea crude oil API 5L X52 steel pipeline which led to leakage has been reported to occur at a horizontal crude oil subsea pipeline after 27 years in service. During operation, crude oil was pumped from subsea wells into the horizontal pipeline. The crude oil then flowed out the pipeline directly into a long radius elbow section which turned the crude oil flow vertically, allowing the flow to pass through a riser for further processing in the platform.

Failure mechanism of the horizontal subsea pipeline due to flow-induced corrosion. According to the flow analysis as previously discussed, the flow

pattern is expected to take place in the form of stratified flow where the gas and liquid completely segregate from each other and the water layer is present at the bottom of the oil pipeline. As the crude oil flows through the elbow section, the flow must turn resulting in impacts on the regions near the bend pipeline wall. The eddy current and possibly entrainment of sand in the pipeline have a potency to destroy the protective film. Once the protective film is destroyed, the pipeline surface is exposed to water and oxidation-reduction reactions are expected to occur.

Nabhani et al. (2007) suggest that the metallurgy of pipelines, vessel, etc. in oil and gas producing systems is usually based on carbon steel. This is because carbon steel has good mechanical properties and is also relatively cost effective. However, carbon steel is strongly susceptible to corrosion attack from the dissolved gases (CO_2 and H_2S) that are present in the produced fluids.

Corrosion rate measurements were obtained using different aqueous environments such as a plain sodium chloride solution, a sodium chloride and carbon dioxide solution, and a sodium chloride and sulphuric acid solution that also contained a small amount of carbon dioxide.

The carbon contents of the steels used to play a part in the corrosion process, especially in the acidic solutions. The mechanism involved in this effect is not clear at this time, but one possibility is the setting up of an electrolytic cell in the surface of the steels exposed to the solution where the carbon contents become significant.

Migahed and Nassar (2008) suggest that the acid fracture is an oil reservoir stimulation technique for increasing well productivity. Hydrochloric acid, HCl, is used in oil and gas. The acid flow occurs in the steel tubes. In the process oil

and gas production is requires a high degree of corrosion inhibition for corrosion protection. The present study deals with the evaluation of the effectiveness of the new synthesized compound namely; 6-methyl-5-[m-nitro styryl]-3-mercapto-1,2,4-triazine as corrosion inhibitor for mild steel in 12% HCl solution at 50°C. The result has shown a very good inhibitive effect for the corrosion of mind steel in 12% HCL solution during oil well acidization process

2.9.2 Study of wear erosion

Martinez et al. (2009) suggests that the oil transporting gas lines are exposed to corrosive-erosive wear mechanisms due to fluid flow conditions in gas transportation processes. Combined parameters like fluid flow regime and chemical composition of the wall deposited products increase oil gas pipes wearing. API X52 steel grade were performed to study corrosion rate effect of inhibitors added to residual water transported with gas in pipelines. Fluid flow conditions were simulated in dynamic laboratory tests which were performed using a rotating cylinder electrode. The corrosive wear of an API X52 steel immersed in condensed salt water with amine as inhibitor was evaluated using the Electrochemical impedance spectroscopy (EIS) technique for static and dynamic conditions.

Zhu et al. (2012) suggests that the according to the erosion theory and actual condition, the erosion of drill pipe is investigated using laboratory experiment and computational fluid dynamics (CFD) simulation technique. Different factors of gas drilling, such as drill pipe centralization, eccentricity of drill pipe, wellbore enlargement, gas injection volume, rate of penetration (ROP) and rotational speed of drill pipe, are considered. The results show that the local erosion rate of drill pipe in horizontal well is larger than that one in vertical well. The increase of drill pipe

eccentricity, wellbore enlargement and ROP, the local peak erosion rate increases. The effect of gas injection volume and rotational speed of drill pipe on the erosion of drill pipe is very little. When the wellbore enlargement occurs severely, the increase of gas injection volume can improve carrying efficiency of cuttings, and the local erosion of drill pipe will be reduced.

Cheng-Hong (2012) suggests that the corroded steel tube joint belonging to an offshore oil well-drilling pipeline was investigated. All of the pits and punctures distributed along the ‘‘steps’’ are formed by off-center machining on the internal tube surface. The pits contour and metallurgical structure indicate that the pits and punctures are characterized by cavitation erosion. The chemical composition of the corroded steel tube joint is similar to 1320, 1330 and L80-1 steels specified in ASTM standards. Appearance observed on location of the penetrating puncture, indicating H_2S and CO_2 assisted corrosion mechanisms. These investigations indicated that failure of the pipeline occurred by erosion corrosion, cavitation erosion and chemical corrosion, which is from both mechanical and chemical actions. The main pits and punctures were distributed along the ‘‘steps’’, which are form by off-center machining on the internal surface of the tube. The metallurgical structure on the subsurface of some corrosion pits and punctures spots displays curved, bending deflections in the banded structure (streamlines). This structure indicates that the pits and punctures were mainly caused by cavitation erosion.

2.9.3 Study of electrochemical (Potentiostat)

Yahya et al. (2014) reveal that corrosion is degradation or destructive attack of metals due to its environments. Most of science and engineering aspects in

the field of corrosion focusing on knowing how to mitigate the impact of corrosion. Generally, the weight lost method is the easy process to determine the corrosion rate.

The uses of those electrochemical techniques are very fast methods since electrochemical instruments polarize the sample to accelerate the corrosion process and make the measurement in minutes or hours. Scan rate is an essential experimental parameter in performing the polarization measurements and measuring the corrosion rate.

The effect of scan rate on the investigation of rice straw extract as corrosion inhibitor has been identified. It was found that the scan rate optimization is necessary to provide corrosion reaction remains fully charged within the electrode and electrolyte. If the scan rate is too rapid, the alteration of potentiodynamic curves may lead to misinterpretation of the polarized electrode process due to charges disturbance and insufficient time during achieving the steady state.

Sekunowo et al. (2013) point out that the most exposed metallic surfaces in air are usually covered with an oxide film thereby limiting spontaneous degradation. However, when a metal is immersed in an aqueous solution, the oxide film tends to dissolve. In particular, the corrosion of mild steel pipes in acid and saline environments has been a major challenge with regard to processed products (oil, gas, chemical, etc.) transportation due to its devastating effects.

The electrochemical polarization method is often preferred because it enables the determination of instantaneous reaction rates at electrode or solution interface in a single experiment while other methods require multiple measurements over time to obtain the required corrosion rate data. This technique is a relatively

short time dependent; it aids the selection of the best protective measures to be used thereby saving cost.

The potentiostat polarization of mild steel in hydrochloric acid and seawater has been investigated. Mild steel intrinsic characteristics approximated by its constituent elements significantly impacted the corrosion responses. The acidity of corrosion product appears to have distinguished the corrosion rates of the mild steel in each of the environments simulated.

Even though there are many works on electrochemical corrosion-erosion on various steel, there are only a few study concerns with steel tubing used in petroleum industry.

Therefore, the main objective of this research is to study the corrosion rate of steel tubing grade L80-13Cr and K55 based on the electrochemical corrosion method and the effects of surface roughness to the corrosion rate.

CHAPTER III

METHODOLOGY

3.1 Research methodology

This research consists of five main steps; 1) specimens preparation from steel tubing grade K55 and L80-13Cr, 2) specimens chemical composition analysis, 3) Specimens corrosion test, 4) specimens surface analysis, and 5) specimens wear test, respectively. Figure 3.1 shows steps of this study activities in brief.

3.2 Materials

3.2.1 Steel tubing specimens

This research selected two steel tubing grade K55 and L80-13Cr according to the API 5CT Standard since they were widely used in the petroleum production system. Their chemical compositions are shown in Table 3.1.

Table 3.1 Chemical composition of steel tubing (after API 5CT)

Grade	Chemical composition (Wt%)								
	C ≤	Si ≤	Mn ≤	P ≤	S ≤	Cr ≤	Ni ≤	Cu ≤	Fe
K55	0.389	0.218	1.27	0.0028	0.0002	0.0794	0.0335	0.0444	Bal.
L80-13Cr	0.221	0.405	0.542	0.0002	0.0002	13.23	0.0749	0.00015	Bal.

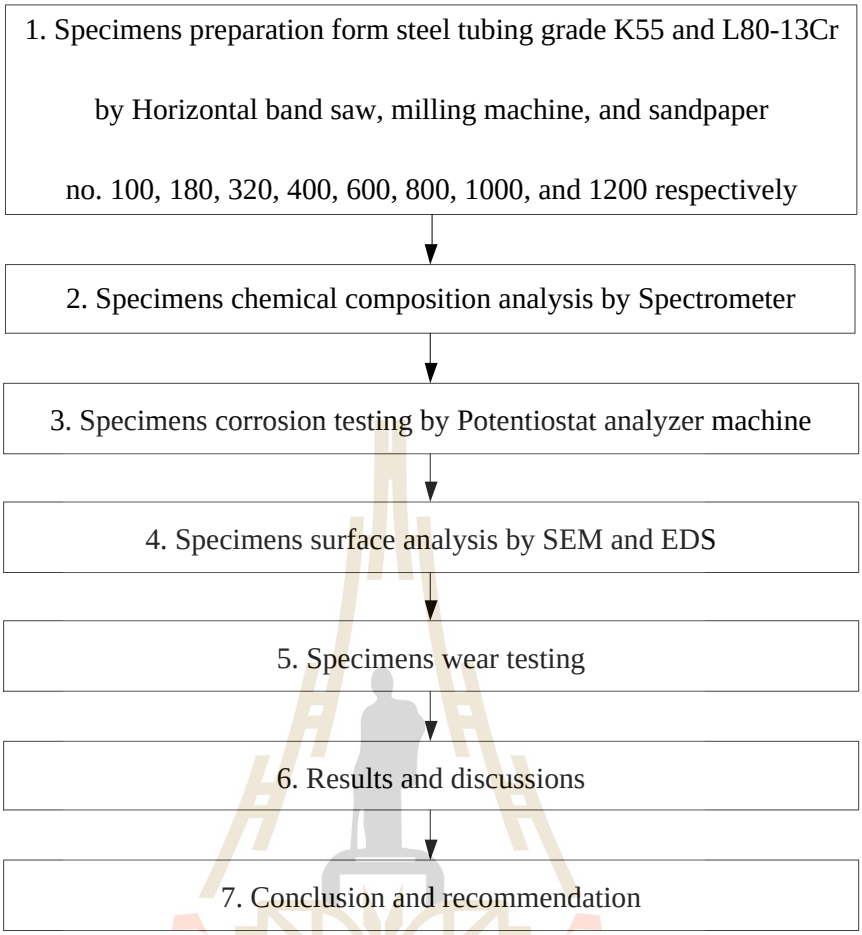

Figure 3.1 Flow chart showing steps of the research activities

Pictures of steel tubing grade K55 and L80-13Cr before cutting are depicted in Figure 3.2.

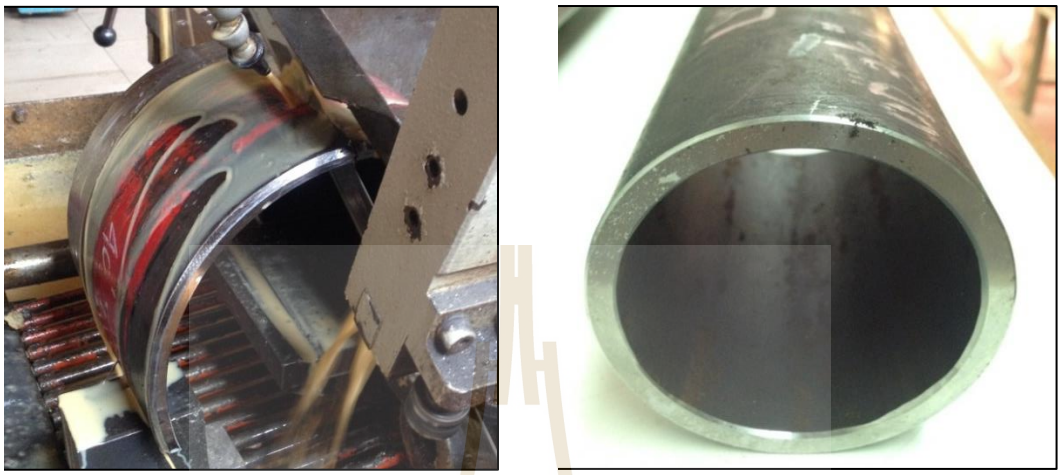

(a) (b)

Figure 3.2 Steel tubing before making specimens (a) K55 (b) L80-13Cr

3.3 Equipment

3.3.1 Equipment for physical properties testing

3.3.1.1 Spectrometer

The spectrometer is a device used to determine chemical properties and elements involved in combustion or heat the material with Spectrometer machine (Figure 3.3). In chemistry, the light from a burning or heated material can be spread into its spectrum which can be used to determine the elements involved. A spectrometer uses a prism or diffraction rating to spread out an incoming beam of light into its spectrum of different colors or wavelengths. Since each element has a unique set of spectral lines, examination of the spectral lines is used to determine which elements are involved, as well as how many elements are in a compound.

Figure 3.3 Spectrometer (Model SPECTRO LAB)

3.3.1.2 Rockwell hardness

The Rockwell hardness test method, as defined in ASTM E-18, is the most commonly used hardness test methods. Rockwell hardness testing machine (Figure 3.4) is a general method for measuring the bulk hardness of metallic materials. Although hardness testing does not give a direct measurement of any performance properties, hardness of a material correlates directly with its strength, wear resistance, and other properties. Hardness testing is widely used for material evaluation because of its simplicity and low cost relative to direct measurement of many properties.

Figure 3.4 Rockwell Hardness (Model: 660RLD/T)

The Rockwell method measures the permanent depth of indentation produced by a force/load on an indenter (Figure 3.5). This load represents the zero or reference position that breaks through the surface to reduce the effects of surface finish. After the preload, an additional load, call the major load, is applied to reach the total required test load. This force is held for a predetermined amount of time (dwell time) to allow for elastic recovery. This major load is then released and the final position is measured against the position derived from the preload, the indentation depth variance between the preload value and major load value. This distance is converted to a hardness number which is presented in Table 3.2.

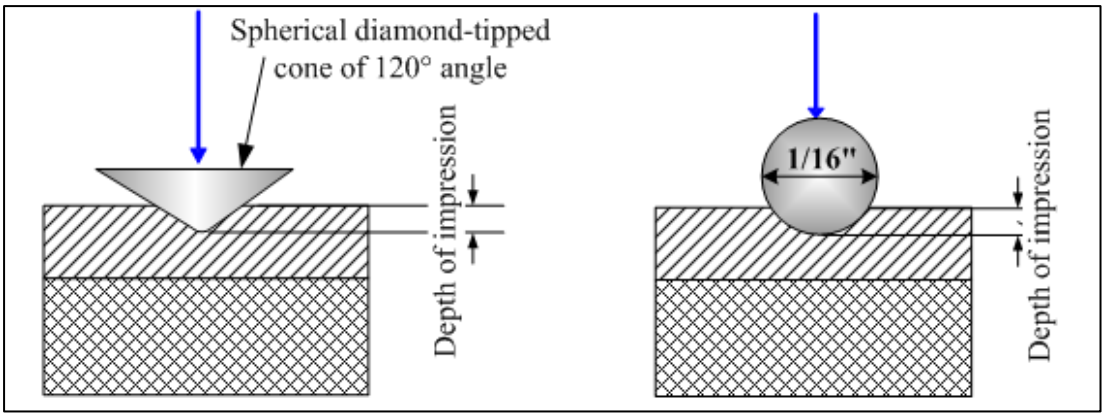

Figure 3.5 Indenters or the Rockwell hardness test (after http://www.vnmachine.com/2014/02/phuong-phap-do-do-cung-rockwell.html)

Table 3.2 Various Rockwell scales (https://sizes.com/units/hardness_rockwell.htm)

Scale	Abbreviation	Load (kgf)	Indenter
A	HRA	60	120° diamond spheroconical
B	HRB	100	1/16 inch diameter steel sphere
C	HRC	150	120° diamond spheroconical
D	HRD	100	120° diamond spheroconical
E	HRE	100	1/8 inch diameter steel sphere
F	HRF	60	1/16 inch diameter steel sphere
G	HRG	150	1/16 inch diameter steel sphere
H	HRH	60	1/8 inch diameter steel sphere
K	HRK	150	1/8 inch diameter steel sphere

3.3.1.3 Milling machine and horizontal band saw machine

In order to make the tubing steel pipe into smaller pieces the milling machine (Figure 3.6) and Horizontal band saw machine (Figure 3.7) were used.

(a)

(b)

Figure 3.6 Milling machine (a) and cutter for milling machine (b) (Model: Full mask)

3.3.1.4 Grinding machine, sandpaper, and polishing machine

In order to prepare the surface of the steel plate specimens for surface analysis grinding machine with various sandpaper number (Figure 3.8 and Figure 3.9) and polishing machine (Figure 3.10) were used in this study.

Figure 3.7 Horizontal band saw machine (Model: Sahinler)

Figure 3.8 Grinding machine (Model ECOMET 6)

Figure 3.9 Sandpaper (Silicon carbide, SiC)

Figure 3.10 Polishing machine (Brand: BUHLER, Model: Phoenix 2000)

3.3.2 Equipment for Metallography

In order to examine microstructure and chemical composition of the steel plate specimens in this study, three types of microscope; Optical microscope (OM), Scanning Electron Microscope (SEM), and Energy-Dispersive X-ray Spectrocope (EDS), were used.

The optical microscope: OM (Figure 3.11), often referred to a light microscope, is a type of microscope which uses visible light and a system of lenses to magnify images of small samples. Basic optical microscopes can be very simple, although there are many complex designs which aim to improve resolution and sample contrast.

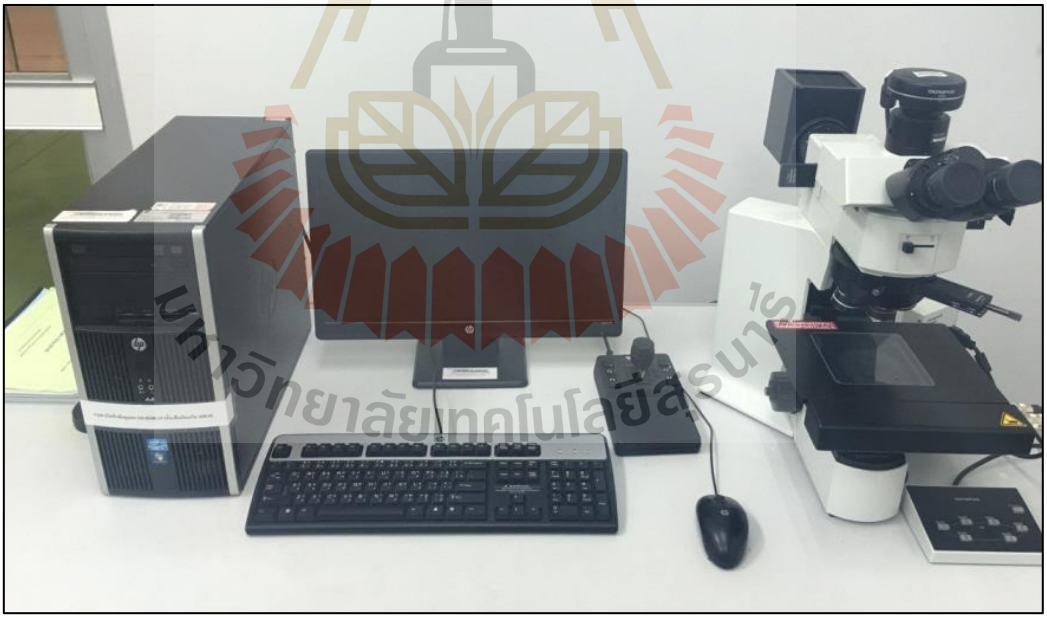

Figure 3.11 Optical Microscope (Model Olympus-BX51M-LED)

Scanning Electron Microscope and Energy-dispersive X-ray spectroscopy (Figure 3.12). In scanning electron microscopy, (SEM) an electron beam is scanned across a sample's surface. When the electrons strike the sample, a variety of signals are generated, and it is the detection of specific signals which produces an image or a sample's elemental composition. The three signals which provide the greatest amount of information in SEM are the secondary electrons, backscattered electrons, and X-rays.

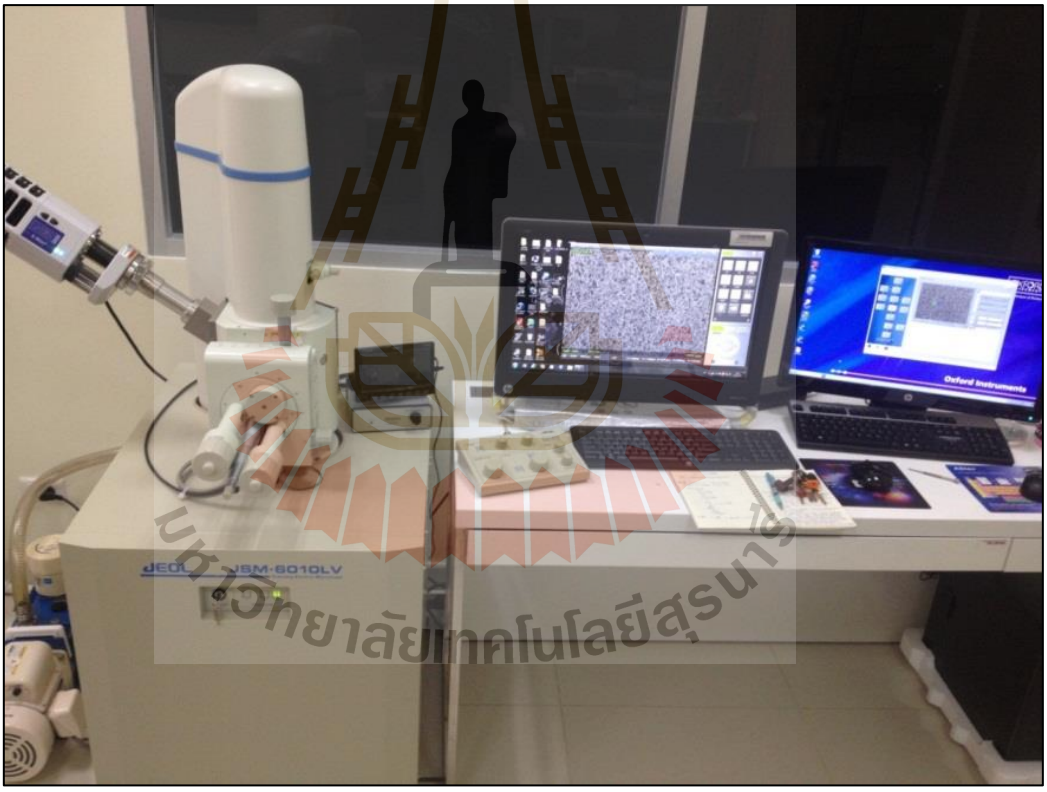

Figure 3.12 Scanning Electron Microscope and Energy-dispersive x-ray spectroscope (Model: JEOL SEM 6010)

Secondary electrons are emitted from the atoms occupying the top surface and produce a readily interpretable image of the surface. The contrast in the image is determined by the sample morphology. A high resolution image can be obtained because of the small diameter of the primary electron beam.

Backscattered electrons are primary beam electrons which are 'reflected' from atoms in the solid. The contrast in the image produced is determined by the atomic number of the elements in the sample. The image will therefore show the distribution of different chemical phases in the sample. Because these electrons are emitted from a depth in the sample, the resolution of the image is not as good as for secondary electrons. The interaction of the primary beam with atoms in the sample causes shell transitions which result in the emission of an X-ray. The emitted X-ray has an energy characteristic of the parent element. Detection and measurement of the energy permit elemental analysis (Energy Dispersive X-ray Spectroscopy or EDS). EDS can provide rapid qualitative or with adequate standards, quantitative analysis of elemental composition with a sampling depth of 1-2 microns. X-rays may also be used to form maps or line profiles, showing the elemental distribution in a sample surface.

3.3.3 Equipment for corrosion testing

Corrosion is an electrochemical process of oxidation and reduction reactions. As corrosion occurs, electrons are released by the metal (oxidation) and gained by elements (reduction) in the corrosive solution. Because there is a flow of electrons (current) in the corrosion reaction, it can be measured and controlled electronically. Therefore, controlled electrochemical experimental methods can be used to characterize the corrosion properties of metals and metal components in

combination with various electrolyte solutions. The corrosion characteristics are unique to each metal/solution system.

In order to study the corrosion rate of the steel plate specimens in this study the potentiostat analyzer machine (Figure 3.13) was applied. A potentiostat is used for dynamic methods when it is necessary to control the potential of the working electrode. Figure 3.14 shows a schematic diagram of the potentiostat setup that can be used to maintain a constant cell potential.

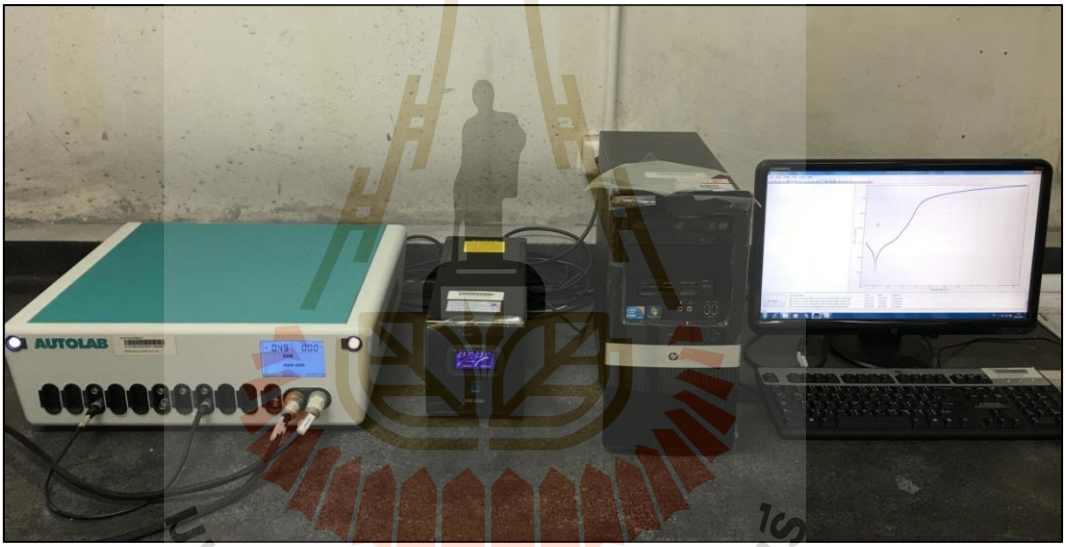

Figure 3.13 Potentistat analyzer machine

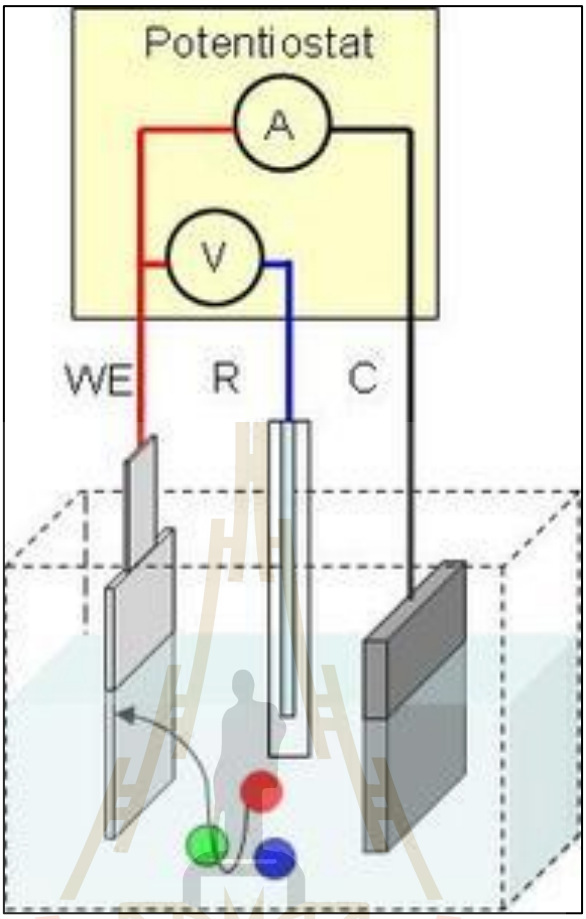

Figure 3.14 A schematic diagram of the potentiostat setup

(a) (b)

Figure 3.15 Reference electrode (a), Counter electrode (b)

However, this study had established a corrosion cell to be used in this experiment. Easy to install specimen test as shown in Figure 3.16.

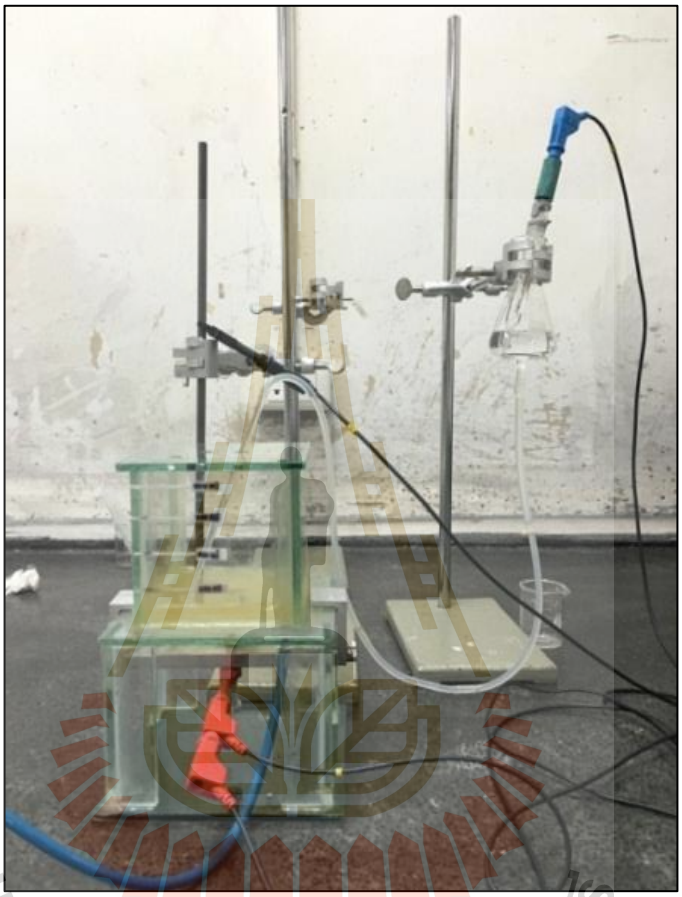

Figure 3.16 A schematic diagram of the corrosion test cell

In order to measure pH of the solution which was used in corrosion test, a pH meter was used. A pH Meter (Figure 3.17) is a scientific instrument used in the measurement of the concentration of hydrogen ion (or pH) in a solution, indicating its acidity or alkalinity. The pH meter measures the difference in electrical potential between a pH electrode and a reference electrode.

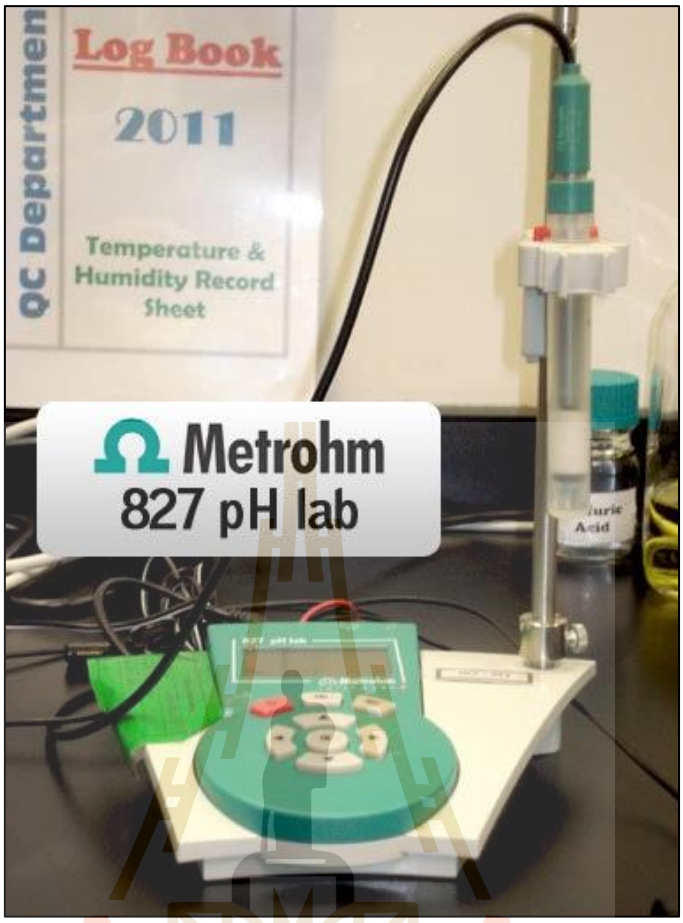

Figure 3.17 pH meter (Model: 827 pH Lab Metrohm)

3.3.4 Equipment for wear testing

Wear is related to interactions between surfaces and specifically the removal and deformation of material on a surface as a result of mechanical action on the opposite surface (Figure 3.18). In materials science, wear is erosion or sideways displacement of material from its "derivative" and original position on a solid surface performed by the action of another surface. Wear of metals occurs by the plastic displacement of surface and near-surface material and by the detachment of particles that form wear debris. This process may occur by contact with other metals,

nonmetallic solids, flowing liquids, or solid particles or liquid droplets entrained in flowing gasses.

Wear can also defined as a process where interaction between two surfaces or bounding faces of solids within the working environment results in the dimensional loss of one solid, with or without any actual decoupling and loss of material. Aspects of the working environment which affect wear include loads and features such as unidirectional sliding, reciprocating, rolling, and impact loads, speed, temperature, but also different types of counter-bodies such as solid, liquid or gas and type of contact ranging between single phase or multiphase, in which the last multiphase may combine liquid with solid particles and gas bubbles.

Figure 3.18 Wear test method (ASTM G65-04)

3.4 Chemical for corrosion testing

In order to set up the experiment condition for the corrosion rate test, some chemicals and substances were used. They are as follows.

1) Solution for corrosion testing is ground water from the separation out of the crude oil, pH values about 6-7.

2) Distilled water, Alcohol solution for cleaning specimen.

3) Silica gel for the moisture absorption.

4) Nital acid 5% (5 cc nitric acid, 95 cc Ethyl alcohol)

5) Carpenter 300 series (Ferric chloride 8.5 g, Cu

6) Nitric chloride 2.4 g, Alcohol 122 ml, Hydrochloride acid 122 ml, Nitric acid 6 ml.

7) Alumina powder for the polishing specimens.

3.5 Specimens preparation

3.5.1 Sample cutting and cleaning

The two tubing steel grade K55 and L80-13Cr were cut to the 20x20x5 mm (wide x long x thick) (Figure 3.19) with the number of each specimen as showed in Table 3.3. After cutting, the surface of specimens had been grinded by grinding machine with sandpaper from coarse-grained to fine-grained (100, 180, 320, 400, 600, 800, and 1200). After grinding, steel plate specimens had been measured their hardness with a Rockwell hardness B scale. The results of the hardness test are showed in Table 3.4.

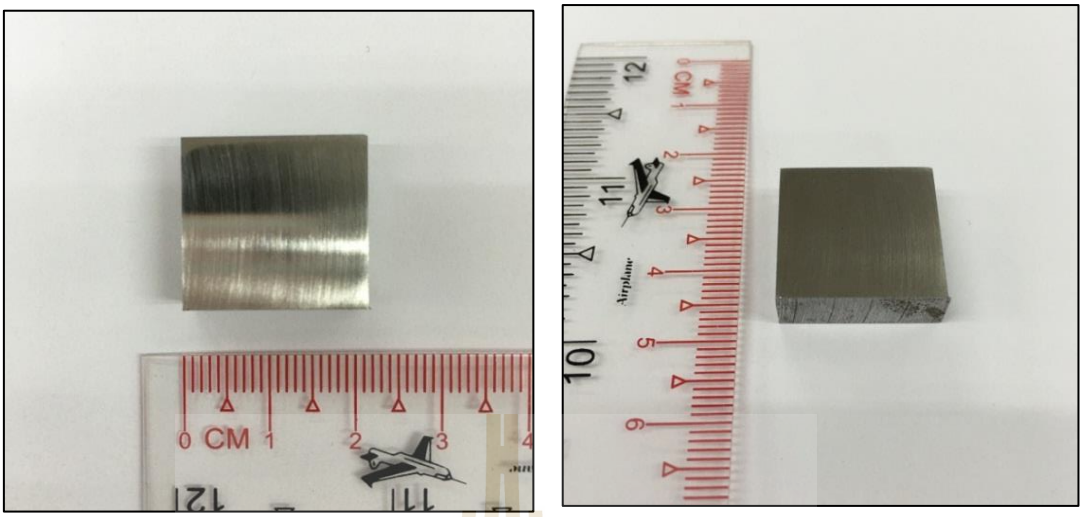

(a) (b)

Figure 3.19 Steel plate specimen size after cutting

Table 3.3 Number of specimen for each tubing grade and surface roughness preparing

Sandpaper (SiC) No.	**K55 (API 5CT)**	**L80-13Cr (API 5CT)**
No. 600	3	3
No. 1200	3	3

Table 3.4 The hardness of steel plate specimens

API 5CT	**Hardness value (HRB)**				
	Point 1	**Point 2**	**Point 3**	**Average**	**SD**
K55	93.80	94.00	94.05	93.95	0.13
L80-13Cr	99.45	99.75	99.80	99.67	0.19

After measuring the hardness, steel plate specimens had been polished with alumina powder by rotation disk machine before etching with Nitral acid 5% (for K55) and Carpenter (for L80-13Cr) about 5 to 10 minutes in order to observe the grain boundary and to take photographs of the microstructure of the two grades specimens. After that, the specimens were cleaned with alcohol and blown to dry.

3.5.2 Specimens corrosion testing

After steel plate specimens had been already prepared, they were conducted corrosion test with electrochemical techniques, by Potentiostat analyzer machine. The solution used in this study was the groundwater from the separation unit of an oil field in the Phitsanulok oil field. Its pH values was range between 6 and 7. Specimens were installed in the corrosion cell which was filled with 100 milliliter of testing solution. The test voltage in this study was range between -200 to 1000 millivolts and the scan rate was 0.01 millivolts per second. In practical, before the start of the scan, it is required to perform the open circuit voltage (OCP) measurement. In this research, OCP testing time was 5 minutes.

3.5.3 Specimens surface analysis

After the corrosion testing, steel plate specimens had been conducted the surface and chemical composition analysis to the areas which were corroded by SEM and EDS method. The result of the experiment was shown as an image and line spectrum. The spectrum can represent the relationship between the energy intensity and photon energy which are difference in each area where it has difference chemical composition. Therefore, it can be used to specify the area where corrosive has been taken place.

3.5.4 Wear test

The steel plate specimens were conducted the wear test according to the Standard G65 to observed the wear caused by abrasion from sand. Sand was dropped pass steel plate specimens and wear with rubber wheels with the speed of 200 rounds per minute under 130 N loaded. The testing time is 10, 20 and 30 minutes respectively. After the test, the specimen weight loss was calculated and recorded.

CHAPTER IV

RESULTS AND DISCUSSIONS

4.1 Chemical composition and physical properties of specimens

4.1.1 Chemical composition

Results from chemical composition analysis of the steel plate specimens by the Energy-Dispersive X-ray Spectreoscopy (EDS) indicate that the chemical compostion of the steel plate specimens of tubing grade K55 and L80-13Cr used in this study is quite similar to those of tubing grade K55 and L80-13Cr according to the API5CT standard. Results of the analysis are shown in Table 4.1 and Table 4.2, respectively.

Table 4.1 Chemical composition of tubing K55 (API5CT) and K55 specimen

Grade	C≤	Si≤	Mn≤	P≤	S≤	Cr≤	Ni≤	Cu≤	Mo≤	V≤	Als≤
K55 (API5CT)	0.34-0.39	0.20-0.35	1.25-1.50	0.02	0.015	0.15	0.2	0.2	-	-	0.02
K55 specimen	0.389	0.218	1.27	0.0028	0.0002	0.0794	0.0335	0.0444	-	-	0.02

Table 4.2 Chemical composition of tubing L80-13Cr (API5CT) and L80-13Cr Specimen

Grade	C≤	Si≤	Mn≤	P≤	S≤	Cr≤	Ni≤	Cu≤	Mo≤	V≤	Fe
L80-13Cr (API5CT)	0.15-0.22	1	0.25-1.00	0.02	0.01	12.0-14.0	0.2	0.2	-	-	bal
L80-13Cr specimen	0.221	0.408	0.542	0.0002	0.0002	13.23	0.0749	0.00015	-	-	bal

4.1.2 Hardness test

The hardness value (Three-point test) of K55 specimen are 93.80, 94.00, 94.05 (average 93.95 HRB) whereas the hardness of L80-13Cr specimen are 99.45, 99.75, 99.80 (average 99.67 HRB). The hardness L80-13Cr is greater than those of K55 as shown in Table 4.3 since L80-13Cr has more alloy and chromium, and it is also passed the heat treatment process.

Table 4.3 The result of hardness tested

Point	K55	L80-13Cr
Point 1	93.80	99.45
Point 2	94.00	99.75
Point 3	94.05	99.80
Avg	93.95	99.67

4.2 Microstructure

4.2.1 Microstructure of steel plate specimens

The microstructure of K55 and L80-13Cr specimens under the 5, 10, 20, 50, and 100 times magnified are shown in Figure 4.1 to Figure 4.5, respectively. Pearlite and Ferrite are dominant in K55 specimens, while Bainite is dominant in L80-13Cr.

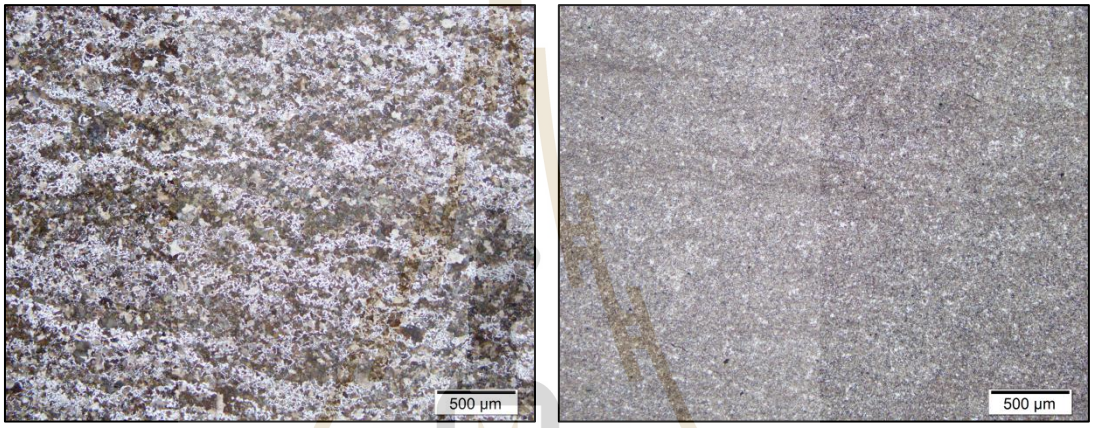

Figure 4.1 Microstructure of K55 (Left) and L80-13Cr (Right), 5X

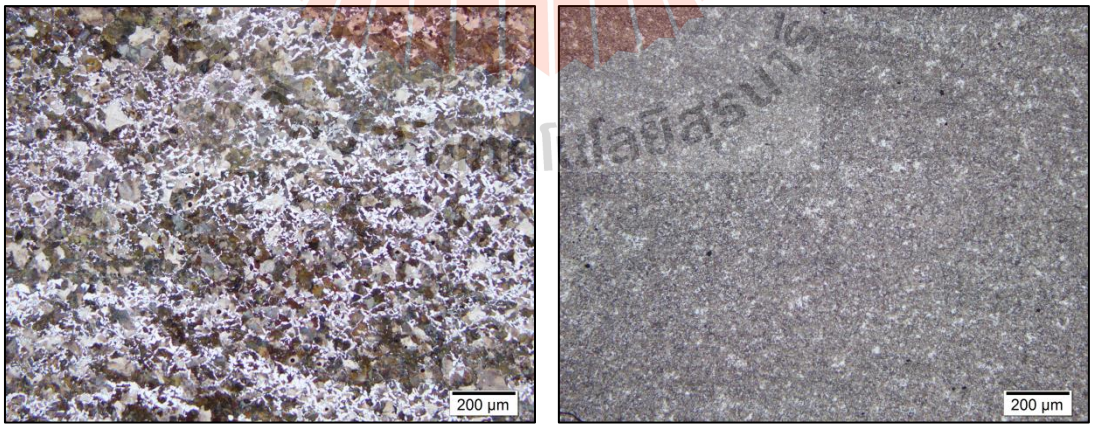

Figure 4.2 Microstructure of K55 (Left) and L80-13Cr (Right), 10X

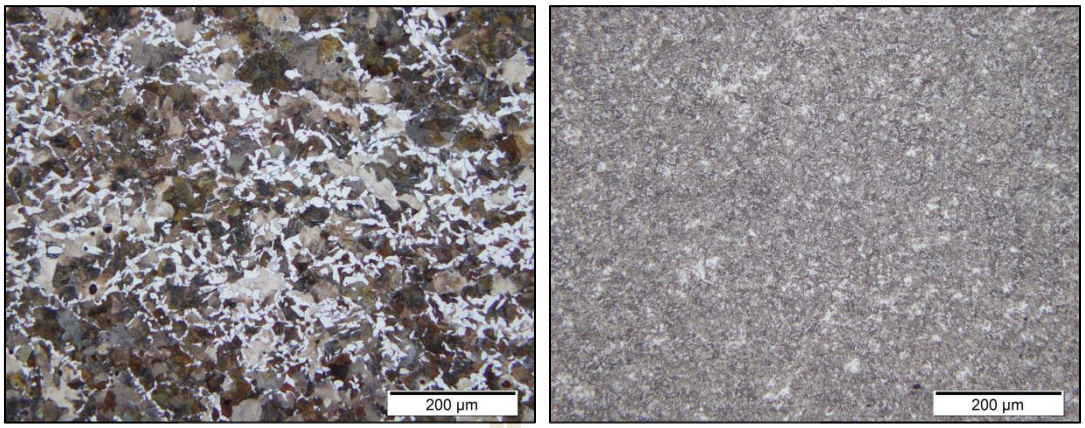

Figure 4.3 Microstructure of K55 (Left) and L80-13Cr (Right), 20X

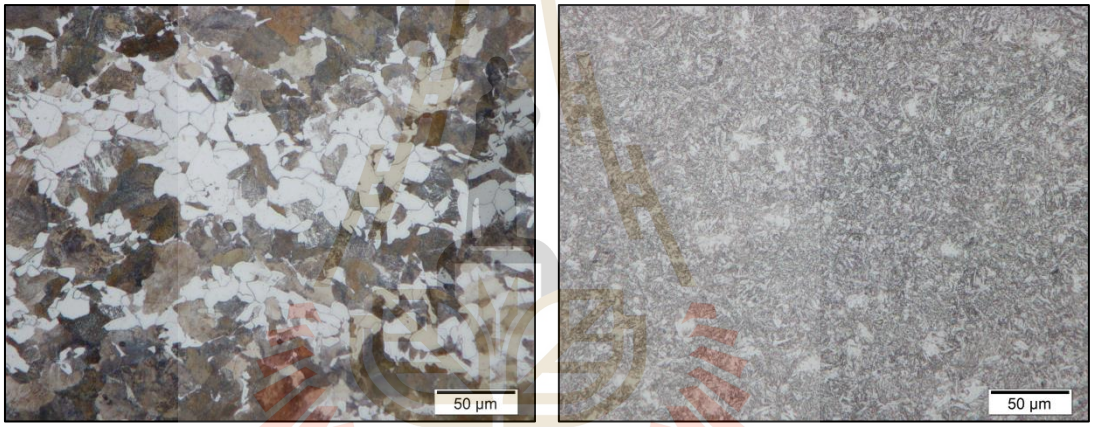

Figure 4.4 Microstructure of K55 (Left) and L80-13Cr (Right), 50X

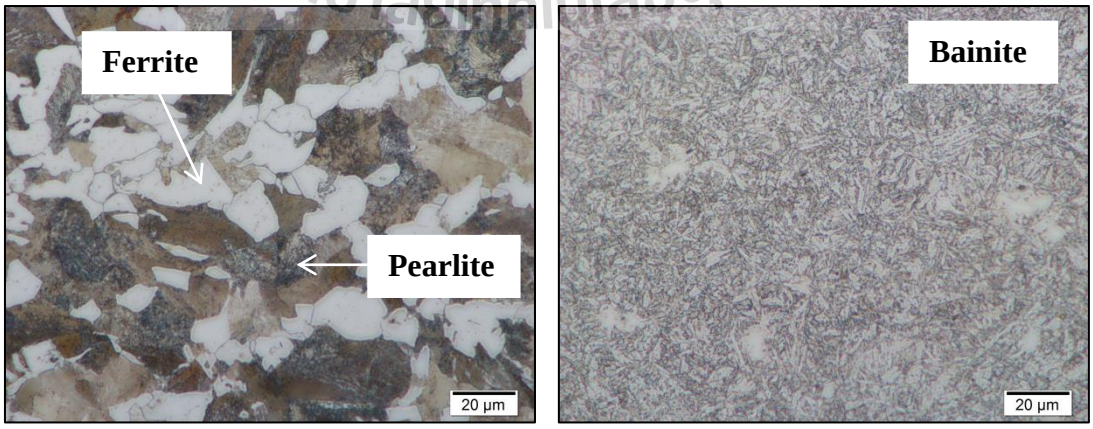

Figure 4.5 Microstructure of K55 (Left) and L80-13Cr (Right), 100X

Ingeneral, the microstructure of the carbon steel is Pearlite and Ferrite. Carbon (wt%) in this grade, it is equal to the 0.39. From lever arm rule, the microstructure normally contains 0.49 Wt% Pearlite and 0.51 Wt% Ferrite, respectively. Pearlite normally appears as the brown area, whereas Ferrite appears as the white area.

The steel tubing grade L80-13Cr is added Chromium (Cr) about 13 Wt% in order to make it has high corrosion resistant, high mechanical properties and can work in high temperature. The internal structure of L80-13Cr is different from K55 since it is passed the heat treatment process. The heat treatment process of metal will make the metal has fine-grained crystal, such as fine-grained Ferrite, acicular Ferrite and retained Ferrite, because of the high cooling rate.

4.2.2 SEM and EDS before taking the corrosion test

Results of surface analysis before taking corrosion test of K55 and L80-13Cr steel plate specimens by SEM Test are shown in Figure 4.6 and Figure 4.8, while Figure 4.7 and Figure 4.9 present the result of EDS Test of K55 and L80-13Cr, respectively.

Results from EDS Test (Figure 4.7 and Figure 4.9) indicate that L80-13Cr has Chromium (Cr) mush more than K55 obviously.

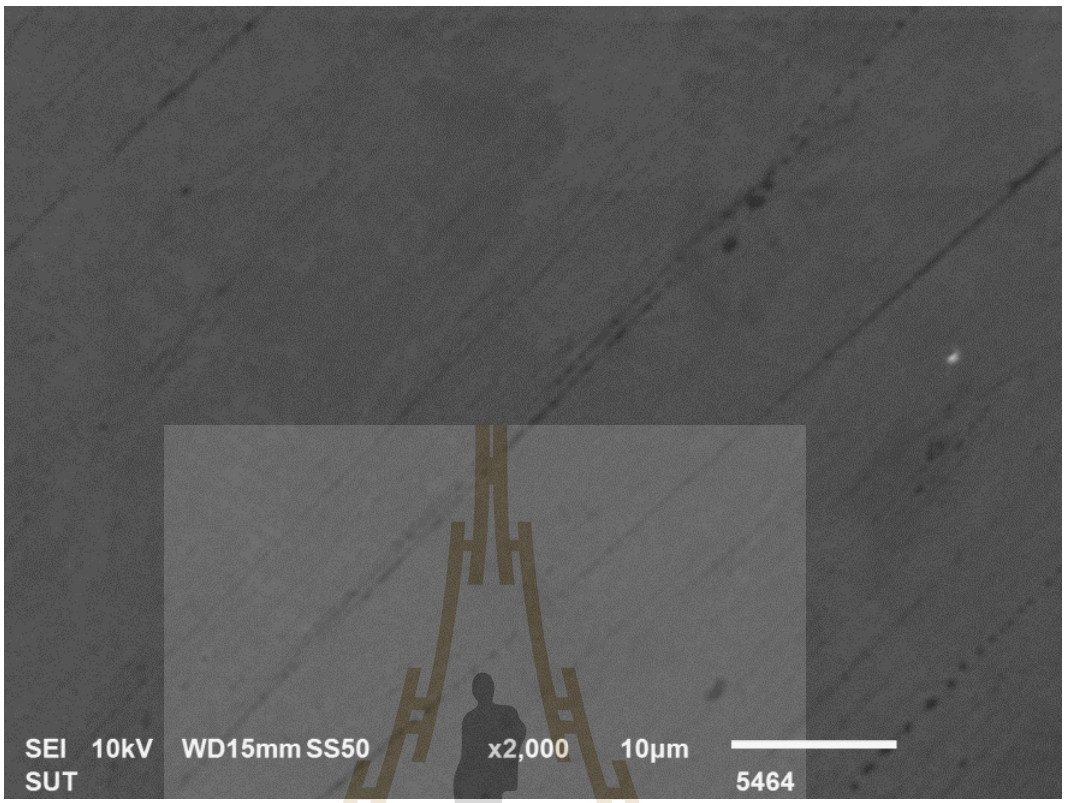

Figure 4.6 Surface of K55 before taking the corrosion test

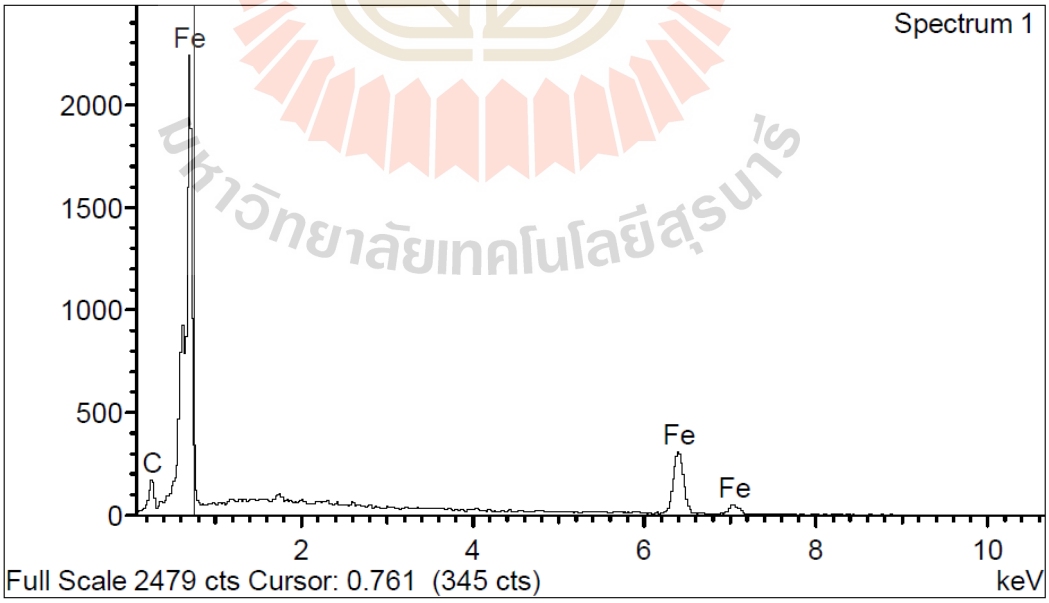

Figure 4.7 Spectrum element of K55 specimen before taking the corrosion test

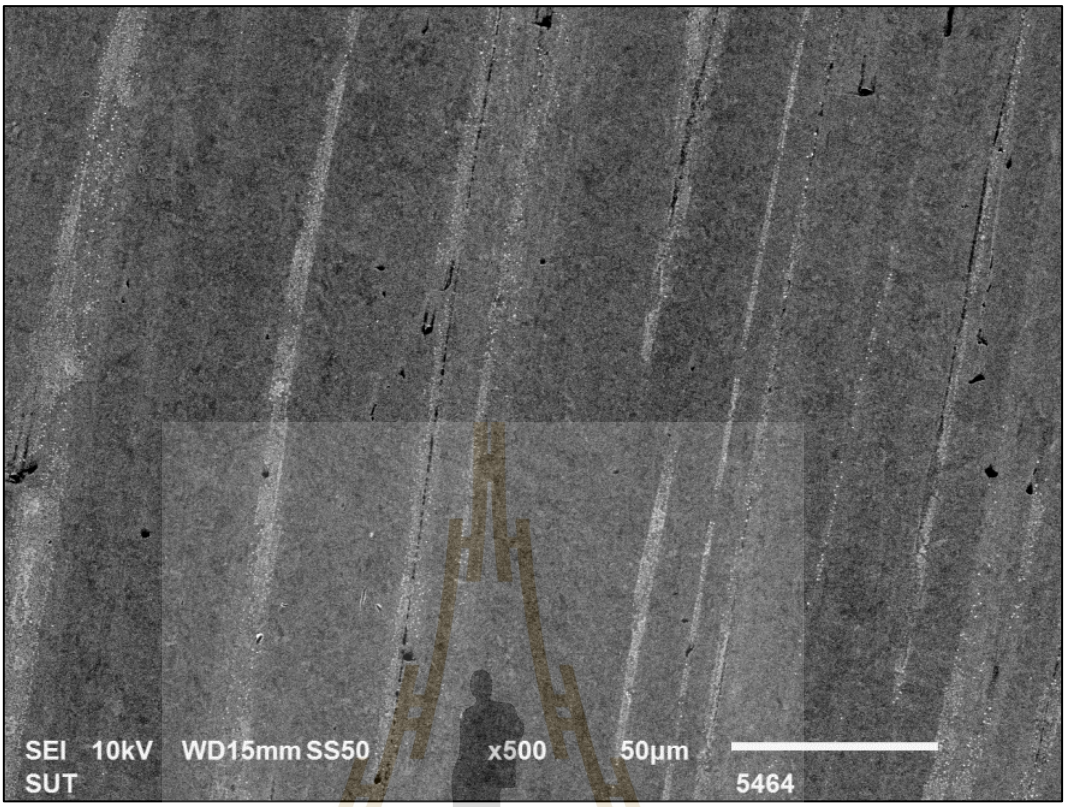

Figure 4.8 Surface of L80-13Cr before taking the corrosion test

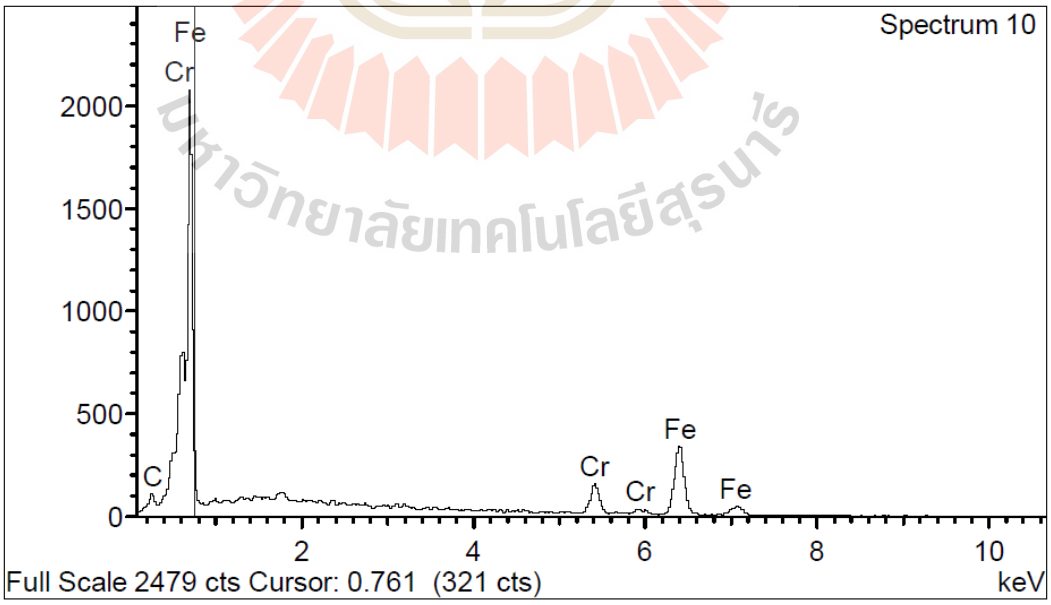

Figure 4.9 Spectrum element of L80-13Cr specimen before taking the corrosion test

4.2.3 SEM and EDS after taking the corrosion test

The microstructure of K55 specimens after taking the corrosion test show the noticeable oxide film on the surface (Figure 4.10), whereas the surface of L80-13Cr after taking the corrosion test show pitting instead (Figure 4.12). Figure 4.11 and Figure 4.13 show results of EDS analysis of K55 and L80-13Cr specimens after taking the corrosion test respectively.

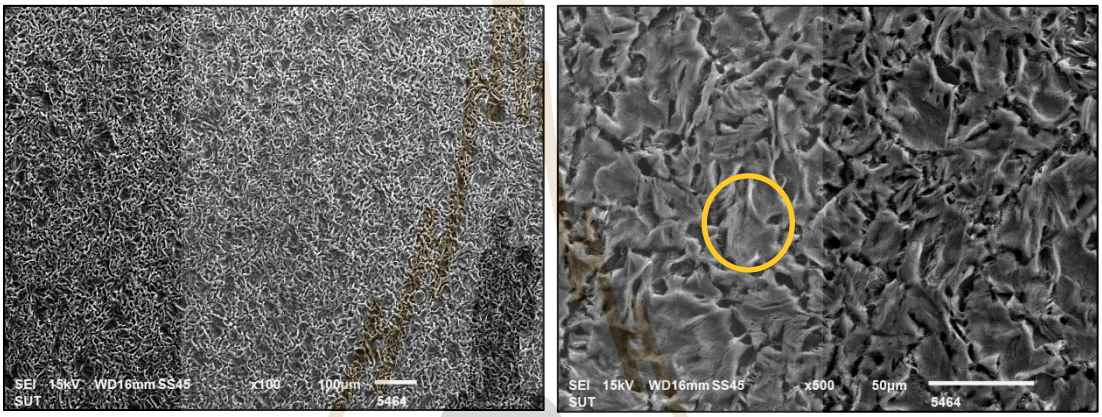

(a) (b)

Figure 4.10 Surface of K55 specimen showing oxide film after taking the corrosion test, (a) 100X (b) 500X

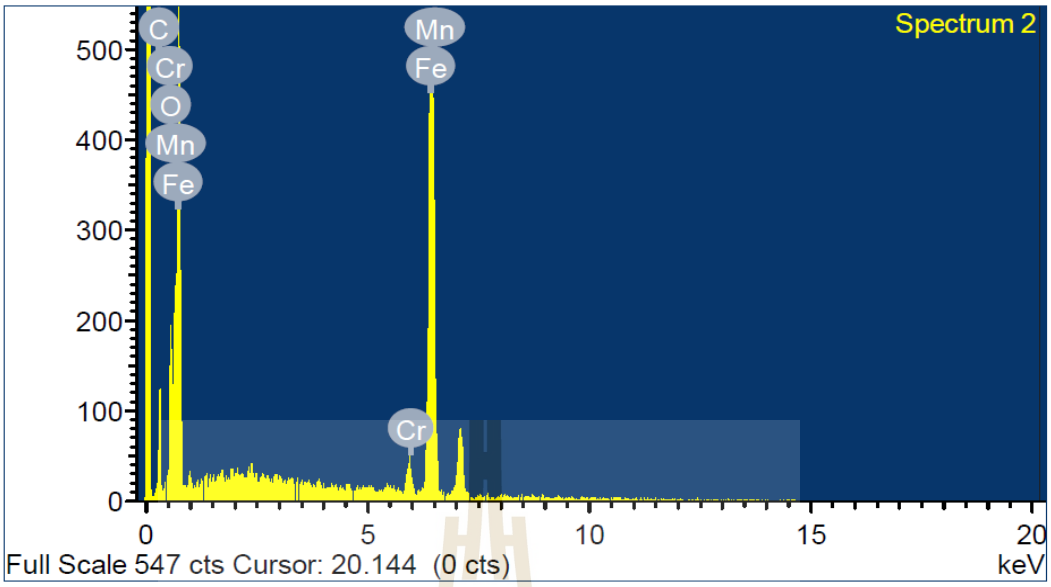

Figure 4.11 Element spectrum of K55 after taking the corrosion test

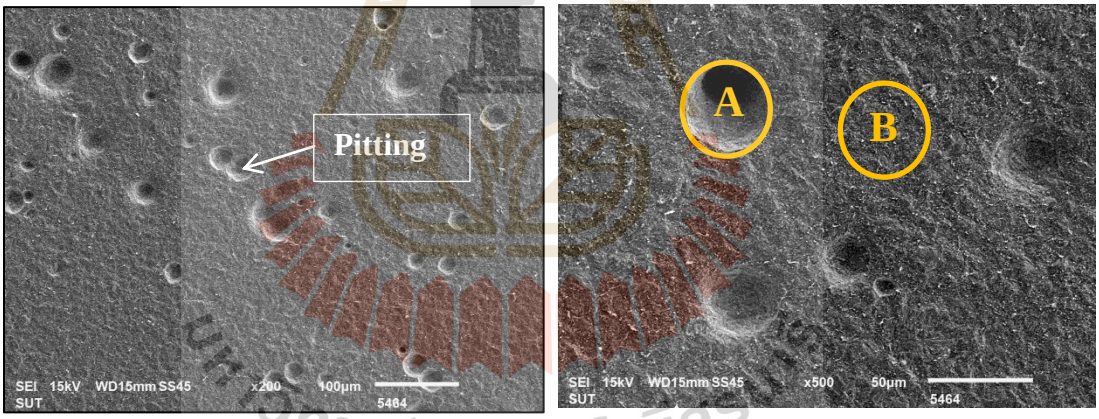

(a) (b)

Figure 4.12 Surface of L80-13Cr specimen showing pitting after taking the corrosion test, (a) 100X (b) 500X

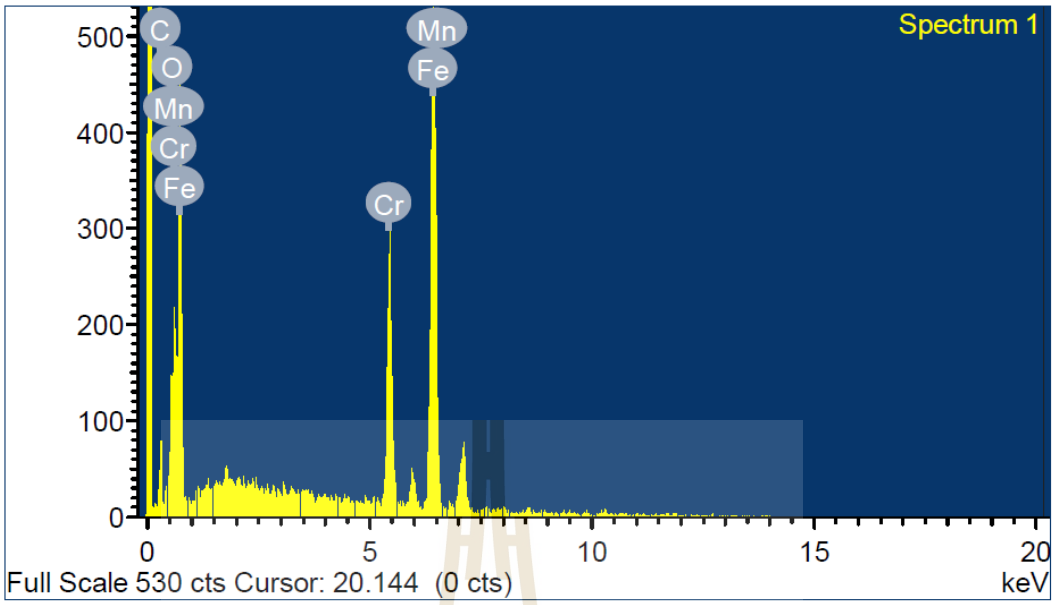

(Point A)

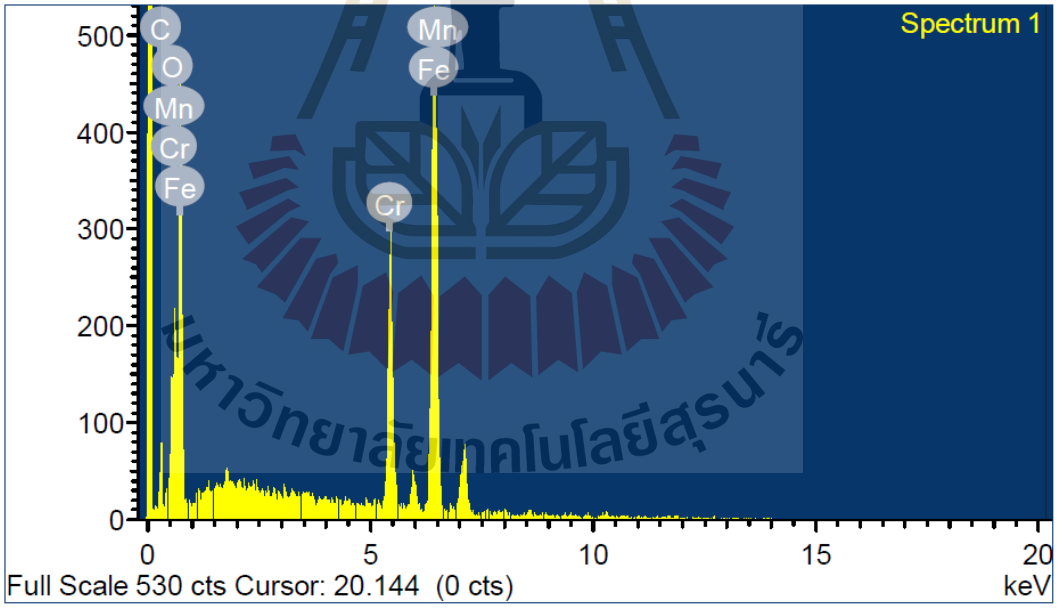

(Point B)

Figure 4.13 Element spectrum of L80-13Cr after taking the corrosion test

4.3 Corrosion rate

4.3.1 Polarization curve

A polarization curve is a plot of current density of corrosion (Icorr) versus electrical potential of corrosion (Ecorr) for a specific electrode-electrolyte combination. Plots of log |Icorr| vs. Ecorr are called polarization curves. The polarization curve is the basic kinetic law for any electrochemical reaction.

Polarization curves are valuable in quantifying the behaviors of metals under various conditions. Polarization curves for passive systems may show active/passive and/or passive/trans-passive transitions.

In order to study the surface roughness on the corrosion rate, K55 and L80-13Cr specimens were prepared their surface with two sandpaper grit number (600 and 1200) before conducting the corrosion test in this study. Results of the experiments are presented in Figure 4.14 to Figure 4.17, respectively.

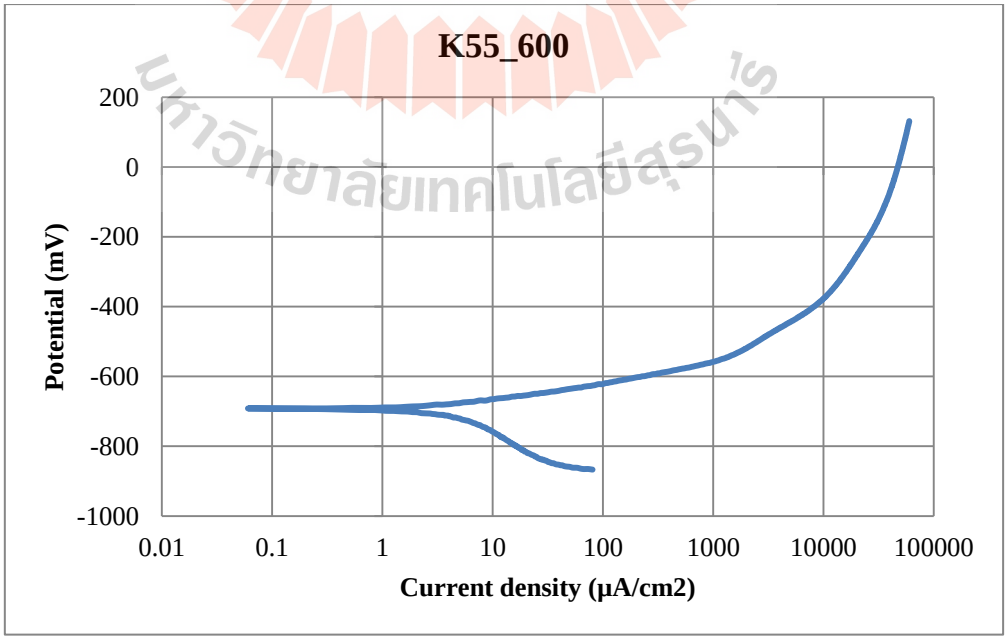

Figure 4.14 Polarization curve of K55, sandpaper No. 600

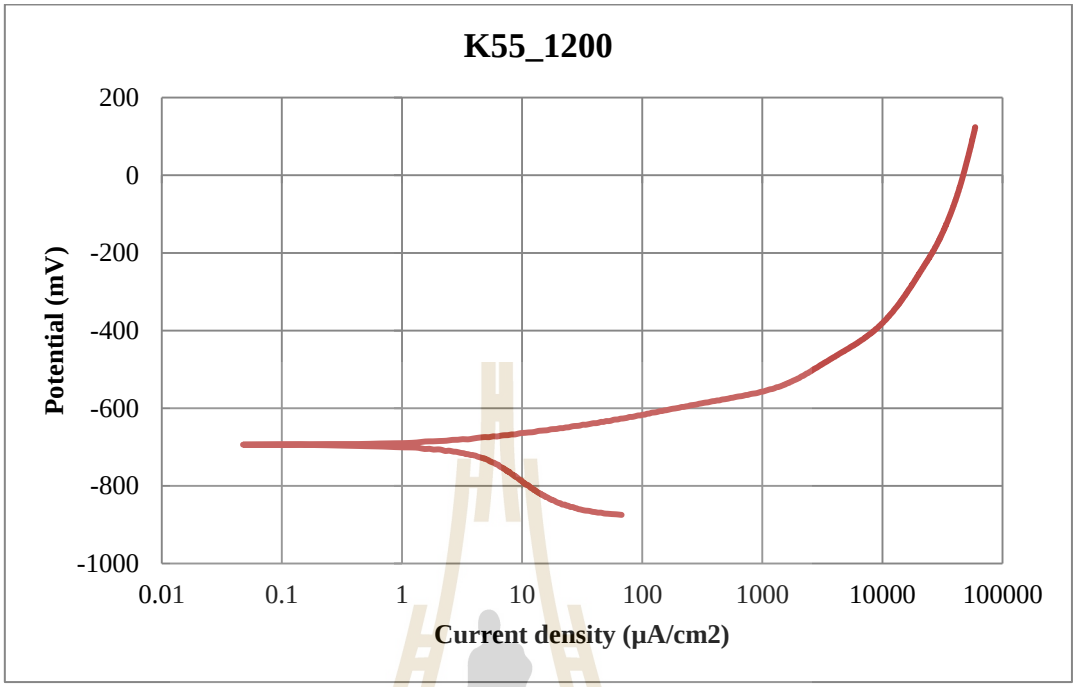

Figure 4.15 Polarization curve of K55, sandpaper No. 1200

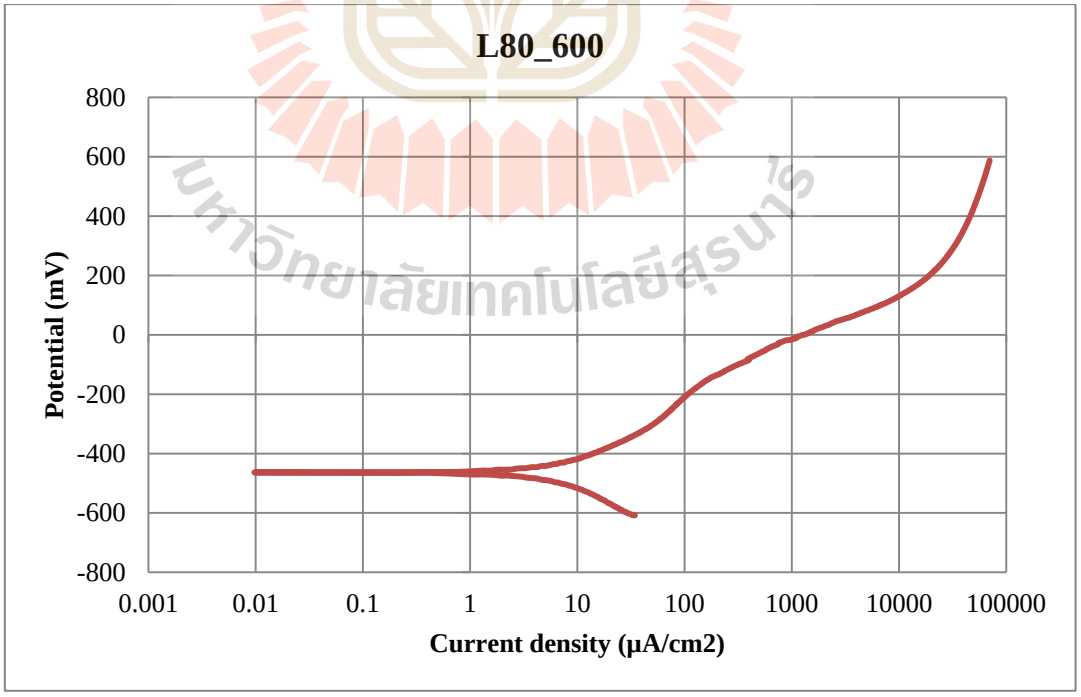

Figure 4.16 Polarization curve of L80-13Cr, sandpaper No. 600

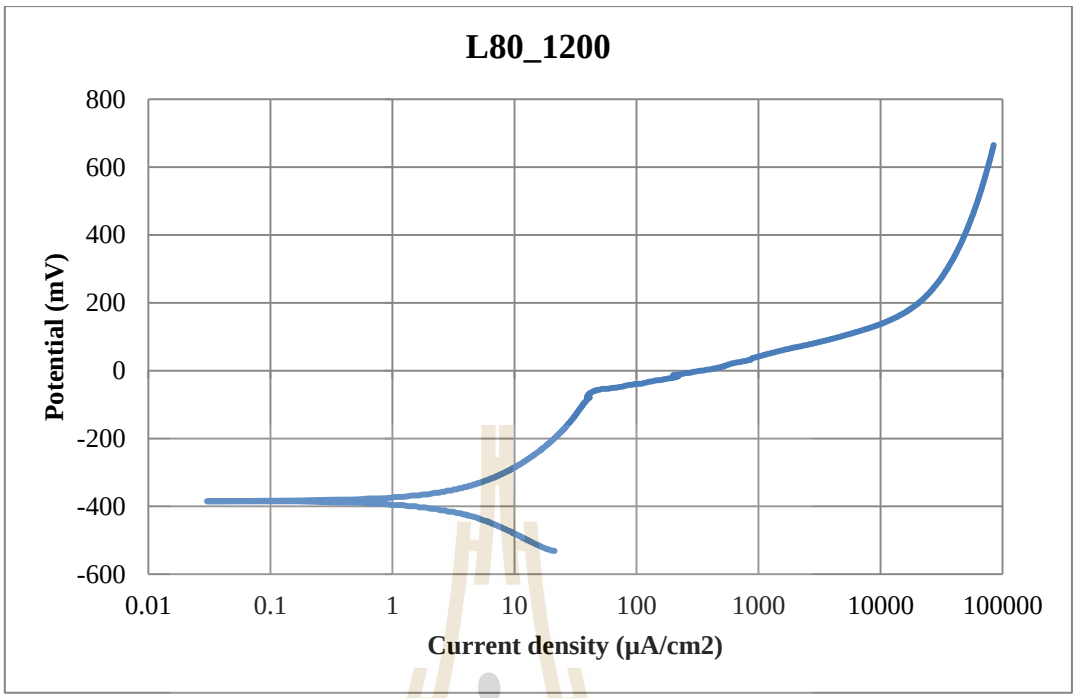

Figure 4.17 Polarization curve of L80-13Cr, sandpaper No. 1200

4.3.2 Calculation corrosion rate

From the polarization curve, value of Ecorr and Icorr which were used for the corrosion rate calculation can be obtained as shown in Table 4.4. The results of the corrosion rate calculations are depicted in Bar Chart as shown in Figure 4.18 to Figure 4.20, respectively.

Table 4.4 Corrosion rate of the steel plate specimens from polarization analyzer

Grade (API 5CT)	Sandpaper (SiC)	pH	Ecorr (mV)	Icorr (µA/ cm2)	CR (mm/year)
K55	600	6.66	-682	5.57	0.0465
K55	1200	6.65	-688	3.47	0.0376
L80-13Cr	600	6.71	-499	1.53	0.0169
L80-13Cr	1200	6.70	-392	1.05	0.0138

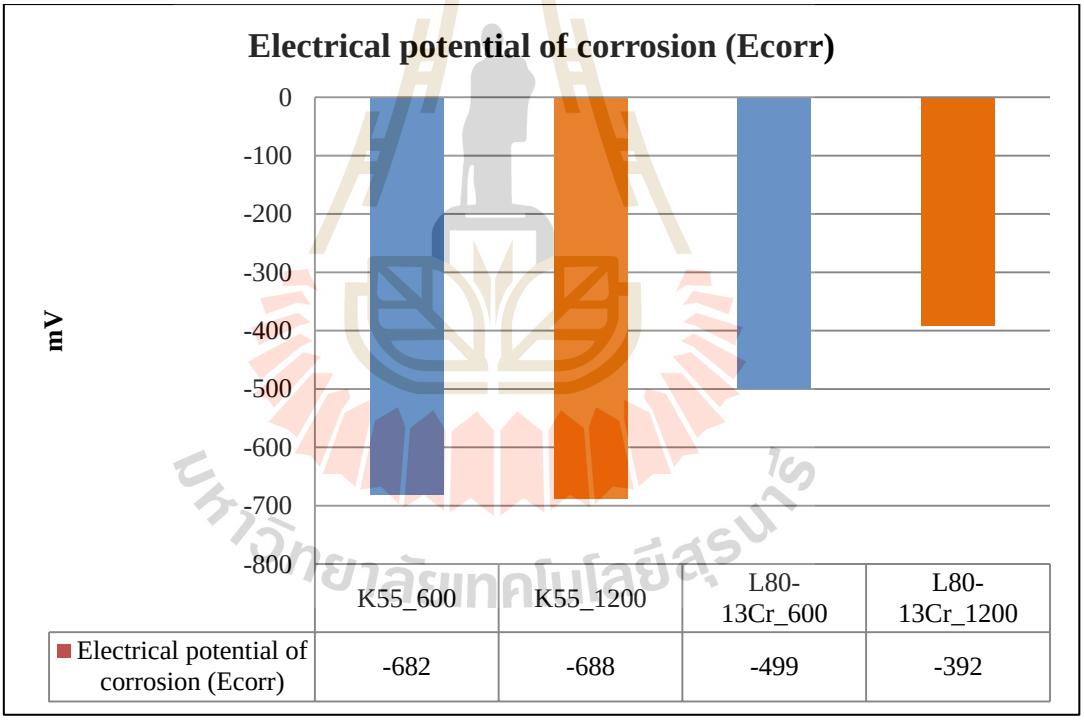

Figure 4.18 Bar chart of electrical potential of corrosion (Ecorr)

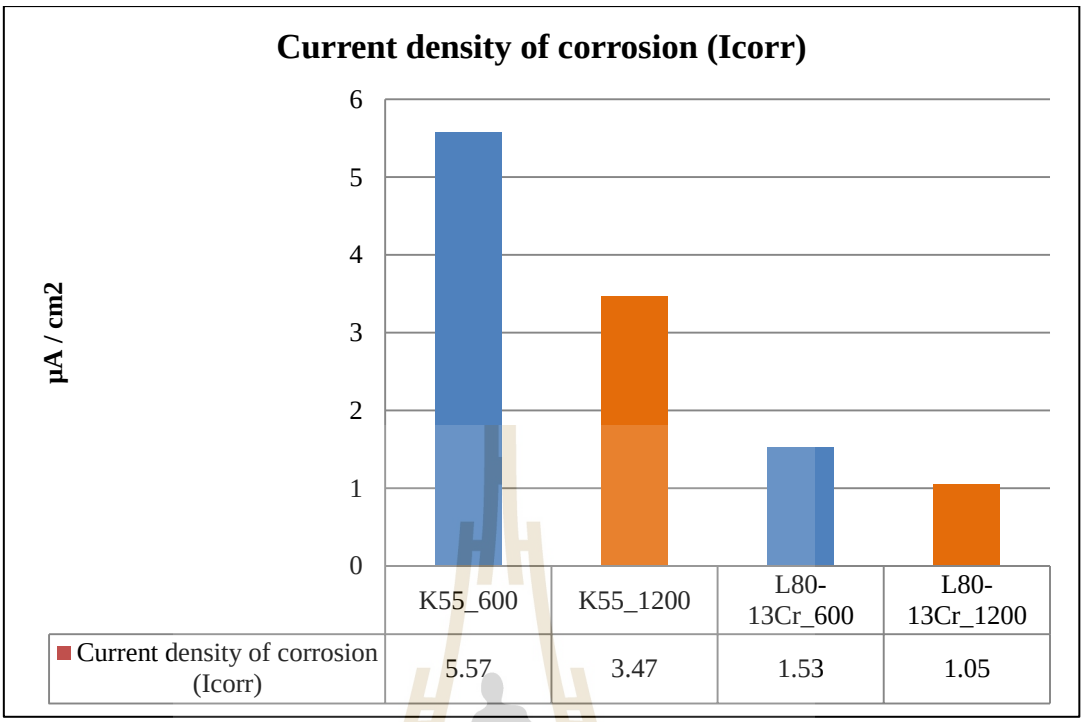

Figure 4.19 Bar chart of current density of corrosion (Icorr)

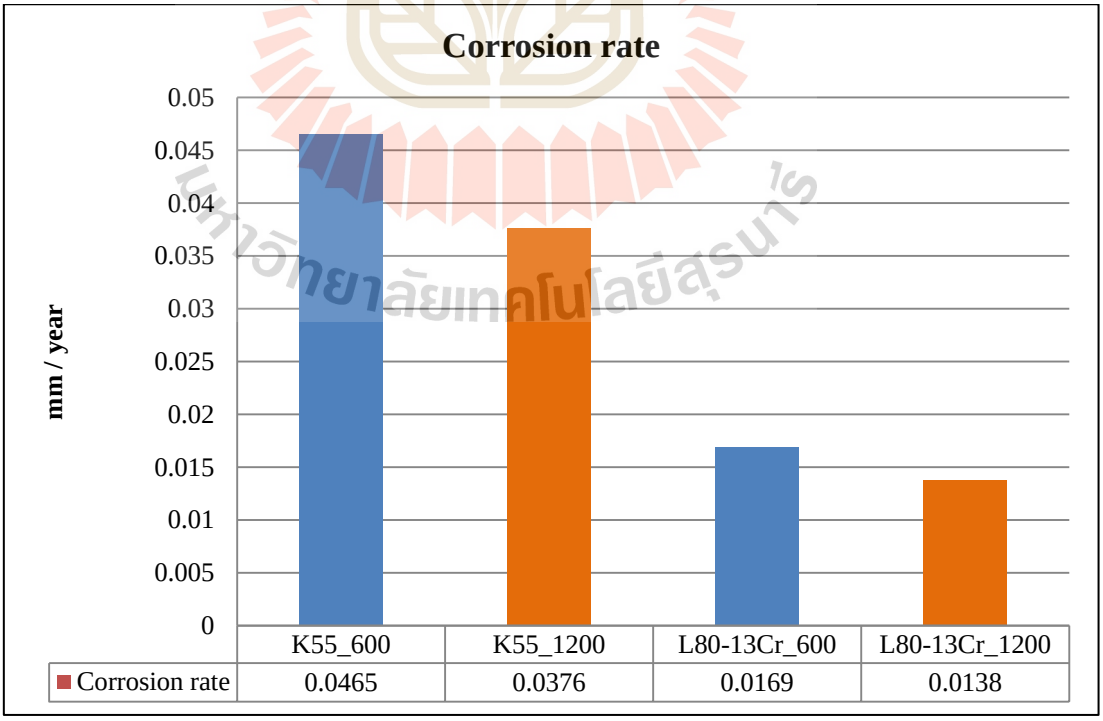

Figure 4.20 Bar chart of corrosion rate (CR)

4.3.3 Wall thickness

Each length of pipe shall be measured to verify conformance with wall thickness requirements. Wall thickness measurements shall be made with a mechanical calliper, a go/no-go gauge or with a properly calibrated of appropriate accuracy.

For pipe, the wall thickness at any place shall not be less than the tabulated thickness the permissible under-tolerance specified is show in Table 4.5.

Table 4.5 Tolerances of the outside diameter and thickness of pipe (Bradley, 1987)

Outside diameter (D)		**Thickness (S)**
Pipe diameter (mm)	**Tolerance (mm)**	**Tolerance (mm)**
< 114.3 (4 1/2 inch.)	± 0.79%	-12.5%
≥ 114.3 (4 1/2 inch.)	-0.5%, +1%	

API tubing and casing: The performance of the tubing that is run inside the casing to conduct oil or gas to ground level is important. But also must resist the corrosive action of well fluid that is some area is severe. The minimum performance properties of tubing are shown in Table 4.6 and the minimum performance properties of casing are shown inTable 4.7 respectively.

Table 4.6 Minimum performance properties of tubing (Bradley, 1987)

OD (in.)	**Nominal weight (lbm/ft)**		**Wall thickness (in.)**	**ID (in.)**
	Non-upset	**Upset**		
2 7/8	6.40	6.50	0.217	2.441
	7.80	7.90	0.276	2.323
	8.60	8.70	0.308	2.259
3 1/2	7.70	-	0.216	3.068
	9.20	9.30	0.254	2.992
	10.20	-	0.289	2.922

Table 4.7 Minimum performance properties of casing (Bradley, 1987)

OD (in.)	Nominal weight (lbm/ft)	Wall thickness (in.)	ID (in.)
9 5/8	32.30	0.312	9.001
	36.00	0.352	8.921
	40.00	0.395	8.835
	43.50	0.435	8.755
	47.00	0.472	8.681
	53.50	0.545	8.535
	58.40	0.595	8.435
	59.40	0.609	8.407
	64.90	0.672	8.281
	70.30	0.734	8.157

Table 4.7 Minimum performance properties of casing (Bradley, 1987)

OD (in.)	Nominal weight (lbm/ft)	Wall thickness (in.)	ID (in.)
9 5/8	71.80	0.750	8.125
	75.60	0.797	8.031
13 3/8	48.00	0.330	12.715
	54.40	0.380	12.615
	61.00	0.430	12.515
	68.00	0.480	12.415
	72.00	0.514	12.347
	77.00	0.550	12.275
	80.70	0.580	12.215
	85.00	0.608	12.159
	86.00	0.625	12.125
	92.00	0.672	12.031
	98.00	0.719	11.937
	72.00	0.734	11.907

Therefore, from the limitation as shown in Table 4.6 and Table 4.7, the lifetime of steel tubing grade K55 and L80-13Cr which are releated to the corrosion rate from this study can be calculated. The results of lifetime calculation of steel tubing grade K55 and L80-13Cr are shown in Table 4.8.

Table 4.8 Lifetime of steel tubing grade K55 and L80-13Cr estimated from corrosion rate (CR) value

Grade (API 5CT)	Sandpaper No.	Corrosion rate (mm/year)	Wall thickness (mm)	Lifetime of steel tubing (years)	API thickness tolerance -12.5% (years)
K55	600	0.0465	6.45	139	17.42
K55	1200	0.0376	6.45	172	21.54
L80-13Cr	600	0.0169	6.45	382	47.93
L80-13Cr	1200	0.0138	6.45	467	58.70

* API thickness tolerance -12.5% (mm) is 5.64 mm

4.3.4 Wear testing

The result from wear testing is presented in weight loss with sand content as shown in Table 4.9 and Figure 4.21. The result from wear testing is used to verify the corrosion rate which is calculated from the electrochemical corrosion testing.

It can be noticeable from Figure 4.21 that the slope of the straight line is direct proportional to the weight loss. Moreover, it can be observed that the steel tubing grade L80-13Cr has the weight loss less than K55 since it contains more Chromium (Cr).

Table 4.9 Weight loss from wear test

Grade (API 5CT)	Weight loss (g)		
	10 minute	20 minute	30 minute
K55	0.1959	0.3755	0.5322
L80-13Cr	0.1102	0.2065	0.2832

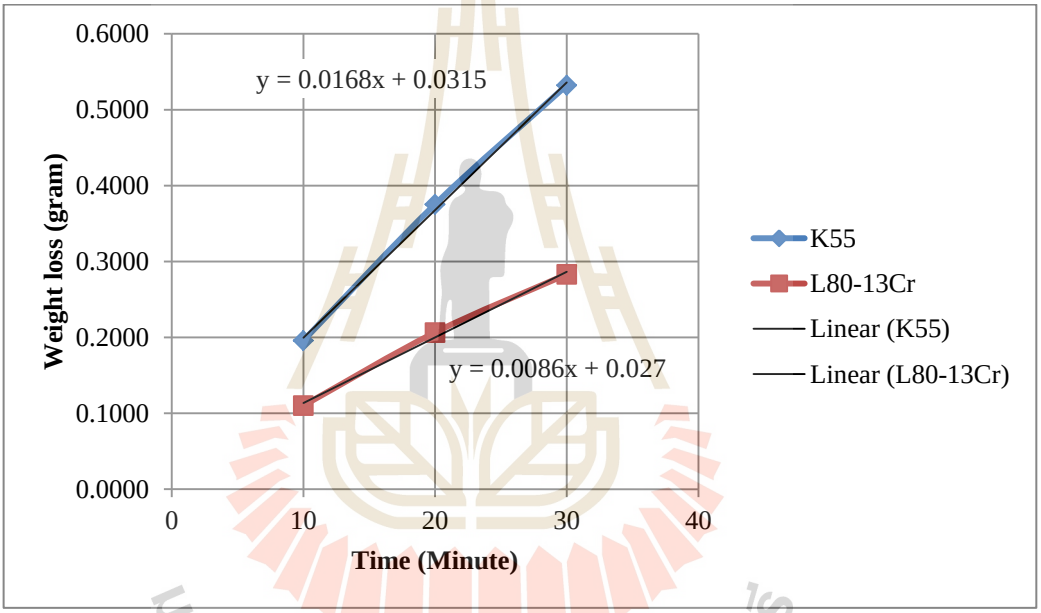

Figure 4.21 Weight loss from wear test

4.3.5 Water analysis

Table 4.10 presents results from separated-water that was used as the corrosion solution in this study. After the corrosion test it was found that water which was used for K55 corrosion test had the Total Dissolved Solid (TDS) more than those of L80-13Cr since some solids were lost from K55 specimen during the test easier than L80-13Cr. This is conform to the result of weight loss and corrosion rate test.

Table 4.10 Water analysis

No.	Testing list	Before test	After testing as K55	After testing as L80-13Cr
1	Conductivity (mS/cm)	105.6	104	105
2	Salinity (ppt)	60	60	60
3	Chloride (mg/l)	44,736	57,283	43.886
4	Sulfate (mg/l)	15	11	12
5	Bicarbonate Alkalinity (mg/l as CaCO3)	233	28	29
6	Carbonate Hardness (mg/l as CaCO3)	233	28	19
7	Total Iron (mg/l)	3.2	1.42	1.16
8	Chromium (Chexavalent) (mg/l)	-	-	1.1
9	Total Dissolved Solids (mg/l)	84,691	96,954	96,612

4.4 Discussions

4.4.1 Corrosion behavior from polarization curve

The corrosion test results as presented in Figure 4.14 to Figure 4.17 indicate that under the corrosion solution which is the groundwater obtained from the separation unit of crude oil of an oil field in the Phitsanulok Basin, pH 6, the severity of corrosion change according to Cr alloy and surface roughness of the steel plate specimens. Like in this study L80-13Cr (Chromium 13Wt%) has the corrosion rate less than K55 (Non-Chromium).

It is also found that the surface roughness has an important role to the electrical potential of corrosion (Ecorr) of the steel plate specimens. For example, in the case of steel tubing L80-13Cr, the specimen which had the surface prepared by sandpaper No. 1200, the Ecorr was in the range between -200 and -400 mV, whereas the Ecorr of the specimen which had the surface prepared by sandpaper No. 600 was in the range between -400 and -600 mV and had resulted in higher corrosion rate. Therefore, It can be concluded that the steel plate specimen surface which is prepared by finer sandpaper is supposed to have the less corrosion rate since the contact area between corrosion solution and specimen surface is lesser. On the other hand, the lower current density of corrosion (Icorr), the lower corrosion rate.

4.4.2 Weight loss from erosion-wear test

From the wear testing by sand it found that the weight loss On-time tested of steel plate specimen of K55 is higher than the steel plate specimen of L80-13Cr at any prepared surface roughness. This is because the steel tubing grade L80-13Cr has high alloy and Chromium composition which make it has more erosion and wear resistance capability.

Moreover, result of the wear test conforms with the hardness and the rate of corrosion test by electrochemical method.

CHAPTER V

CONCLUSIONS AND RECCOMMENDATIONS

5.1 Conclusions

This research is focused on the corrosion rate of the steel tubing used in the petroleum production system which is caused by produced groundwater from the separation unit from an oil field in the Phitsanulok Basin. This research consists of five main steps; 1) specimens preparation from steel tubing grade K55 and L80-13Cr, 2) specimens chemical composition analysis, 3) specimens corrosion test, 4) specimens surface analysis, and 5) specimens wear test, respectively.

Results from chemical composition analysis of the steel plate specimens by the Energy-Dispersive X-ray Spectroscopy (EDS) indicate that the chemical composition of the steel plate specimens of tubing grade K55 and L80-13Cr used in this study is quite similar to those of tubing grade K55 and L80-13Cr according to the API5CT standard.

This study uses the electrochemical corrosion process to determine the corrosion rate (CR) by using the Potentiostat analyzer machine. The calculated corrosion rate (CR) is then used in determining the lifetime of the steel tubing. Moreover, this research also study the effect of surface roughness of the steel plate specimens which were prepared by sandpaper number 600 and 1200 on the corrosion rate.

The results from this study indicate that the Ecorr and Icorr can be used for corrosion rate calculation and estimate the lifetime of steel tubing. The calculated corrosion rate (CR) of steel tubing caused by the produced groundwater of steel tubing grade K55 which its surface was prepared by sandpaper number 600 and 1200 is 0.0465 and 0.0376 mm/year respectively. While The calculated corrosion rate (CR) of steel tubing caused by the produced groundwater of steel tubing grade L80-13Cr which its surface was prepared by sandpaper number 600 and 1200 is 0.0169 and 0.0138 mm/year respectively. Therefore, the lifetime of the steel tubing grade K55 which its surface was prepared by sandpaper number 600 and 1200 is 12 years and 15 years. Whereas the lifetime of the steel tubing grade L80-13Cr which its surface was prepared by sandpaper number 600 and 1200 is 33 years and 40 years, respectively. Therefore, it can be conclude that at any steel stubbing grade the finer surface steel plate will have the less corrosion rate than the coarser surface steel plate.

Moreover, after the corrosion test had been completed it was found that the groundwater which was used for K55 corrosion test had the Total Dissolved Solid (TDS) more than those of L80-13Cr since some solids were lost from K55 specimen during the test easier than L80-13Cr. This is also conform to the result of weight loss and corrosion rate test. It can be also noticeable from the wear test that the steel tubing grade L80-13Cr has the weight loss less than K55 since it contains more Chromium (Cr).

5.2 Recommendations

This study has some limitations on steel tubing samples, corrosions solution, and some equipment capability which were used in this study. In order to improve the

condition of corrosion and erosion, the future study might be considered the following issues.

1) The corrosion solution should be changed and collected from various sources to study the effect of corrosion solution composition.

2) Surface roughness of the specimens should be varied.

3) The corrosion solution should be test at various temperatures to study the effect of temperature on the corrosion rate.

REFERENCES

Ahmad, Z. (2006). **Principles of Corrosion Engineering and Corrosion Control**. Boston: Elsevier.

ASTM Standard G65-16 (2007). **Standard Test Method for Measuring Abrasion Using the Dry Sand/Rubber Wheel Apparatus**. Annual Book of ASTM Standards, American Society for Testing and Materials, West Conshohocken, PA.

API Specification 5CT (2005). **Specification for Casing and Tubing** (8th ed). Petroleum and natural gas industries - Steel pipes for use as casing or tubing for wells, American Petroleum Institute, API Publishing Services, Washington, D.C.

Bellarby, J. (2009). **Well completion design.** Amsterdam, Netherlands: Elsevier Science.

Bhavsar, R. B., and Montani, R. (1998). **Application of Martensitic Modified Martensitic and Duplex Stainless Steel Bar Stock for Completion Equipment.** United States: NACE International, Houston, TX.

Blackburn, N. A. (1994). **Downhole Material Selection for Clyde Production Wells: Theory and Practice.** Society of Petroleum Engineers.

Bradford, S. A. (2001). **Corrosion Control** (2nd ed). Edmonton: CASTI Pub.

Chen, C. F., Lu, M. X., and Sun, D. B. (2005). Effect of Chromium on the Pitting Resistance of Oil Tube Steel in a Carbon Dioxide Corrosion System. **Corrosion Engineering.** 61(6): 594-601.

Cheng-Hong, P., Zheng-Yi L., and Xing-Zhao, W. (2012). Failure analysis of a steel tube joint perforated by corrosion in a well-drilling pipe. **Engineering Failure Analysis**. 25: 13-28.

Clark, D. S., and Varney, W. R. (1962). **Physical Metallurgy for Engineers**. Van Nostrand Reinhold Company.

Fontana, M. G. (1986). **Corrosion Engineering**. New York: McGraw-Hil.

Gair, D. J., and Moulds, T. P. (1988). **Tubular Corrosion in the West Sole Gas Field**. Society of Petroleum Engineers.

Heidersbach, R. (2011). **Metallurgy and corrosion control in oil and gas production**. New Jersey: Wiley

Ilman, M. N., and Kusmono, (2014). Analysis of corrosion in subsea oil pipeline. **Case studies in Engineering Failure Analysis**. 2(1): 1-8.

Jones, D. A. (1997). **Principles and Prevention of Corrosion** (2nd ed). New York: Maxwell Macmillan International Pub. Group.

Kane, R. (2006). **Corrosion in Petroleum Production Operations**. ASM Handbook Corrosion: Environments and Industries, Vol. 13C, ASM International Material Park.

Kimura, M., Sakata, K., and Shimamoto, K. (2007). **Corrosion Resistance of Martensitic Stainless Steel OCTG in Severe Corrosion Environments**. Corrosion. NACE Press book.

Martinez, D., et. Al. (2009). Amine type inhibitor effect on corrosion–erosion wear in oil gas pipes. **Wear**. 267(1-4): 255-258.

McCafferty, E. (2009). **Introduction to Corrosion Science**. New York: Springer.

Migahed, M. A., and Nassar, I. F. (2008). Corrosion inhibitor of tubing steel during acidization of oil and gas wells. **ElectrochimicaActa.** 53(6): 2877-2882.

Nabhani, F., Jasim, A. M., and Graham, S.W. (2007). Electrochemical Behaviour of Low Carbon Steel in Aqueous Solutions. In **Proceedings of the World Congress on Engineering** 2007 (Vol. 2). London, U.K.

Palmer, A. C., and King, R. A. (2004). **Subsea pipeline engineering**. United States of America: PennWell.

Papadakis, G. A. (1999). Major hazard pipelines: a comparative study of onshore transmission accidents. **Journal of Loss Prevention in the Process Industries.** 12: 91-107.

Pollack, H. W. (1988). **Materials Science and Metallurgy** (4th ed). Englewood Cliffs, N.J.: Prentice-Hall

Revie, R. W., and Uhlig, H. H. (2008). **Corrosion and Corrosion Control: An introduction to corrosion science and engineering** (4th ed). New York: Wiley.

Roberge, P. R. (2006). **Corrosion Basics: An Introduction** (2nd ed). NACE Press book.

Rodriguez, H. M. A. L., et al. (2007). Corrosion wear failure analysis in a nature in a nature gas pipeline. **Wear**. 263(1-6): 567-571.

Sekunowo, O. I., Adeosun, S. O. and Lawal, G. I. (2013). Potentiostatic Polariaztion Responser Of Mild Steel In Seawater And Acid Environments. **International Journal of Scientific & Technology research.** 2(10): 139-145.

Shreir, L. L. (1979). **Corrosion Volume 1: Metal/environmental reactions** (2nd ed). London, Boston: Newnes-Butterworths.

Tawancy, H. M., Al-Hadhrami, L. M., and Al-yourself, F. K. (2013). Analysis of corroded elbow section of carbon steel piping system of oil-gas separator vessel. **Case studies in Engineering Failure Analysis.** 1(1): 6-14.

Trethewey, K. R., and Chamberlain, J. (1995). **Corrosion for Science and Engineering** (2^{nd} ed). Harlow, England: Longman.

Waard, D. C., Lotz, U., and Milliams, E. D. (1991). Predictive Model for CO_2 Corrosion Engineering in Wet Natural Gas Pipelines Corrosion. **Corrosion Engineering.** 47(12): 976-985.

Yahya, S., Othman, N. K., Daud, A. R., and Jalar, A. (2014). Effect of Scan Rate on Corrosion Inhibition of Carbon Steel in the Presence of Rice Straw Extract-Potentiodynamic Studies. **Sains Malaysiana**. 43(7): 1083-1087.

Zhu, X., Liu, S., Tong, H., Huang, X., and Li, J. (2012). Experimental and numerical study of drill pipe erosion wear in gas drilling. **Engineering Failure Analysis.** 26: 370-380.

APPENDIX A

POLARIZATION OF THE CORROSION RATE

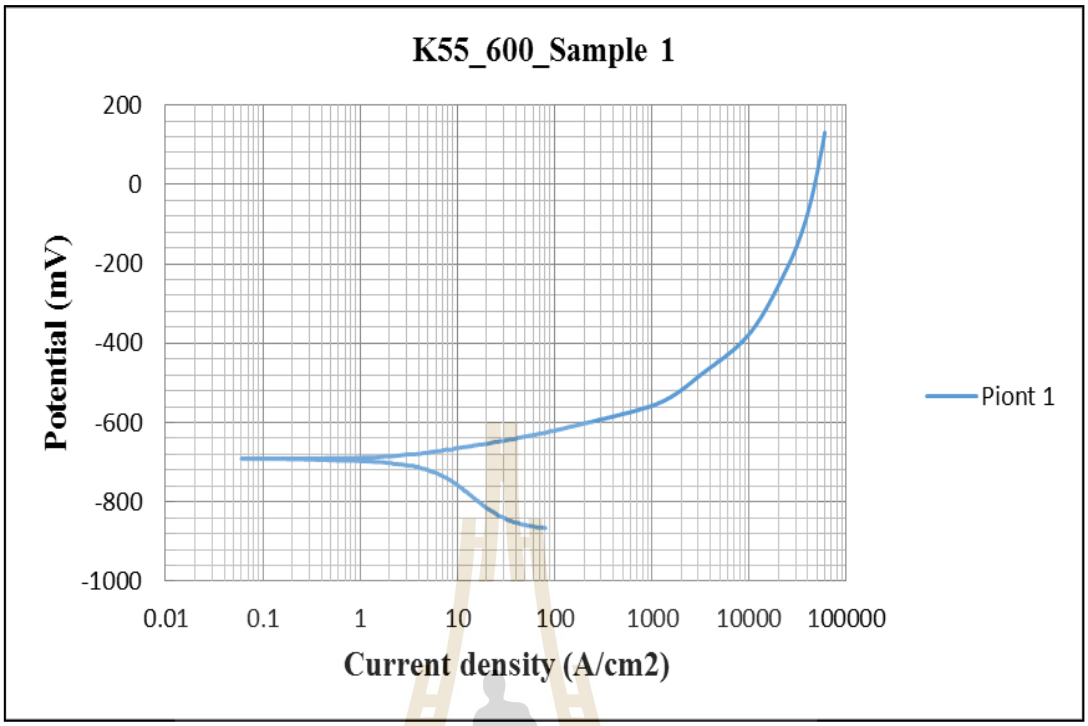

Figure A1 Polarization of K55 (API 5CT), No.600, Sample 1, Point 1

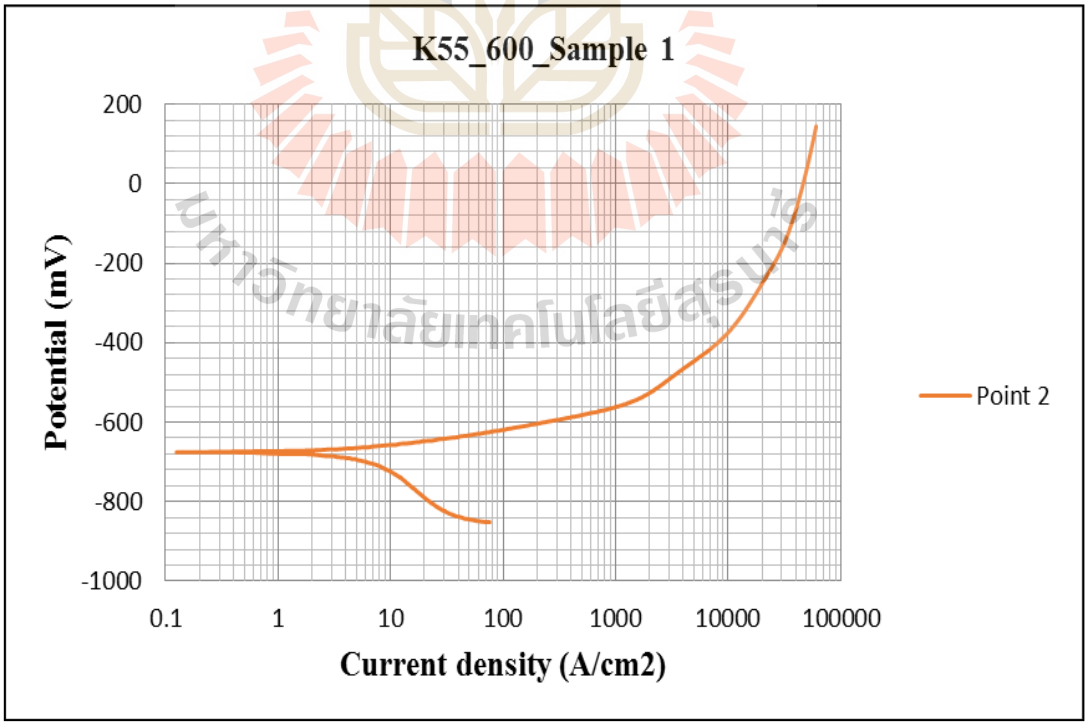

Figure A2 Polarization of K55 (API 5CT), No.600, Sample 1, Point 2

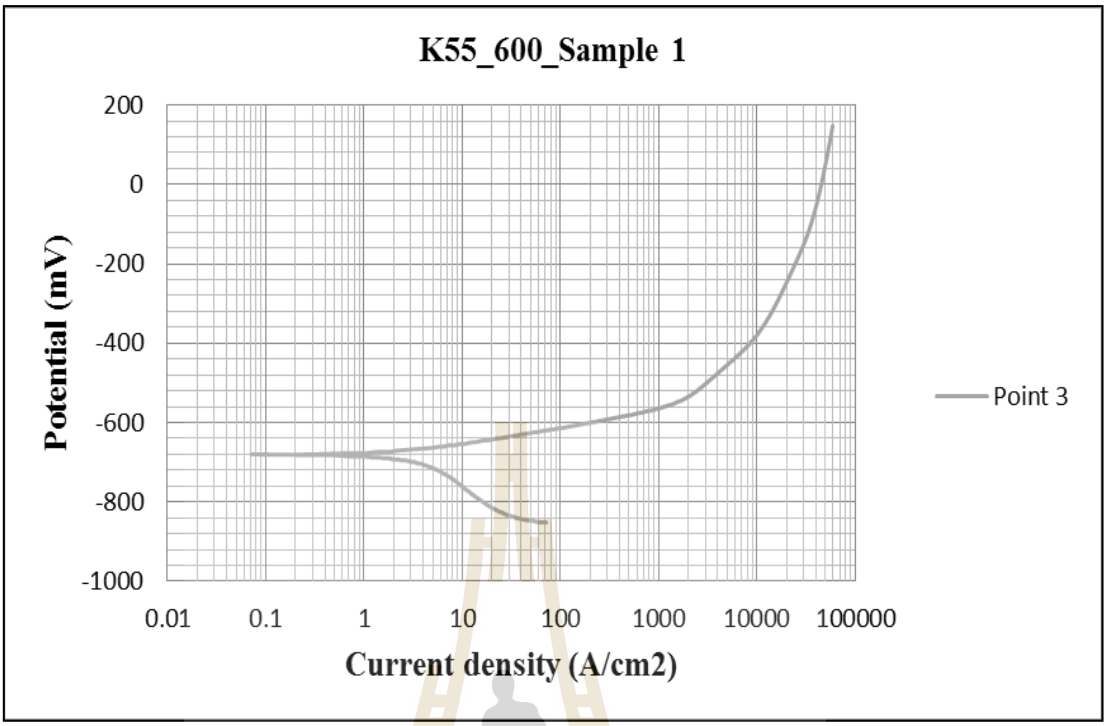

Figure A3 Polarization of K55 (API 5CT), No.600, Sample 1, Point 3

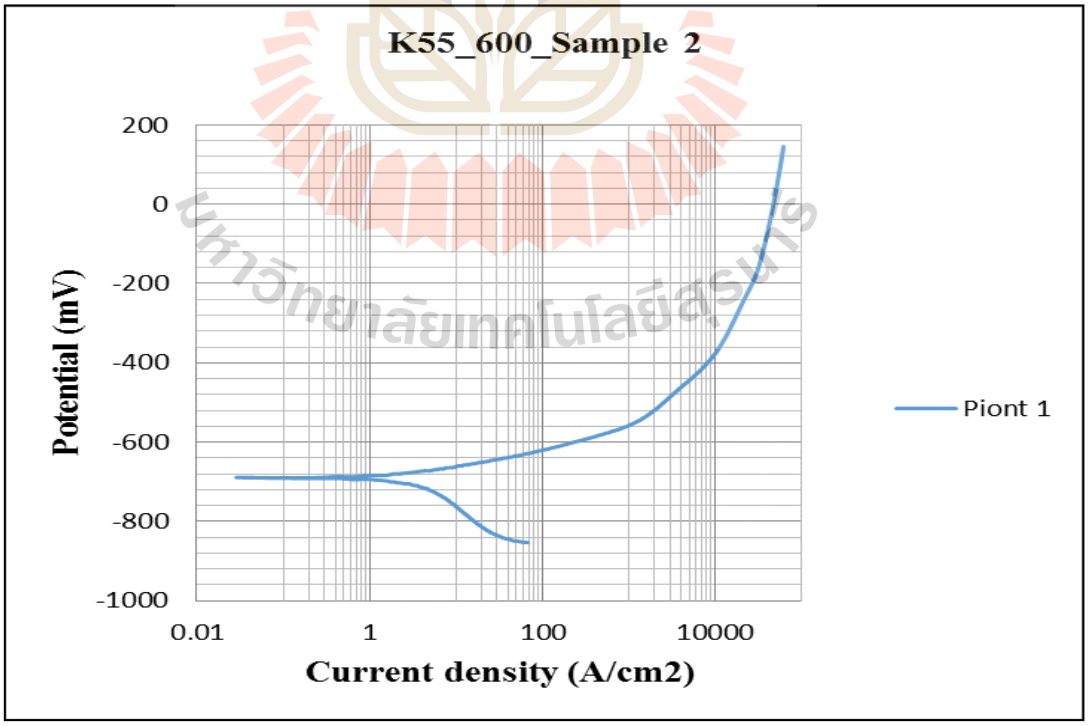

Figure A4 Polarization of K55 (API 5CT), No.600, Sample 2, Point 1

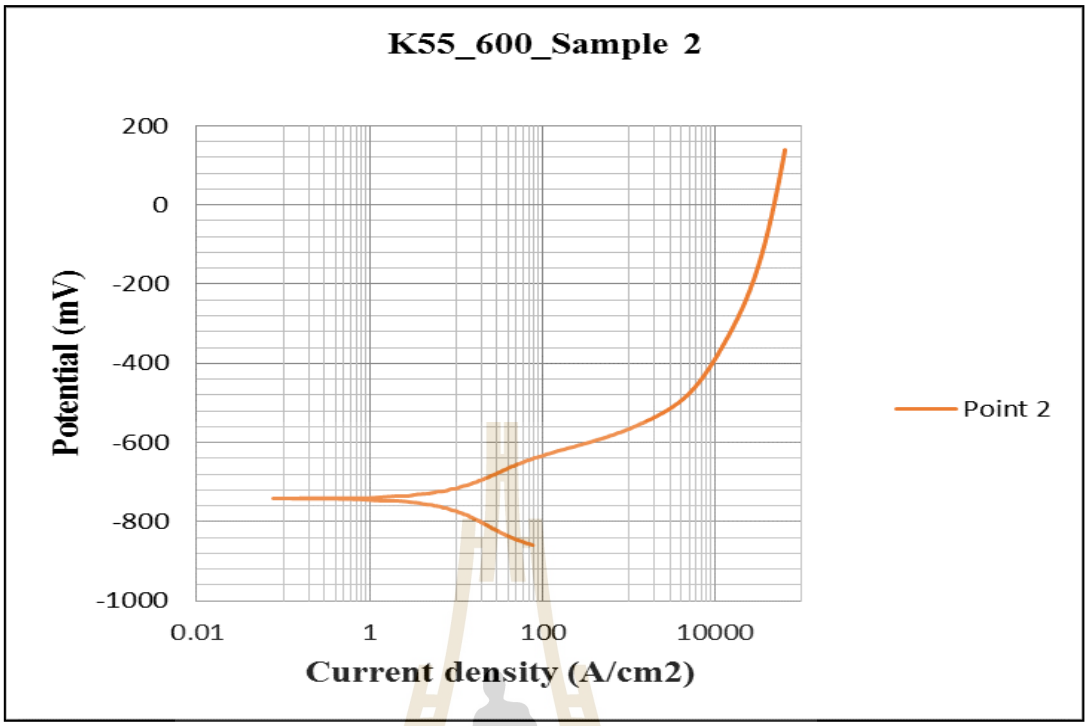

Figure A5 Polarization of K55 (API 5CT), No.600, Sample 2, Point 2

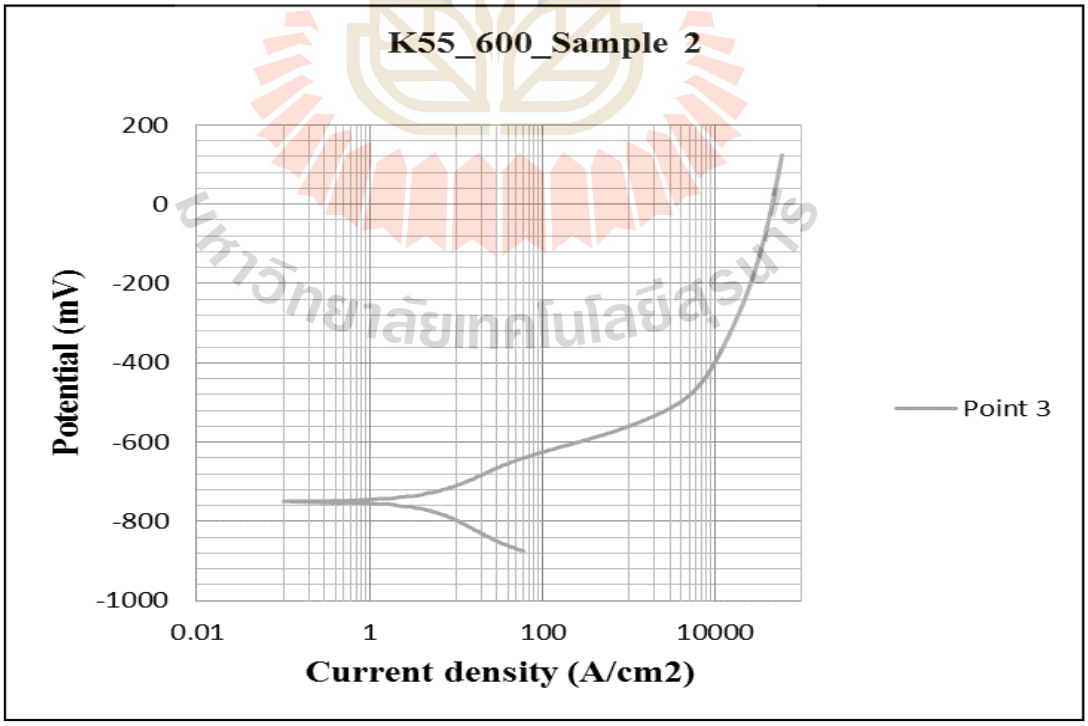

Figure A6 Polarization of K55 (API 5CT), No.600, Sample 2, Point 3

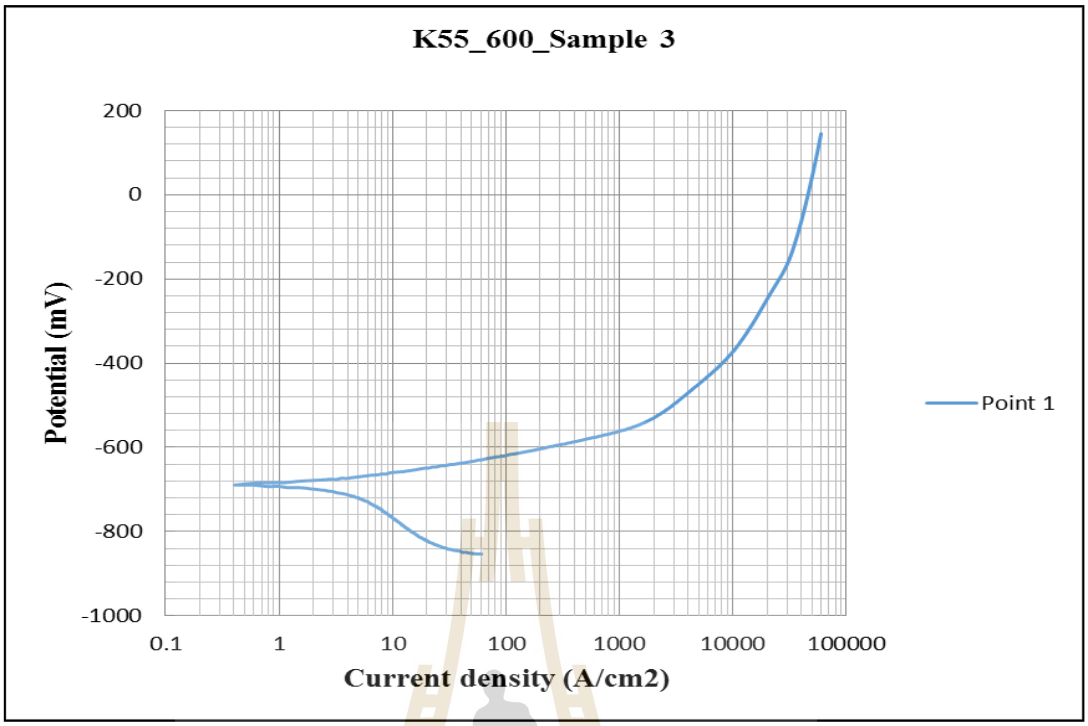

Figure A7 Polarization of K55 (API 5CT), No.600, Sample 3, Point 1

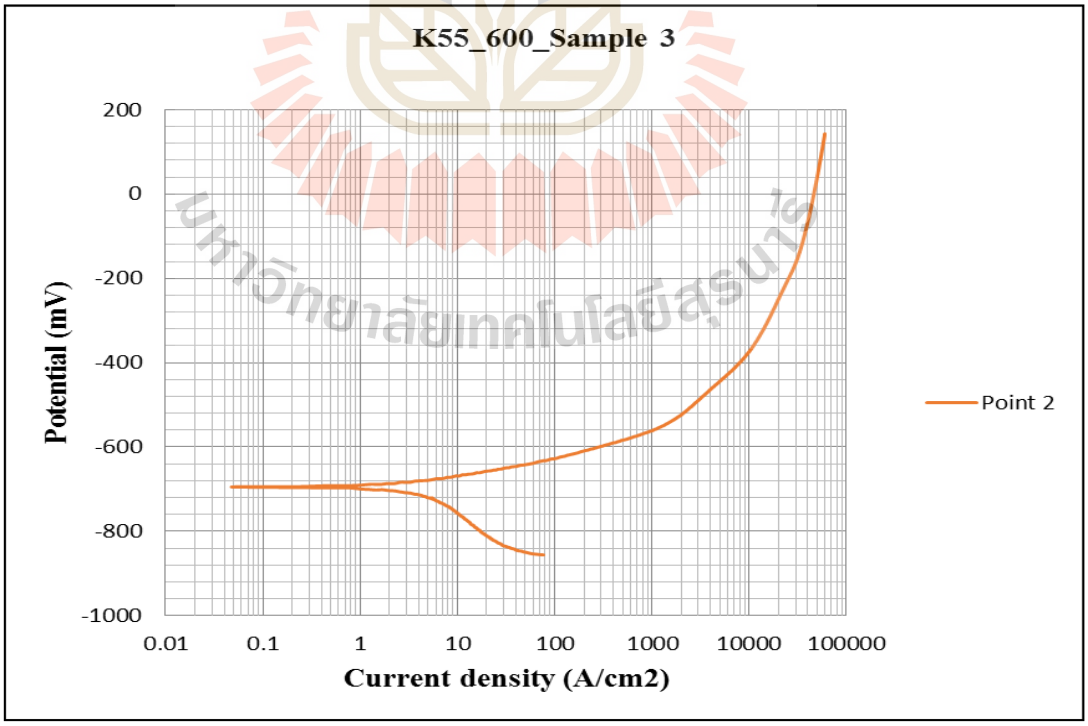

Figure A8 Polarization of K55 (API 5CT), No.600, Sample 3, Point 2

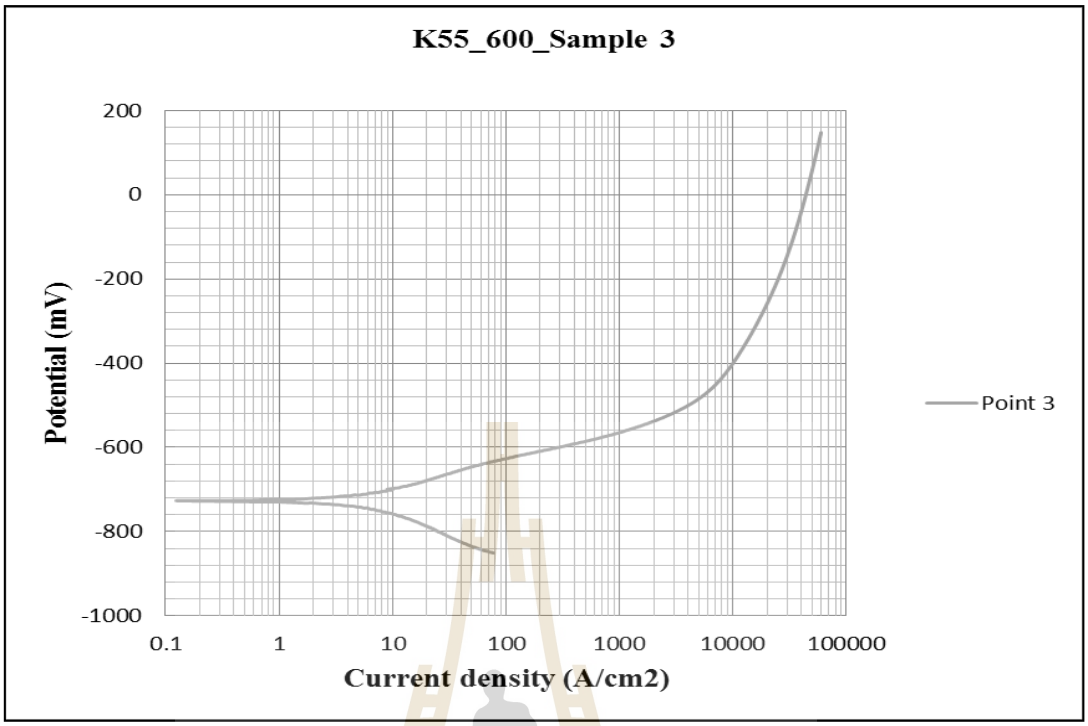

Figure A9 Polarization of K55 (API 5CT), No.600, Sample 3, Point 3

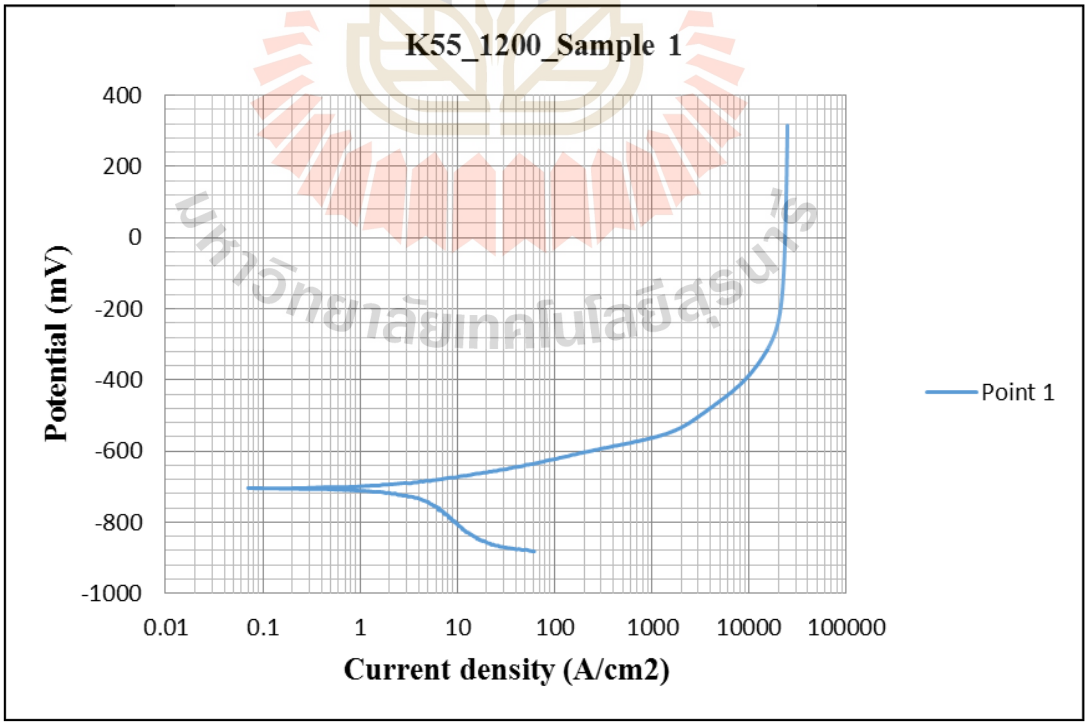

Figure A10 Polarization of K55 (API 5CT), No.1200, Sample 1, Point 1

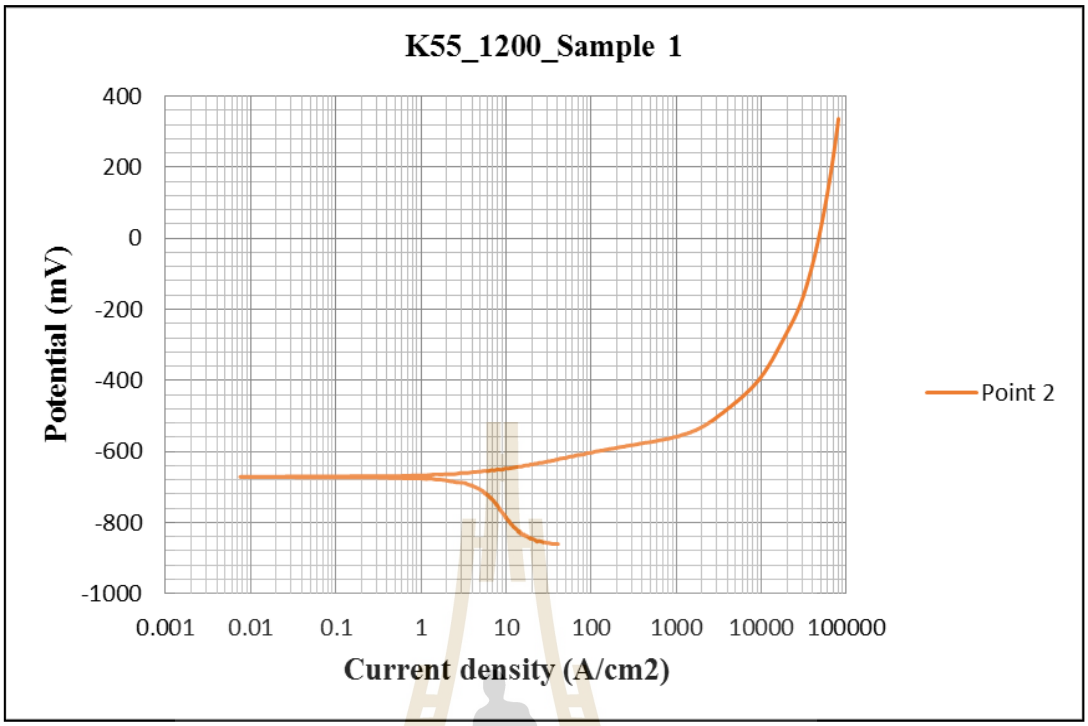

Figure A11 Polarization of K55 (API 5CT), No.1200, Sample 1, Point 2

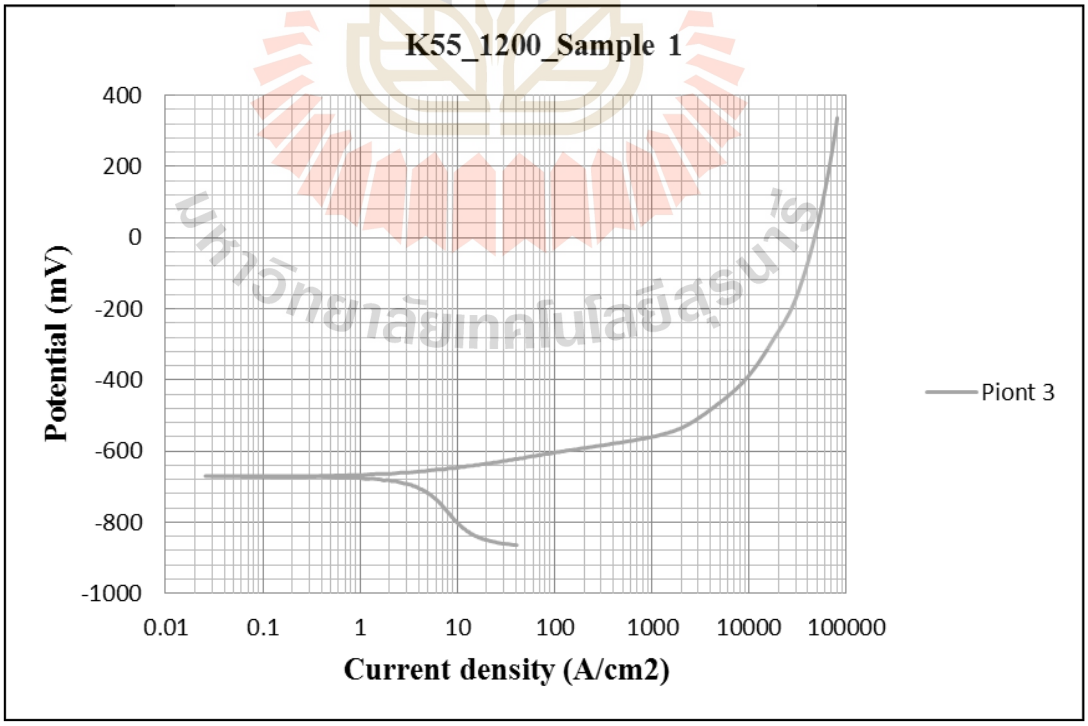

Figure A12 Polarization of K55 (API 5CT), No.1200, Sample 1, Point 3

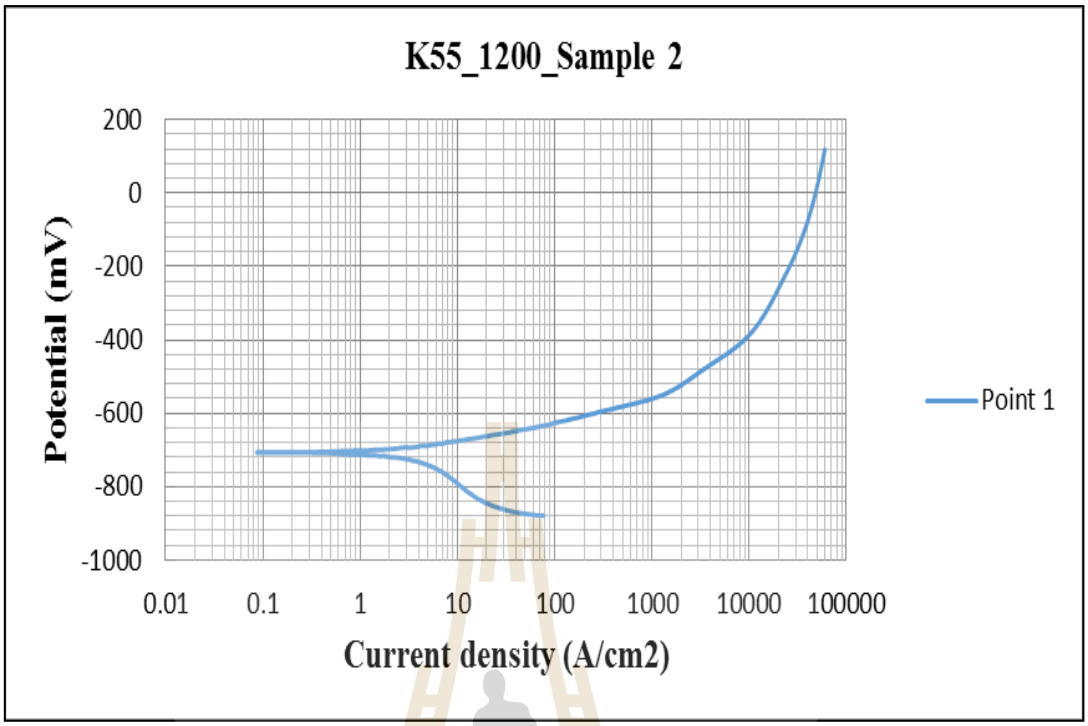

Figure A13 Polarization of K55 (API 5CT), No.1200, Sample 2, Point 1

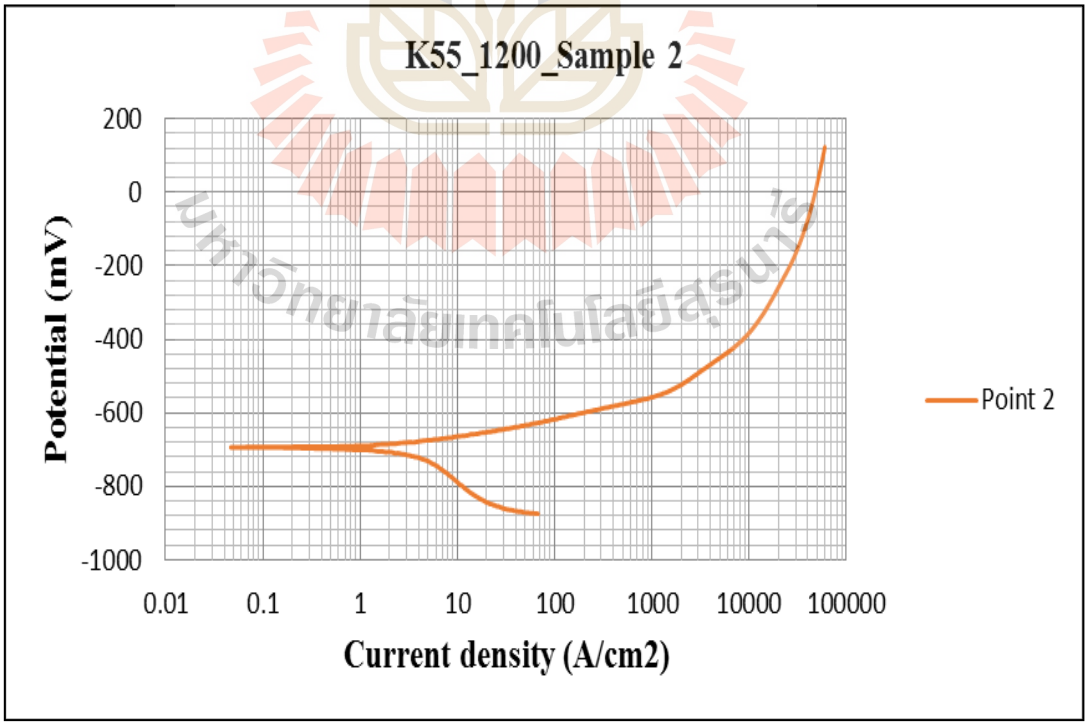

Figure A14 Polarization of K55 (API 5CT), No.1200, Sample 2, Point 2

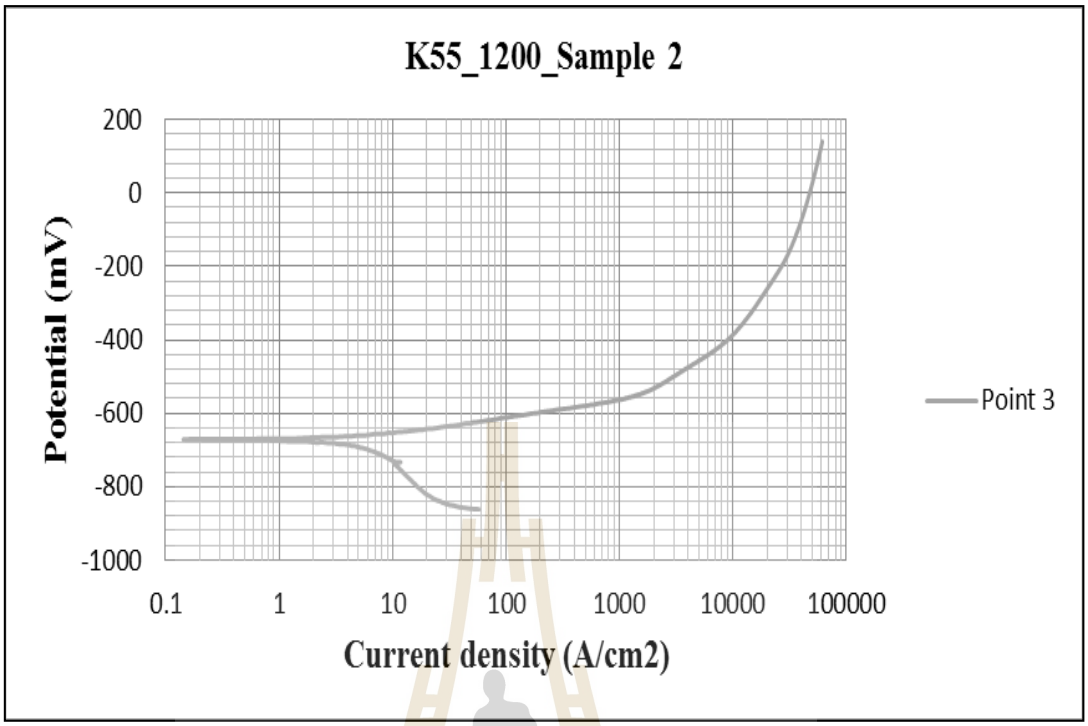

Figure A15 Polarization of K55 (API 5CT), No.1200, Sample 2, Point 3

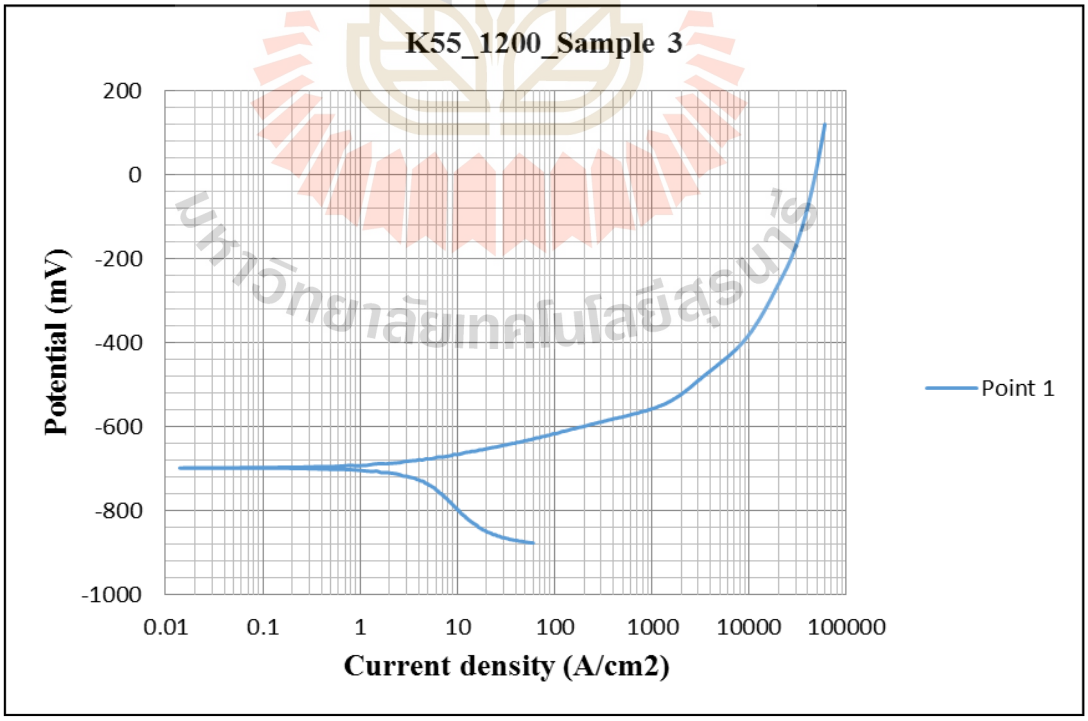

Figure A16 Polarization of K55 (API 5CT), No.1200, Sample 3, Point 1

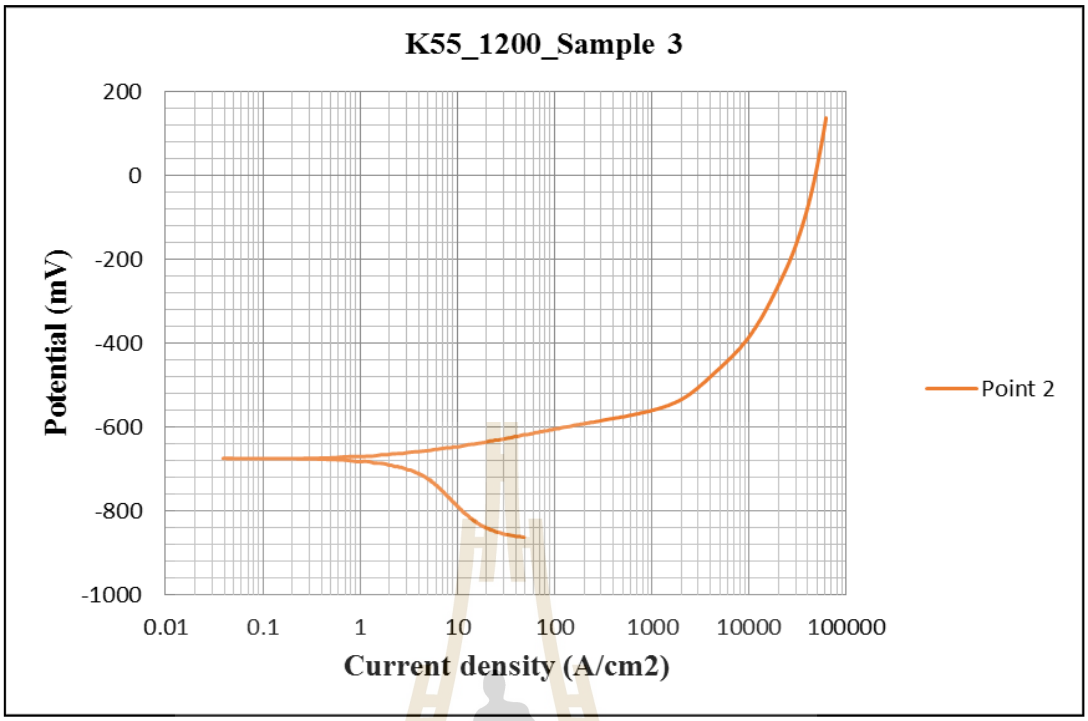

Figure A17 Polarization of K55 (API 5CT), No.1200, Sample 3, Point 2

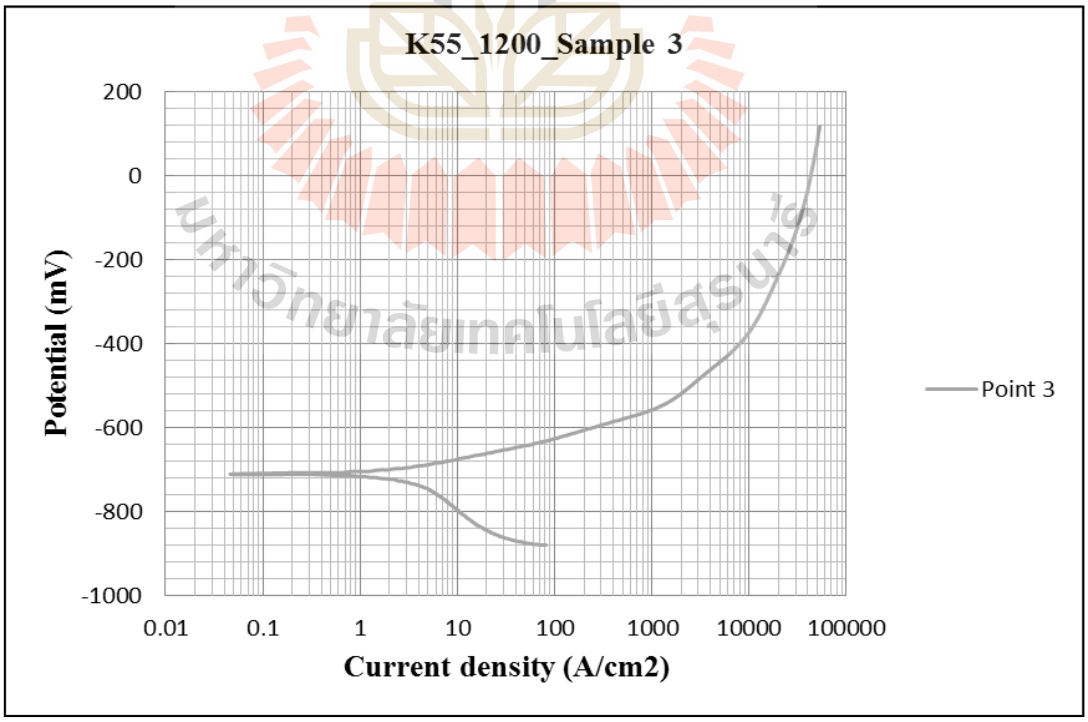

Figure A18 Polarization of K55 (API 5CT), No.1200, Sample 3, Point 3

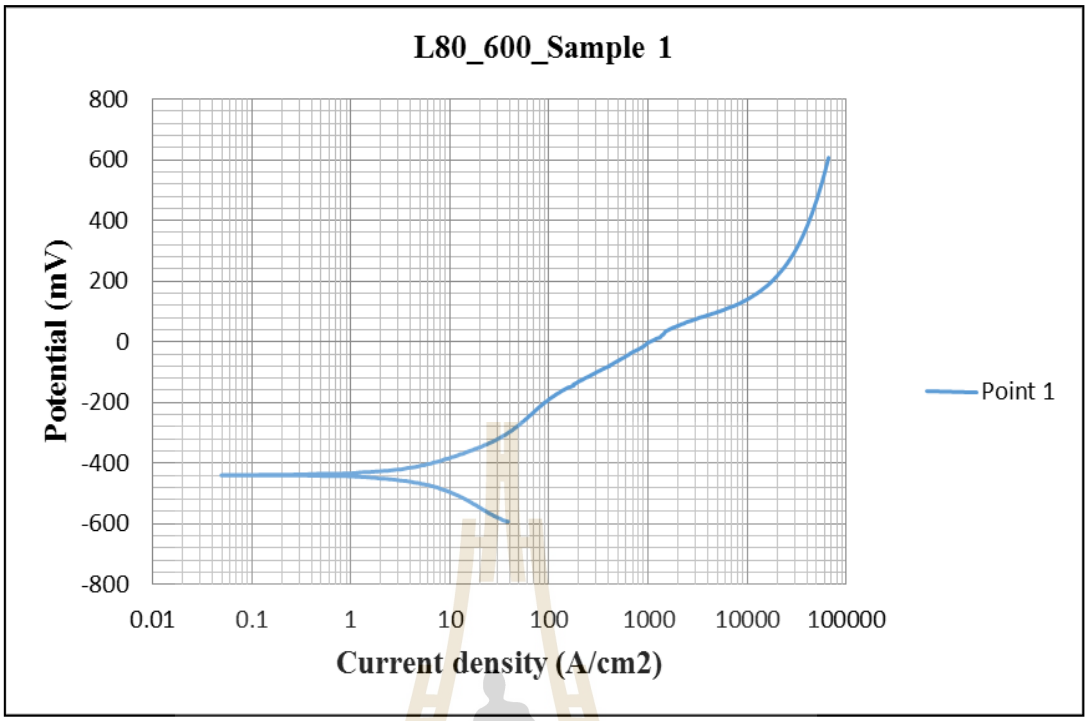

Figure A19 Polarization of L80 (API 5CT), No.600, Sample 1, Point 1

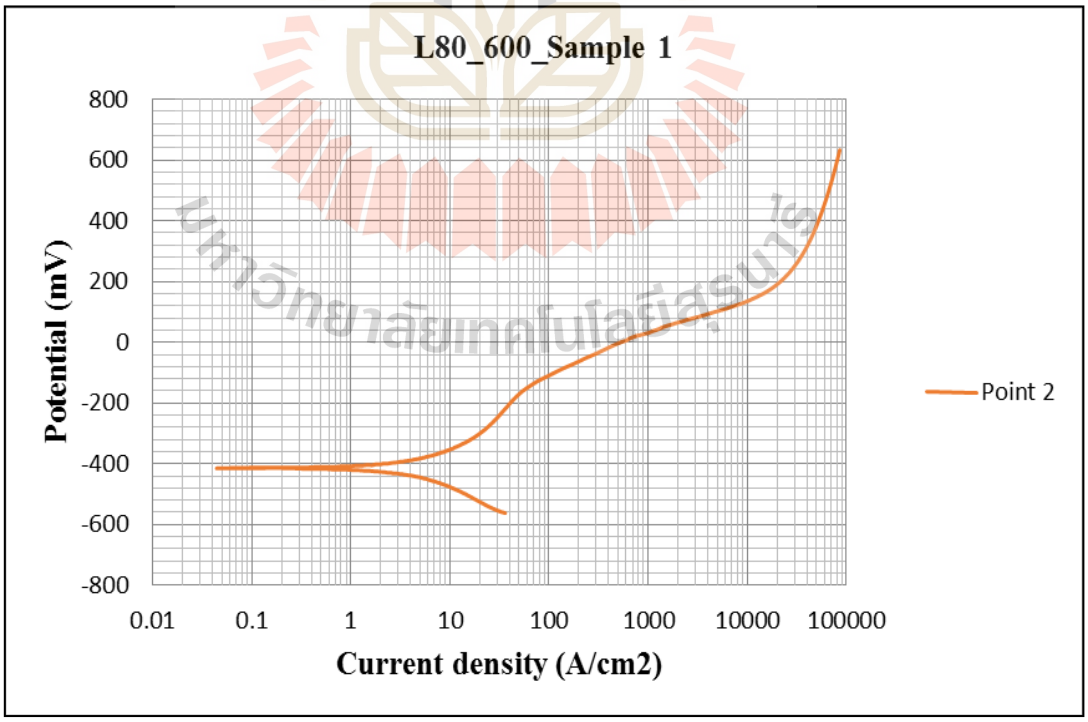

Figure A20 Polarization of L80 (API 5CT), No.600, Sample 1, Point 2

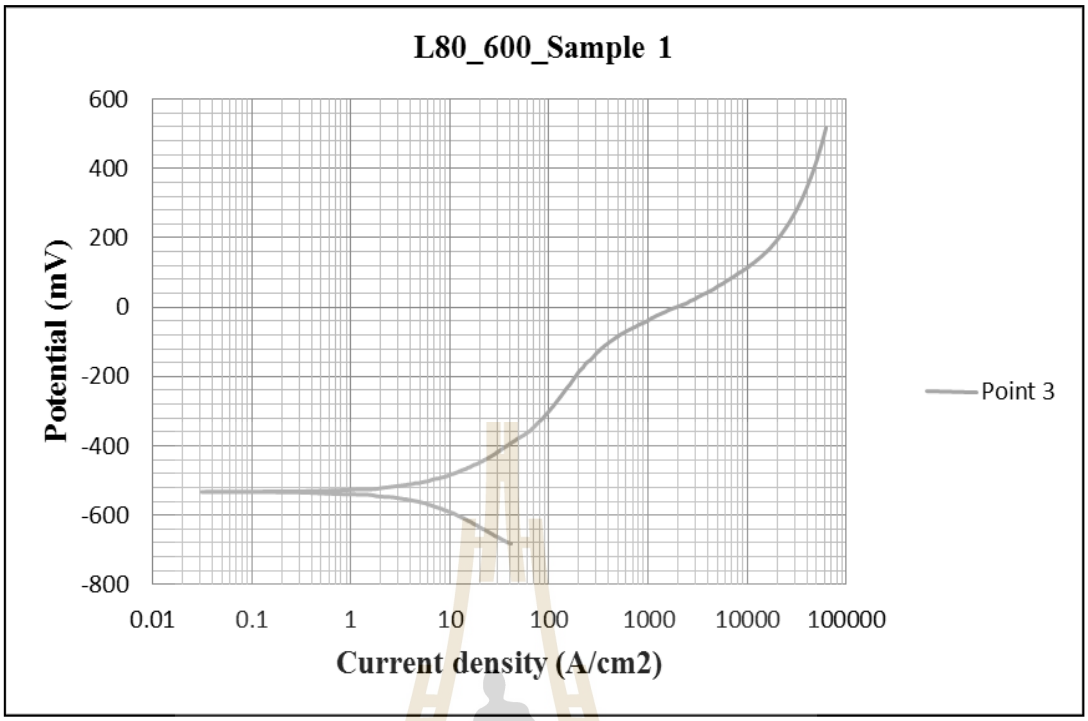

Figure A21 Polarization of L80 (API 5CT), No.600, Sample 1, Point 3

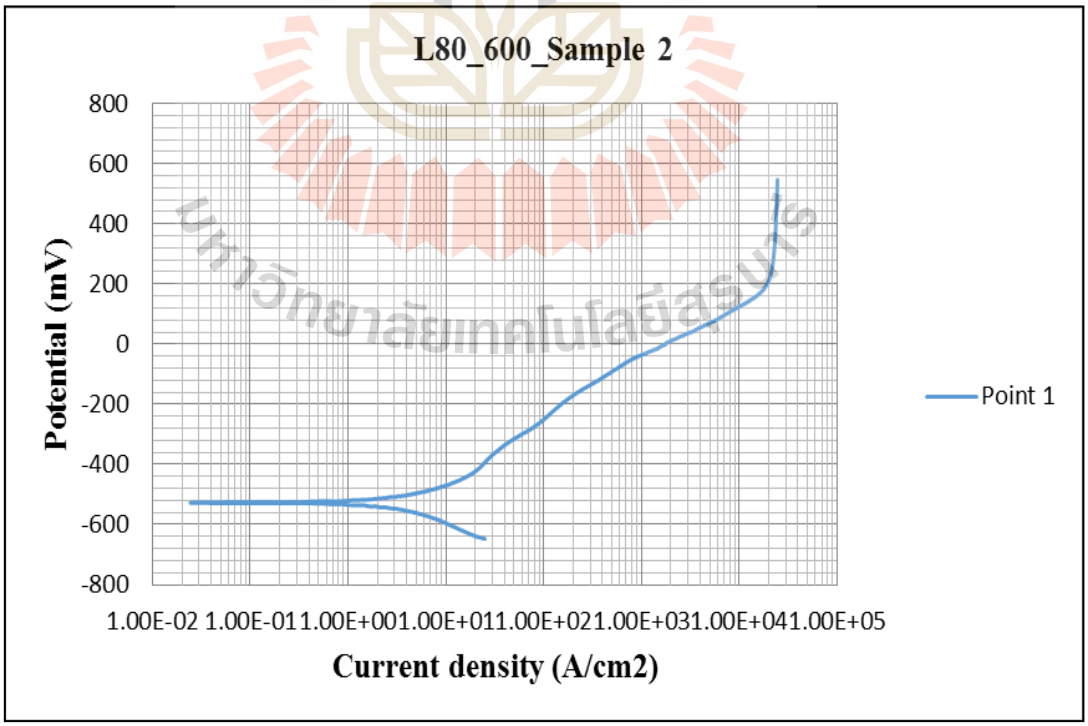

Figure A22 Polarization of L80 (API 5CT), No.600, Sample 2, Point 1

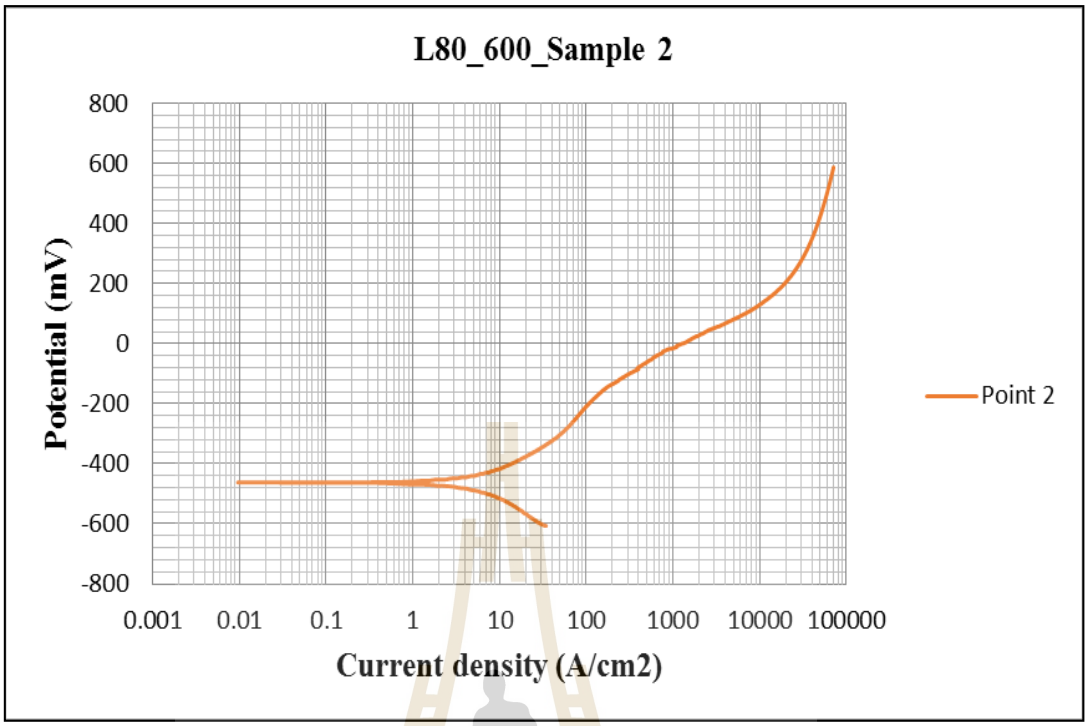

Figure A23 Polarization of L80 (API 5CT), No.600, Sample 2, Point 2

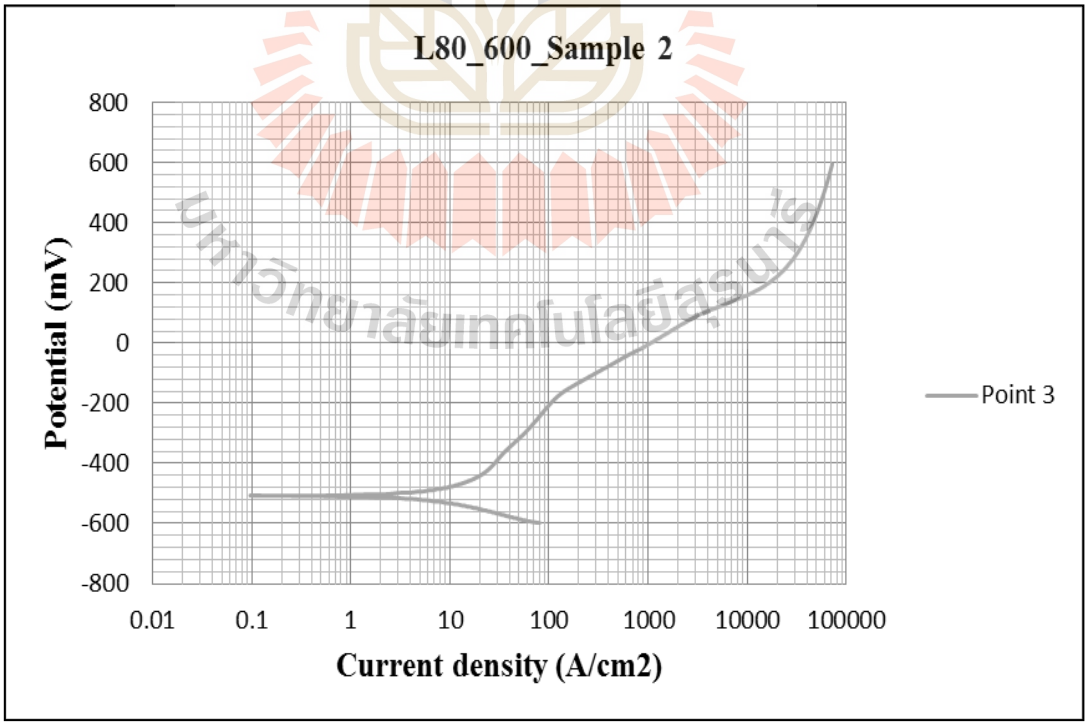

Figure A24 Polarization of L80 (API 5CT), No.600, Sample 2, Point 3

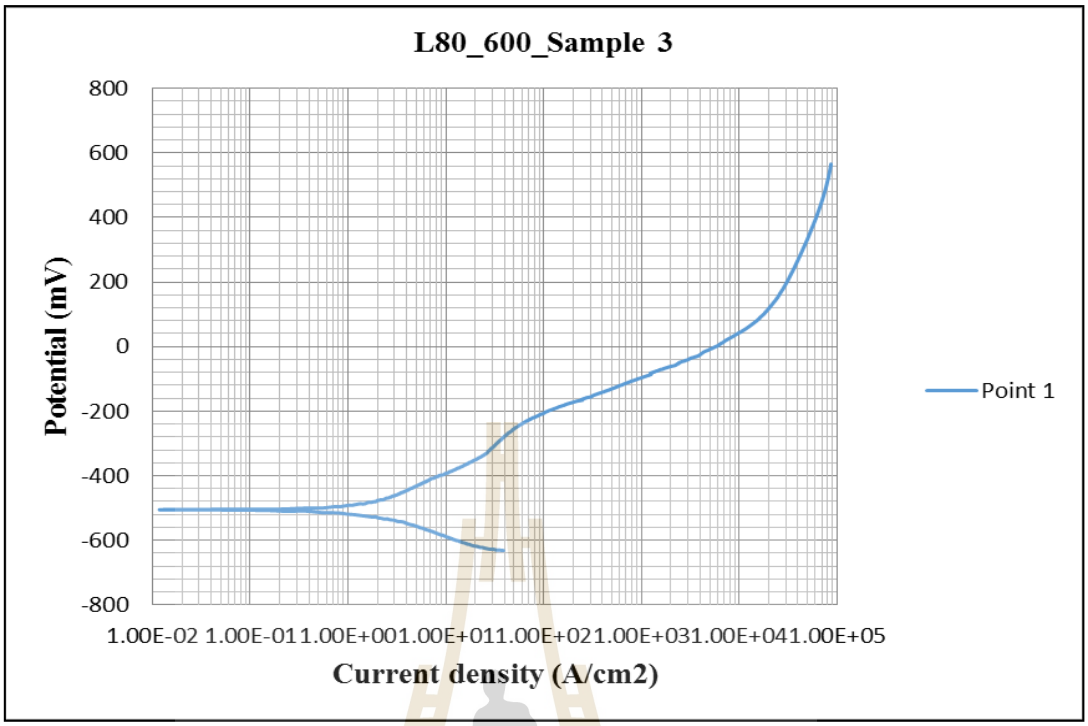

Figure A25 Polarization of L80 (API 5CT), No.600, Sample 3, Point 1

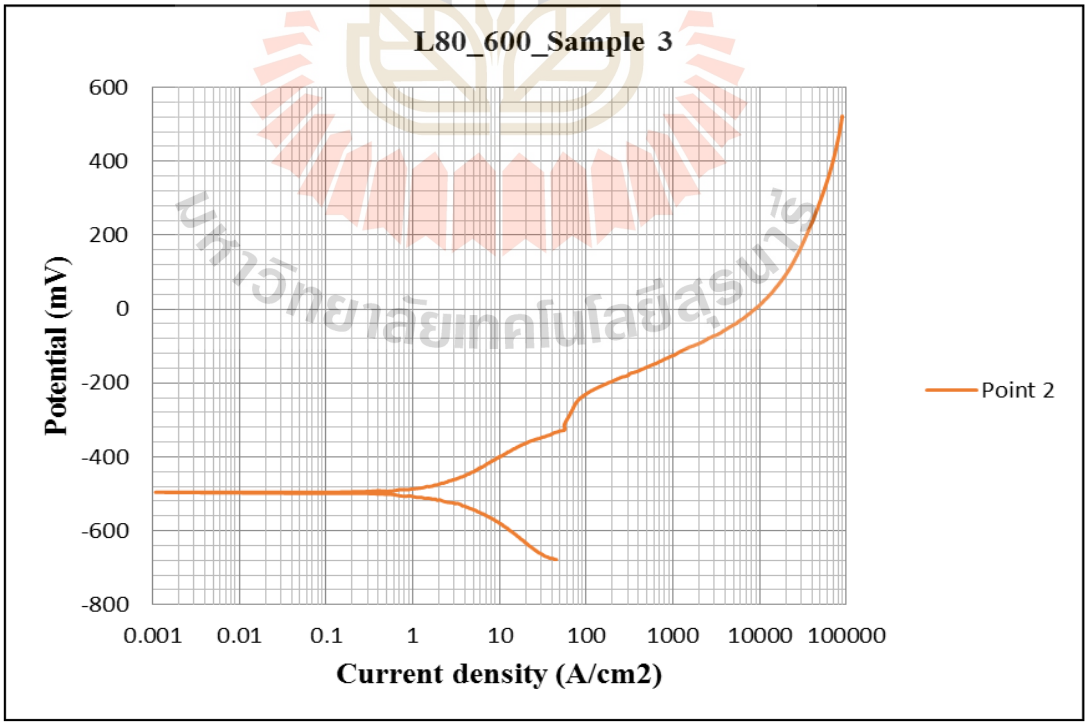

Figure A26 Polarization of L80 (API 5CT), No.600, Sample 3, Point 2

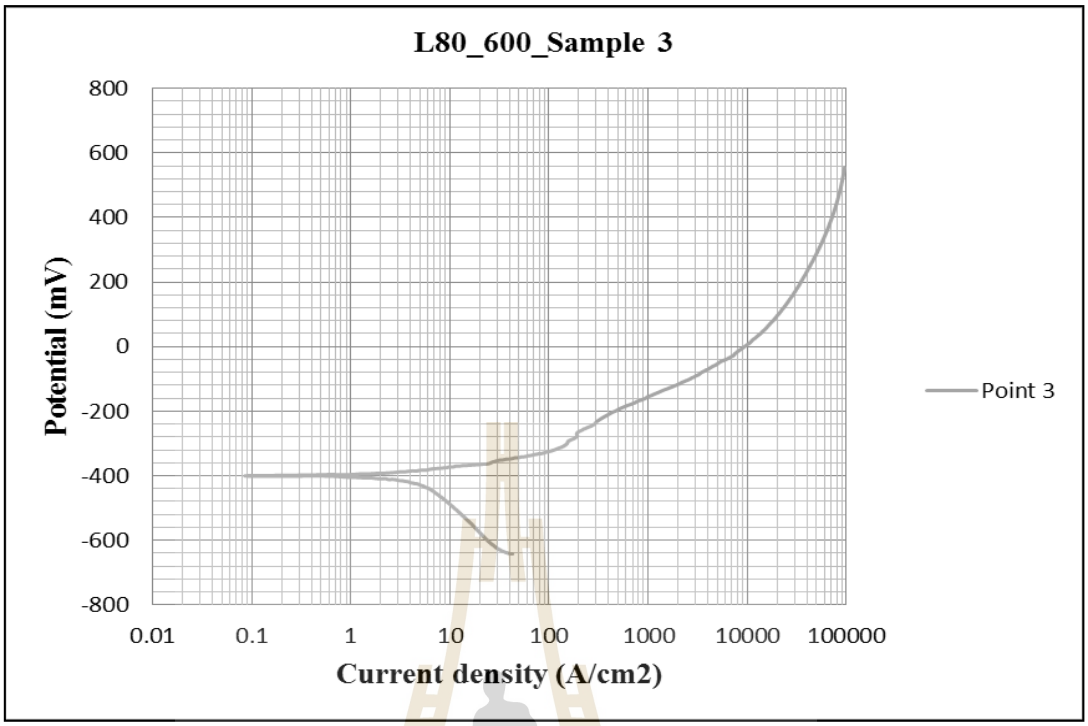

Figure A27 Polarization of L80 (API 5CT), No.600, Sample 3, Point 3

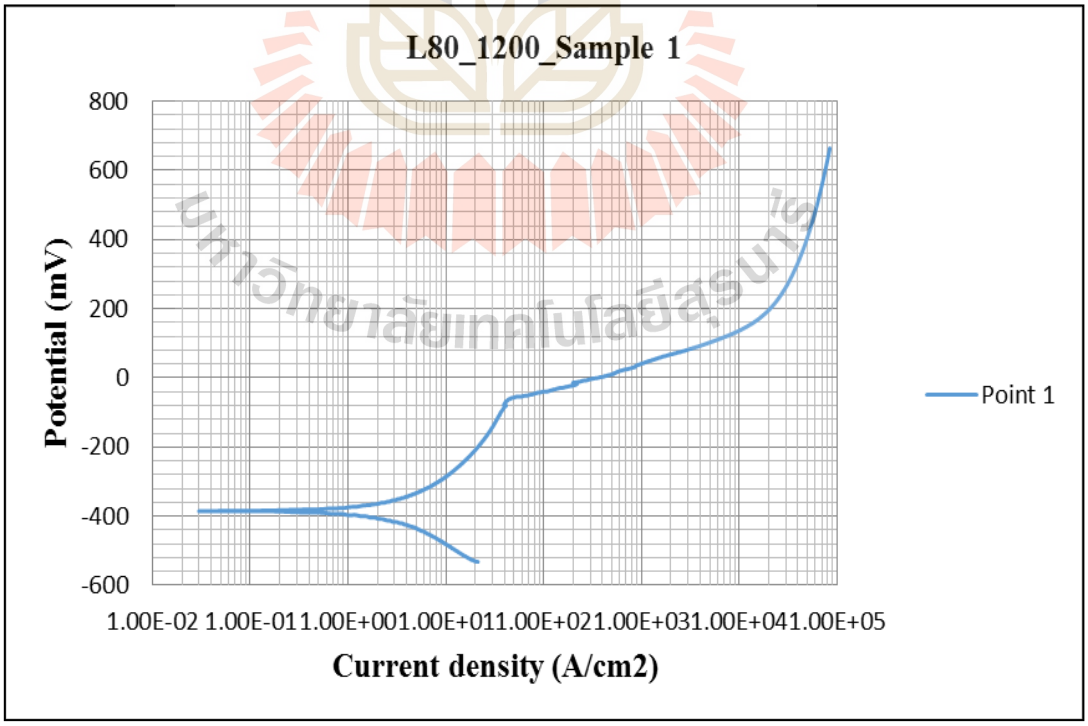

Figure A28 Polarization of L80 (API 5CT), No.1200, Sample 1, Point 1

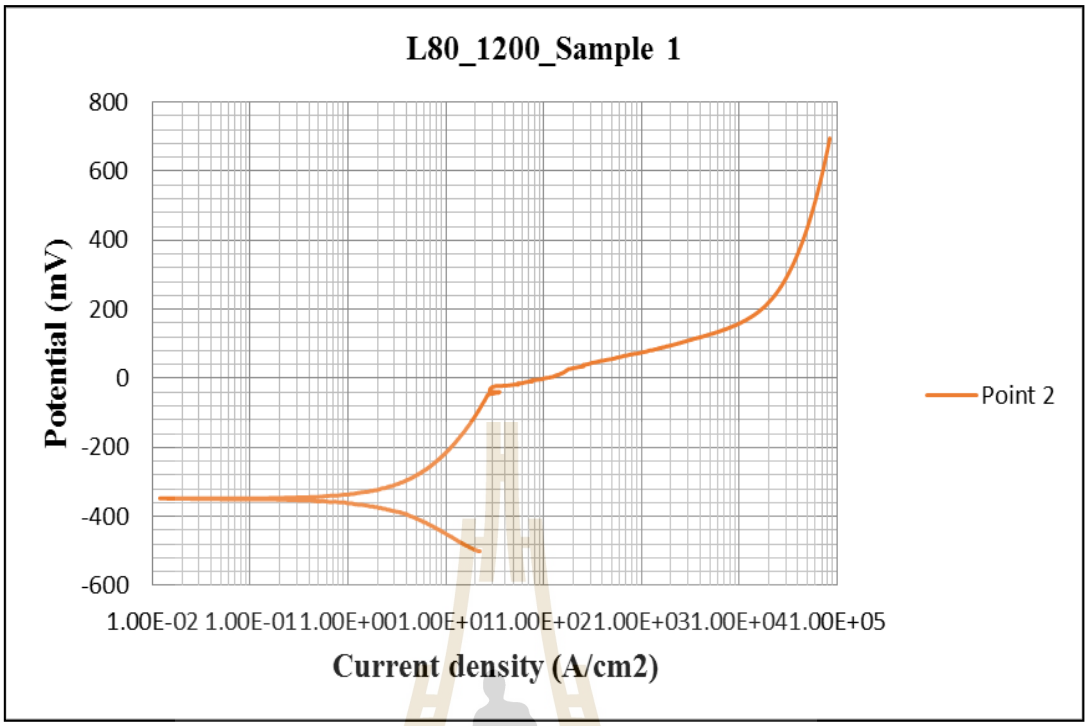

Figure A29 Polarization of L80 (API 5CT), No.1200, Sample 1, Point 2

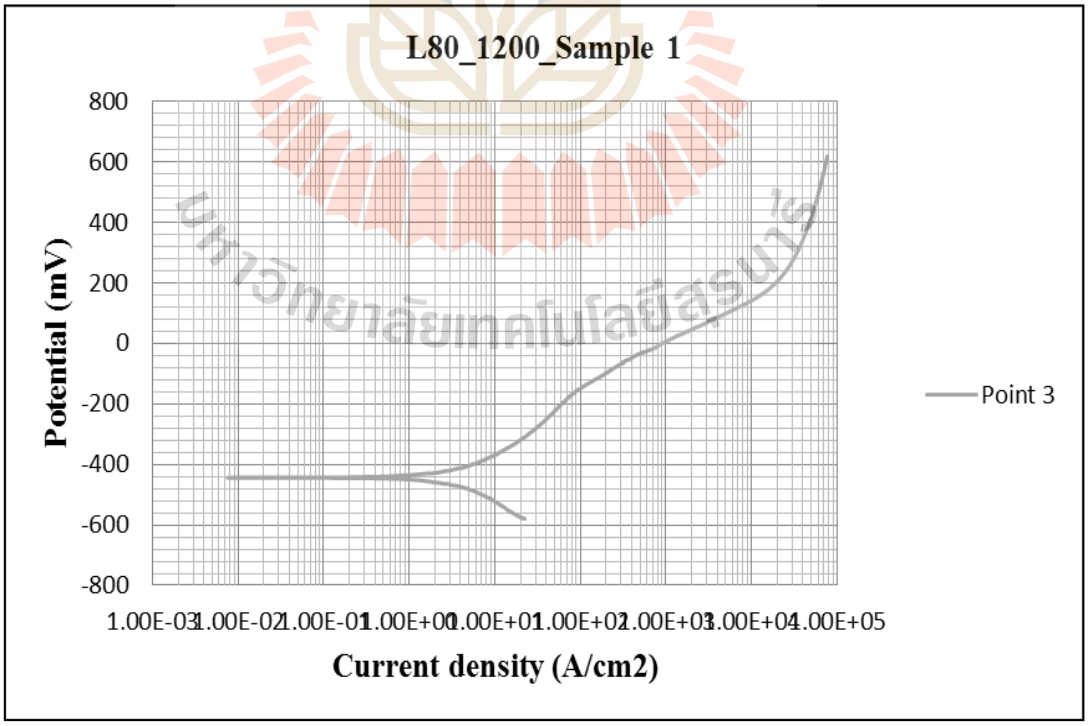

Figure A30 Polarization of L80 (API 5CT), No.1200, Sample 1, Point 3

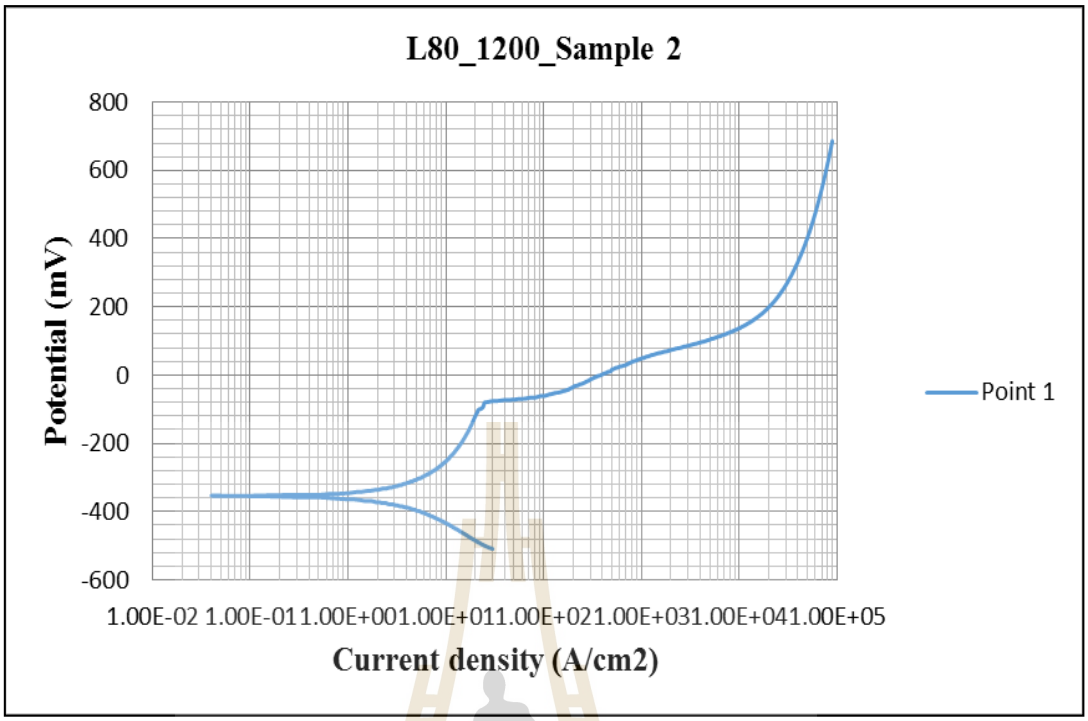

Figure A31 Polarization of L80 (API 5CT), No.1200, Sample 2, Point 1

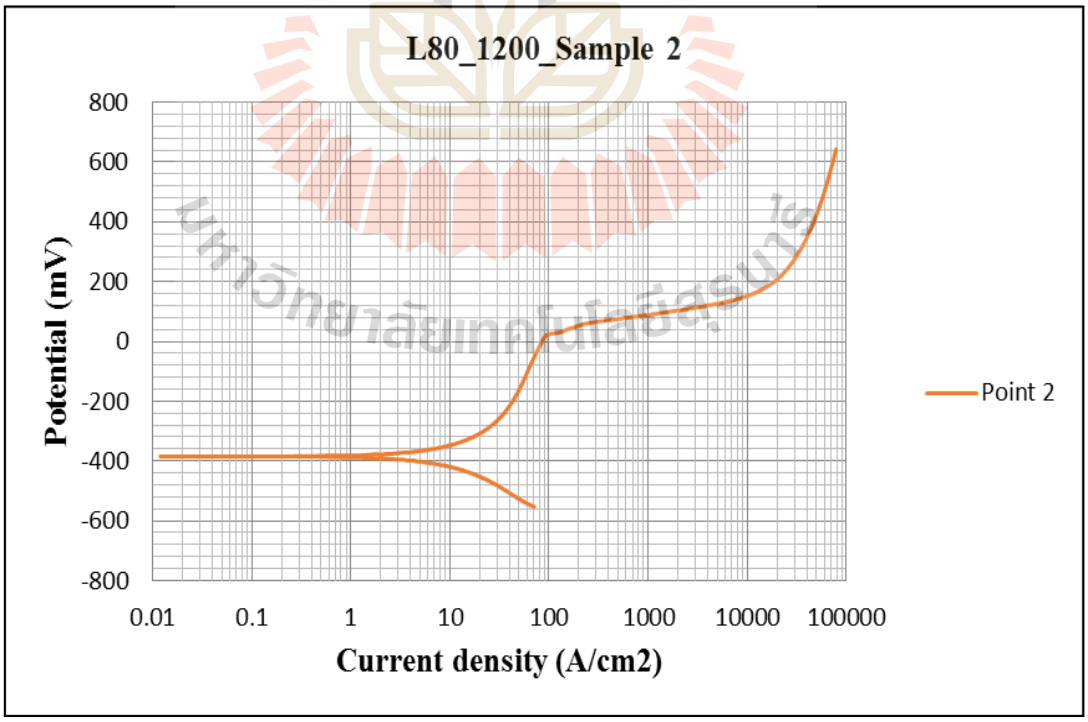

Figure A32 Polarization of L80 (API 5CT), No.1200, Sample 2, Point 2

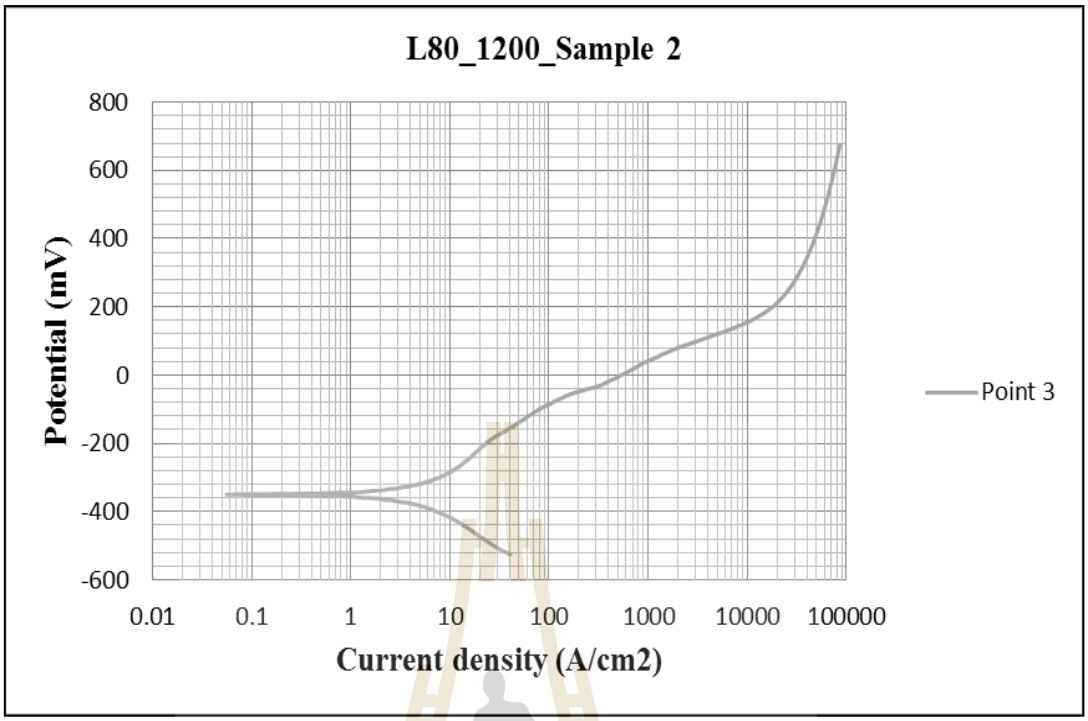

Figure A33 Polarization of L80 (API 5CT), No.1200, Sample 2, Point 3

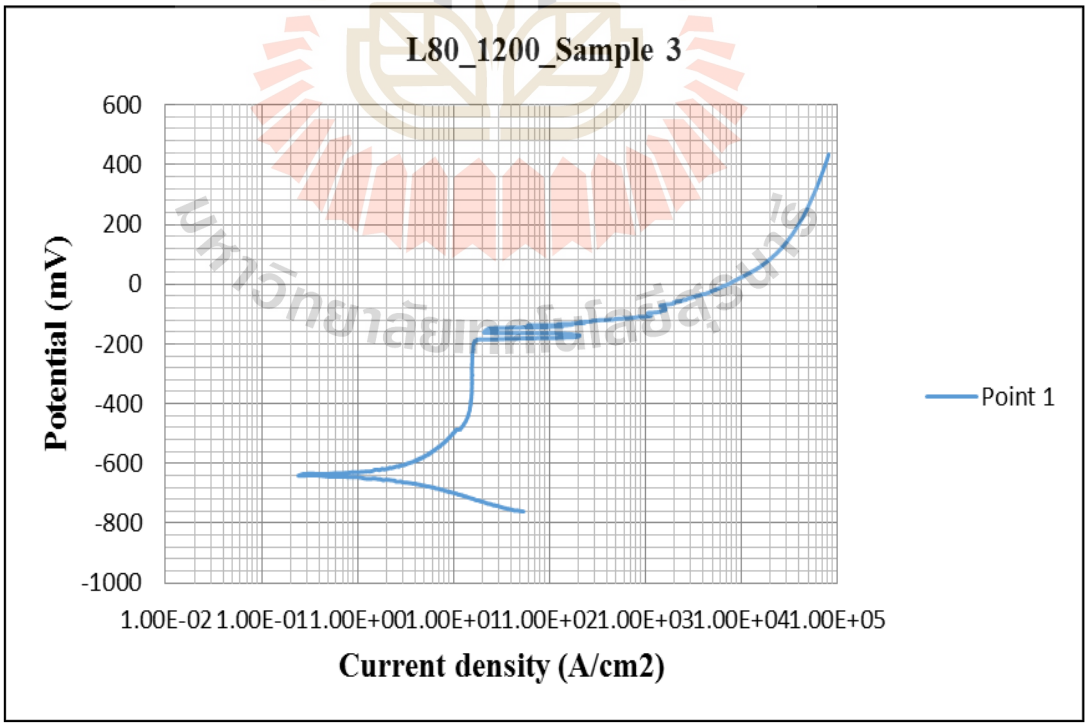

Figure A34 Polarization of L80 (API 5CT), No.1200, Sample 3, Point 1

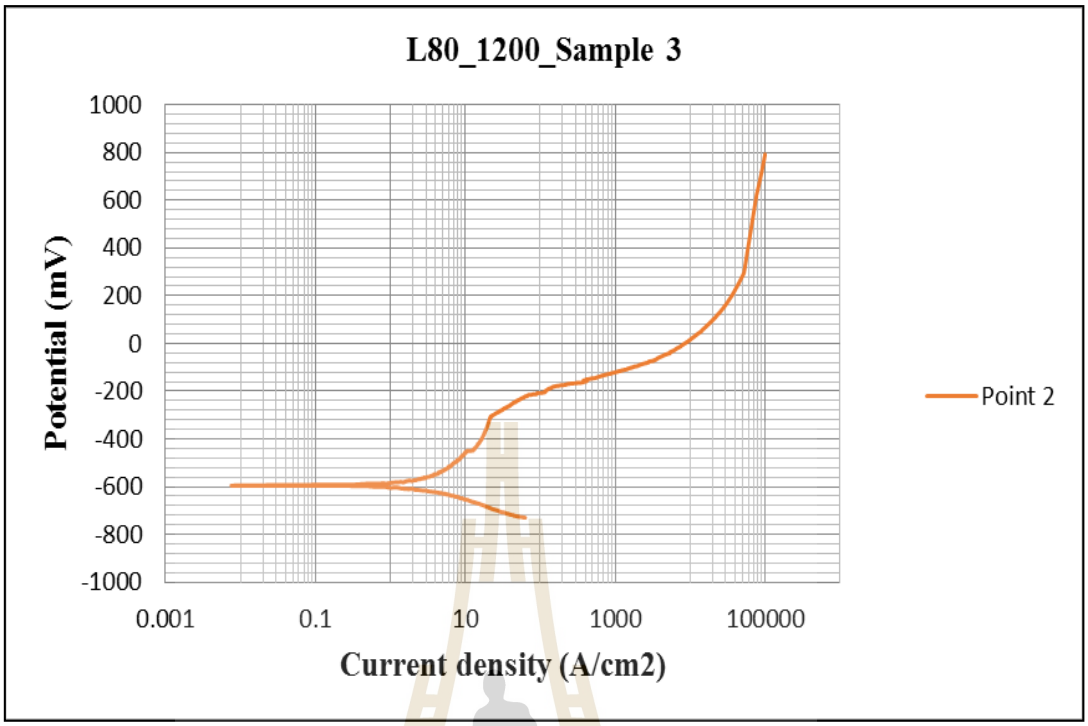

Figure A35 Polarization of L80 (API 5CT), No.1200, Sample 3, Point 2

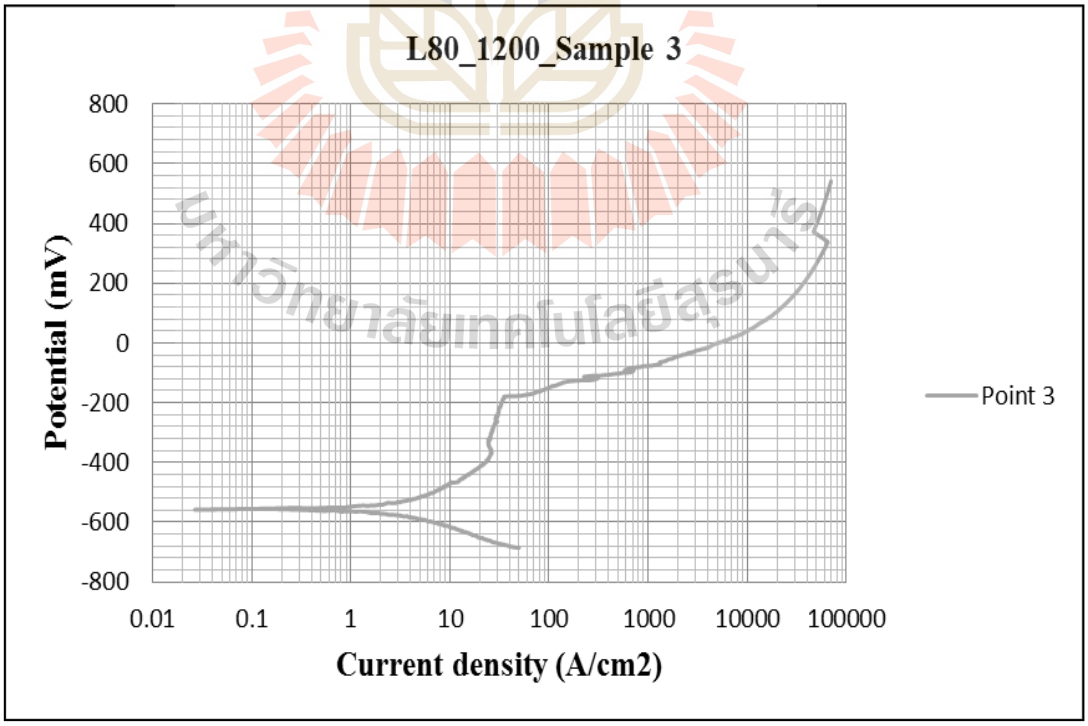

Figure A36 Polarization of L80 (API 5CT), No.1200, Sample 3, Point 3

Table A1.1 The corrosion rate of K55, No.600.

Sample 1	pH	I corr (µA/ cm^2)	E corr (mV)	CR (mm/year)
Point 1	6.59	4.2	-694	0.0482
Point 2	6.69	6.5	-675	0.0746
Point 3	6.69	3	-678	0.0344
avg	6.66	4.57	-682.33	0.0524
S.D	0.06	1.78	10.21	0.0204

Table A1.2 The corrosion rate of K55, No.600.

Sample 2	pH	I corr (µA/ cm^2)	E corr (mV)	CR (mm/year)
Point 1	6.74	3.2	-689	0.0367
Point 2	6.87	5	-742	0.0574
Point 3	6.92	3.5	-750	0.0402
avg	6.84	3.90	-727.00	0.0448
S.D	0.09	0.96	33.15	0.0111

Table A1.3 The corrosion rate of K55, No.600.

Sample 3	pH	I corr (µA/ cm^2)	E corr (mV)	CR (mm/year)
Point 1	6.54	1.8	-688	0.0207
Point 2	6.65	4	-691	0.0459
Point 3	6.75	5.3	-727	0.0608
avg	6.65	3.70	-702.00	0.0425
S.D	0.11	1.77	21.70	0.0203

Table A2.1 The corrosion rate of K55, No.1200

Sample 1	pH	I corr (µA/ cm^2)	E corr (mV)	CR (mm/year)
Point 1	6.66	2.5	-706	0.0287
Point 2	6.76	3.4	-669	0.0390
Point 3	6.89	3.6	-668	0.0413
avg	6.77	3.17	-681.00	0.0363
S.D	0.12	0.59	21.66	0.0067

Table A2.2 The corrosion rate of K55, No.1200

Sample 2	pH	I corr (µA/ cm^2)	E corr (mV)	CR (mm/year)
Point 1	6.62	3.1	-704	0.0356
Point 2	6.64	3.2	-691	0.0367
Point 3	6.7	4.1	-669	0.0470
avg	6.65	3.47	-688.00	0.0398
S.D	0.04	0.55	17.69	0.0063

Table A2.3 The corrosion rate of K55, No.1200

Sample 3	pH	I corr (µA/ cm^2)	E corr (mV)	CR (mm/year)
Point 1	6.74	3.5	-693	0.0402
Point 2	6.79	3	-672	0.0344
Point 3	6.93	3.1	-705	0.0356
avg	6.82	3.20	-690.00	0.0367
S.D	0.10	0.26	16.70	0.0030

Table A3.1 The corrosion rate of L80-13Cr, No.600.

Sample 1	pH	I corr (µA/ cm^2)	E corr (mV)	CR (mm/year)
Point 1	6.71	1.5	-435	0.0159
Point 2	6.80	1.3	-415	0.0138
Point 3	6.87	1.9	-533	0.0202
avg	6.79	1.57	-461.00	0.0166
S.D	0.08	0.31	63.15	0.0032

Table A3.2 The corrosion rate of L80-13Cr, No.600.

Sample 2	pH	I corr (µA/ cm^2)	E corr (mV)	CR (mm/year)
Point 1	6.61	1.4	-528	0.0149
Point 2	6.68	1.2	-462	0.0128
Point 3	6.85	2	-509	0.0213
avg	6.71	1.53	-499.67	0.0163
S.D	0.12	0.42	33.98	0.0044

Table A3.3 The corrosion rate of L80-13Cr, No.600.

Sample 3	pH	I corr (µA/ cm^2)	E corr (mV)	CR (mm/year)
Point 1	6.95	1.6	-502	0.0170
Point 2	6.68	1.9	-496	0.0202
Point 3	6.89	1.5	-400	0.0159
Avg	6.84	1.67	-466.00	0.0177
S.D	0.14	0.21	57.24	0.0022

Table A4.1 The corrosion rate of L80-13Cr, No.1200.

Sample 1	pH	I corr (µA/ cm^2)	E corr (mV)	CR (mm/year)
Point 1	6.95	1	-385	0.0106
Point 2	6.55	0.85	-350	0.0090
Point 3	6.61	1.3	-443	0.0138
Avg	6.70	1.05	-392.67	0.0112
S.D	0.22	0.23	46.97	0.0024

Table A4.2 The corrosion rate of L80-13Cr, No.1200.

Sample 2	pH	I corr (µA/ cm^2)	E corr (mV)	R mpy (mm/year)
Point 1	6.71	1.4	-353	0.0149
Point 2	6.69	2.2	-385	0.0234
Point 3	6.72	1.5	-350	0.0159
Avg	6.71	1.70	-362.67	0.0181
S.D	0.02	0.44	19.40	0.0046

Table A4.3 The corrosion rate of L80-13Cr, No.1200.

Sample 3	pH	I corr (µA/ cm^2)	E corr (mV)	CR (mm/year)
Point 1	6.49	0.85	-640	0.0090
Point 2	6.56	1	-595	0.0106
Point 3	6.46	1.6	-555	0.0170
Avg	6.50	1.15	-596.67	0.0122
S.D	0.05	0.40	42.52	0.0042

BIOGRAPHY

Mr. Atiwat Ketsukmanote was born on the 4th of May 1988 in Chonburi province. He earned his high school diploma in science-math from Chonburi Sukkhabot School in 2003 and his bachelor's degree in Metallurgical Engineering from Institute of Engineering, Suranaree University of Technology (SUT) in 2011. After graduation, he has been worked about production engineering until 2013.

During 2013-2016, he studied for master's degree in the School of Geotechnology, Institute of Engineering at SUT with the major in Petroleum Engineering. His strong background is in drilling, reservoir engineering, corrosion analysis and Non Destructive Testing (NDT).